HEINRICH EVENTS: MASSIVE LATE PLEISTOCENE DETRITUS LAYERS OF THE NORTH ATLANTIC AND THEIR GLOBAL CLIMATE IMPRINT

Sidney R. Hemming

*Department of Earth and Environmental Sciences
and Lamont-Doherty Earth Observatory of Columbia University
Palisades, New York, USA*

[1] Millennial climate oscillations of the glacial interval are interrupted by extreme events, the so-called Heinrich events of the North Atlantic. Their near-global footprint is a testament to coherent interactions among Earth's atmosphere, oceans, and cryosphere on millennial timescales. Heinrich detritus appears to have been derived from the region around Hudson Strait. It was deposited over approximately 500 ± 250 years. Several mechanisms have been proposed for the origin of the layers: binge-purge cycle of the Laurentide ice sheet, jökulhlaup activity from a Hudson Bay lake, and an ice shelf buildup/collapse fed by Hudson Strait. To determine the origin of the Heinrich events, I recommend (1) further studies of the timing and duration of the events, (2) further sedimentology study near the Hudson Strait, and (3) greater spatial and temporal resolution studies of the layers as well as their precursory intervals. Studies of previous glacial intervals may also provide important constraints.   *INDEX TERMS:* 4267 Oceanography: General: Paleoceanography; 1040 Geochemistry: Isotopic composition/chemistry; 1620 Global Change: Climate dynamics (3309); 3022 Marine Geology and Geophysics: Marine sediments—processes and transport; 1045 Geochemistry: Low-temperature geochemistry; *KEYWORDS:* climate, Heinrich layers, Heinrich events, ice-rafted detritus.

1. INTRODUCTION

[2] Few discoveries have focused the attention of the paleoclimate community more than "Heinrich events," which are documented in the North Atlantic as anomalous occurrences of ice-rafted detritus (IRD) (Figures 1 and 2). As pointed out by *Bond et al.* [1993] and *Broecker* [1994], the timing of Heinrich events is in striking coincidence with the pattern of climate fluctuations documented from ice cores. There is also good evidence for a global, or at least a Northern Hemisphere-wide, footprint [e.g., *Broecker*, 1994]. Although the mechanism that drives the events remains a matter of debate, there is no doubt that they are spectacular examples of interactions among Earth's atmosphere, oceans, and cryosphere [*Broecker*, 1994]. Most of the individual studies of sites outside the North Atlantic ice-rafting zone (Figures 3 and 4) conclude that the Heinrich-correlated events are caused by changes in winds: stronger trade winds in the tropics [e.g., *Arz et al.*, 1998; see also *McIntyre and Molfino*, 1996], stronger winter monsoon winds in China [e.g., *Porter and An*, 1995; *Wang et al.*, 2001] and the Arabian Sea [e.g., *Schulz et al.*, 1998], and stronger northerly winds in the western Mediterranean [e.g., *Cacho et al.*, 1999]. *Lund and Mix* [1998] also found evidence of greater northeast Pacific ventilation at intervals approximately coincident with Heinrich events. When compared to the ambient glacial conditions, there appears to be a general pattern of a tendency for wetter (milder?) conditions along the western North Atlantic margin during Heinrich events [e.g., *Grimm et al.*, 1993] and perhaps along the eastern South Atlantic margin [*Little et al.*, 1997; *Kanfoush et al.*, 2000]. In contrast, more extreme cold/dry glacial conditions prevailed during Heinrich intervals on the eastern North Atlantic margin and western Mediterranean [e.g., *Cacho et al.*, 1999; *Bard et al.*, 2000]. The pattern of difference in Heinrich events compared to ambient glacial, as well as the geographic distribution of sites that are sensitive to Heinrich events, versus Dansgaard-Oeschger (D-O) events may provide important clues to the driving forces of these abrupt climate changes. Global climate correlatives are discussed in section 6.

[3] *Heinrich* [1988] documented layers with extremely high lithic fragment percentages (approaching 100%) by taking the ratio of lithic grains to total entities in the 180 μm to 3 mm (sand is 63 μm to 2 mm) sediment fractions of sediment cores from the eastern North Atlantic (Figures 1 and 2). Several subsequent studies have found correlative horizons of high lithic percentages or high magnetic susceptibility in a band approximately coinciding with the North Atlantic Current (Table 1 and Figure 2) and the ice-
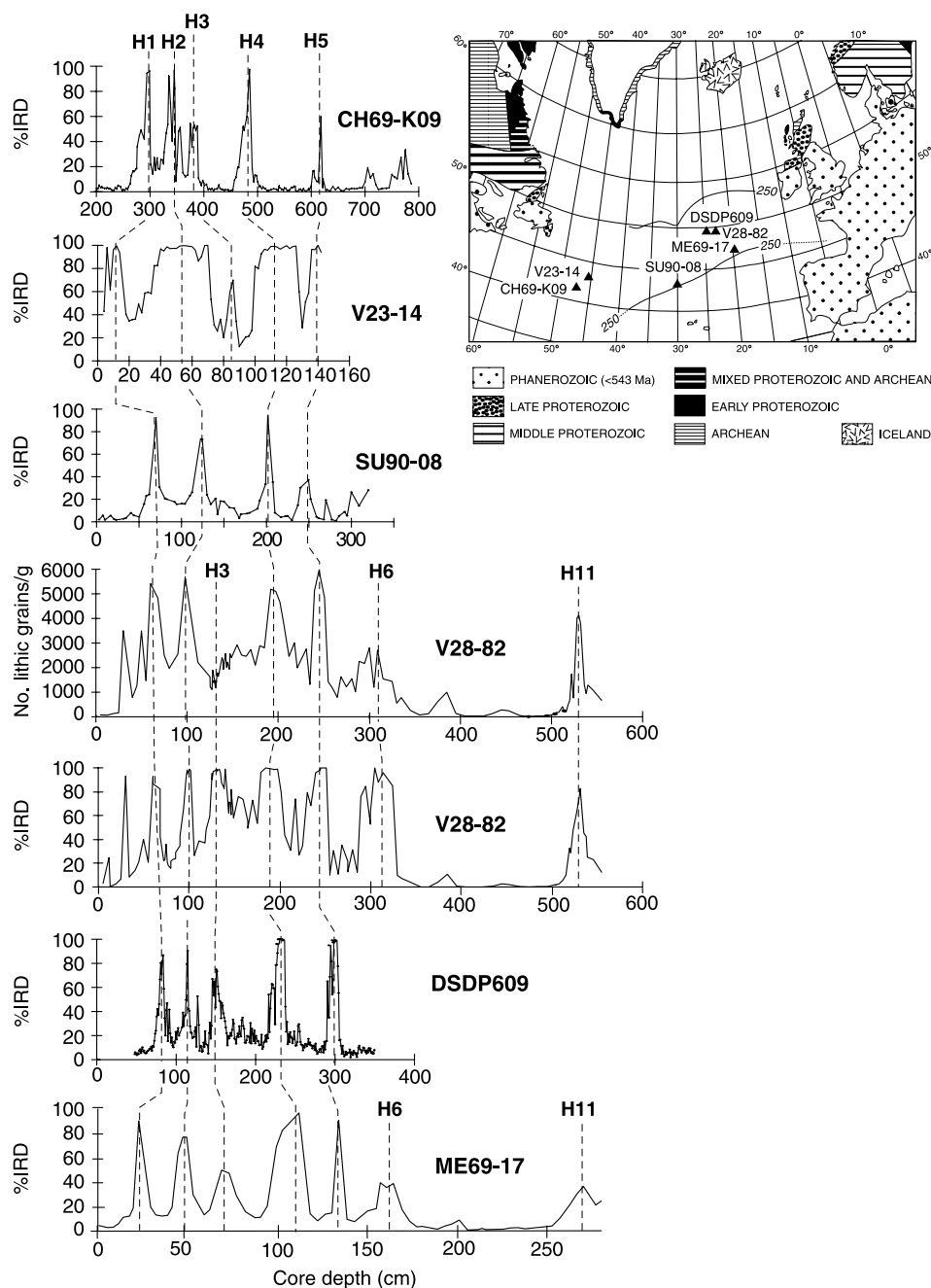

Figure 1. Ice-rafted detritus (IRD) data for North Atlantic sediment cores with Heinrich layers. Most of the data are the percentage of lithic grains in the >150 μm fraction; however, the data from ME69-17 [*Heinrich*, 1988] is the percentage of lithic grains in the 180–3000 μm fraction. Also shown is the record of number of lithic grains >150 μm per gram of dry sediment from core V28-82. The map shows the location of the cores. Data sources are CH69-K09 [*Labeyrie et al.*, 1999], V23-14 [*Hemming and Hajdas*, 2003], SU90-08 [*Grousset et al.*, 1993], V28-82 [*Gwiazda et al.*, 1996a; *McManus et al.*, 1998; *Hemming et al.*, 1998], DSDP609 [*Broecker et al.*, 1992; *Bond et al.*, 1992], and ME69-17 [*Heinrich*, 1988].

rafted detritus (IRD) belt of *Ruddiman* [1977]. The layers are generally considered to fall within six brief time intervals during the last glacial period, which are labeled "H1" through "H6" from youngest to oldest [*Bond et al.*, 1992; *Broecker et al.*, 1992].

[4] In the North Atlantic the Heinrich layers are also anomalous in their abundance of detrital carbonate [*Bond et al.*, 1992; *Broecker et al.*, 1992]. Parallel observations

of high detrital carbonate concentrations within approximately correlative intervals [*Andrews and Tedesco*, 1992] suggested that the Heinrich layers were formed by "armadas of icebergs" launched from Hudson Strait [*Broecker et al.*, 1992]. Hudson Strait is a major trough and likely the location of an ice stream capable of draining the eastern portion of the Laurentide ice sheet. *MacAyeal* [1993] proposed a "binge-purge" mechanism, which could oper-
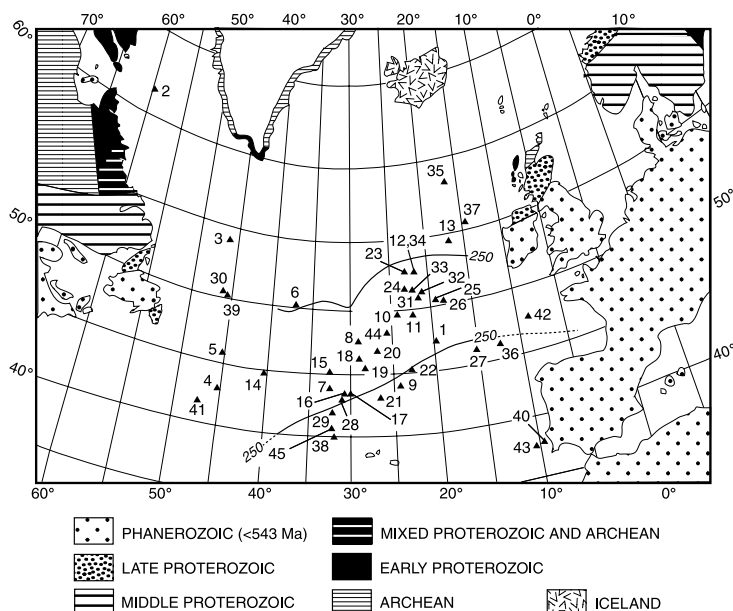
Figure 2. Map showing locations of cores with identified Heinrich layers. Data sources are given in Table 1. Simplified geological provinces are shown for reference. The map template is from *Ruddiman* [1977], and the 250 mg cm^{-2} kyr^{-1} flux lines from 25 to 13 kyr, *Ruddiman*'s [1977] "IRD belt," are shown for reference.

ate independently of climate changes, to account for the armadas of icebergs, and he further proposed that the Paleozoic carbonates lining Hudson Bay and Hudson Strait provided a relatively soft substrate that significantly helped foster an ice stream. More recently, other models have been proposed, but the notion of a binge-purge cycle remains attractive. *Bond et al.* [1999] pointed out that there is no doubt that the enormous amounts of ice discharged during Heinrich events H1, H2, H4, and H5 require glaciological processes, probably involving massive surging or collapse of ice in Hudson Strait. However, they also emphasize that the temporal pattern appears to require a climate trigger.

[5] In the 10 years since Heinrich layers gained prominence because of discoveries of North Atlantic and Labrador Sea correlatives [*Andrews and Tedesco*, 1992; *Bond et al.*, 1992; *Broecker et al.*, 1992], more than 200 papers have been published from studies of the layers or purported global equivalents. In this paper I review the research to date on Heinrich layers (events). I discuss the ice-rafted detritus (section 2.1) setting that encompasses them, the physical and chemical evidence that characterizes them, the processes that may explain them, and the global signals that may relate to them. It is important to understand the global footprint of Heinrich events [e.g., *Leuschner and Sirocko*, 2000; *Broecker and Hemming*, 2001] and how it compares to that of the more frequent Dansgaard-Oeschger cycles that are so prominent in the Greenland ice cores. I use the information I have compiled here to suggest a means of constraining the origin of

Heinrich layers and to propose key areas that need further research.

2. BACKGROUND

2.1. Definition of Ice-Rafted Detritus

[6] Ice-rafted detritus (IRD) is sediment that was entrained in floating ice, either icebergs or sea ice, and that settled to the seafloor when the enclosing ice melted. Considerable disagreement exists about the quantification of IRD in marine sediment cores. *Heinrich* [1988] used the percentage of IRD: the percentage of mineral or rock fragments compared to all entities (what is not mineral or rock fragments is almost exclusively foraminifera). Heinrich counted the 180 μm to 3 mm fraction, whereas most subsequent counts are from the >150 μm fraction, and some from the Nordic Seas are from a much larger size fraction. Another IRD indicator is the lithic portion, measured by weight, of a sample's coarse fraction.

[7] Three complications exist for choosing appropriate grain-size intervals to study IRD. First, the coarse fraction of marine sediments is generally small [*Andrews*, 2000]. *Andrews* [2000] has emphasized the point that the <63 μm fraction, not the >63 μm fraction, is far more abundant and representative in glacial deposits on land and near marine outlets. In core V28-82, Heinrich layers H1, H2, H4, and H5 contain approximately 5000–6000 lithic grains (>150 μm) per gram of dry bulk sediment, and H3 and H6 have only about 3000 (see Figure 5). Second, the provenance of sediments eroded by glaciers profoundly influences their
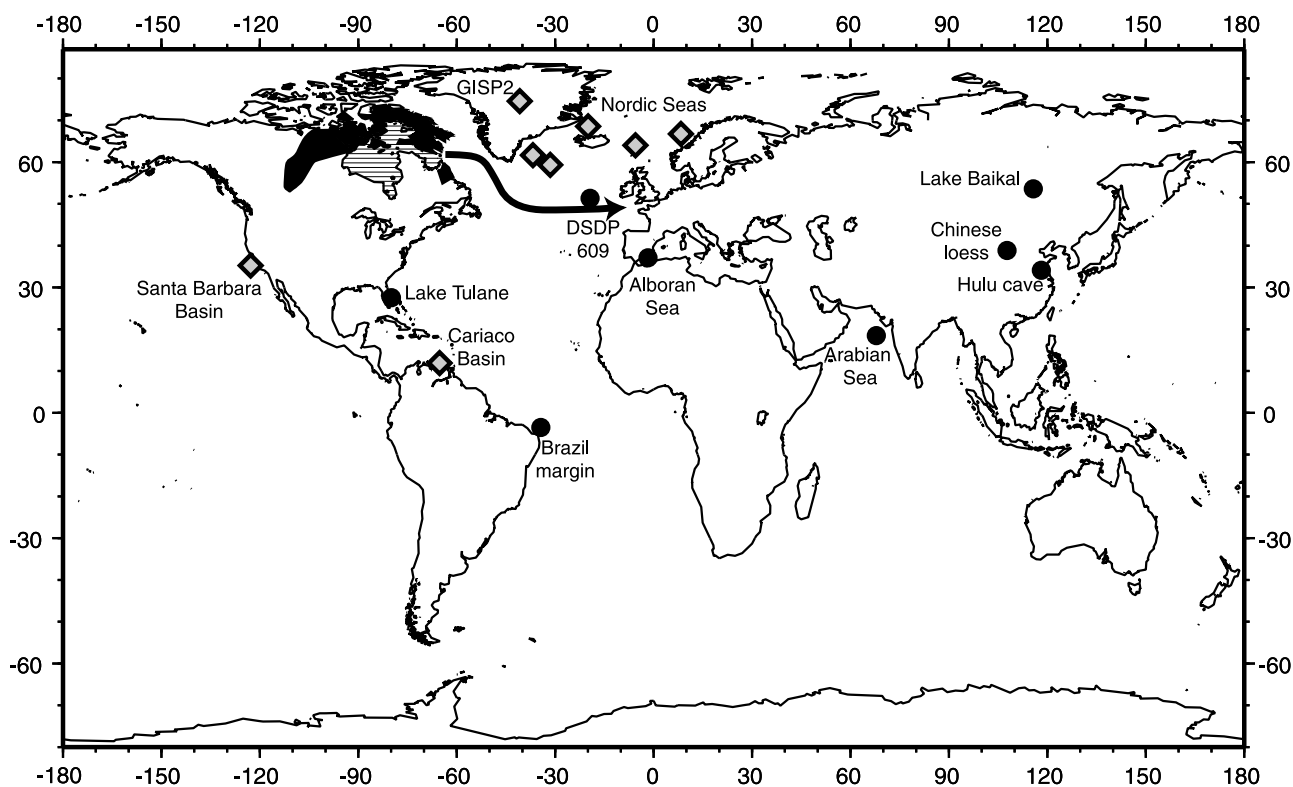
Figure 3. Map showing locations of records of abrupt climate events discussed in this paper. The Greenland Ice Sheet Project 2 (GISP2) $\delta^{18}O$ (Figure 4), Nordic Seas and Irminger Basin ice-rafted detritus (IRD) [e.g., *Rasmussen et al.*, 1997; *Elliot et al.*, 1998; *Voelker et al.*, 1998; *Dokken and Jansen*, 1999; *van Kreveld et al.*, 2000], Santa Barbara Basin anoxia [*Behl and Kennett*, 1996; *Kennett et al.*, 2000], and Cariaco Basin runoff [*Peterson et al.*, 2000] do not record more extreme climate conditions during Heinrich events. DSDP609 detrital carbonate concentration (Figure 4) Lake Tulane pine pollen [*Grimm et al.*, 1993], Brazil margin terrigenous concentration [*Arz et al.*, 1998], Lake Baikal (Selenga delta) runoff [*Prokopenko et al.*, 2001], and Chinese loess average grain size [*Porter and An*, 1995] have approximately the same number of peaks as Heinrich events and do not seem to record the other millennial climate shifts. Alboran Sea sea surface temperature (Figure 4), Arabian Sea organic carbon (Figure 4), and Hulu cave $\delta^{18}O$ (Figure 4) appear to record all the GISP2 events in the last 50 kyr, and Heinrich events are pronounced extrema.

grain-size distribution; thus different grain-size ranges should arguably be examined to identify different fundamental rock-type contributions. Third, distance of transport under the glacier is a strong control on the ultimate grain size.

[8] These complications mean that the coarse-grain fractions are inevitably biased toward rocks near the ocean margin and toward rocks that tend to break into grains of the size range examined. (For example, shale would be underrepresented in the >63 μm fraction.) While recognizing the inevitable complexity of glacial sediment [e.g., *Dreimanis*, 1976; *Dowdeswell and Dowdeswell*, 1989; *Dowdeswell and Murray*, 1990; *Dowdeswell et al.*, 1998; *Andrews*, 1998, 2000], in the open ocean it is necessary to use a fraction that is coarse enough to not have been transported by means other than ice rafting. Away from turbidite aprons (shown by *Ruddiman* [1977]), >63 μm grains are most likely derived by ice rafting and grains >150 μm definitely are.

[9] Depositional and bottom current processes in the ocean can also modify the grain-size distributions. For example, in drift deposits, there is a very large fraction of sortable silt [e.g., *McCave*, 1995], and some depositional sites must be quantitatively losing their fine fraction to scouring by bottom currents. Core V28-82 in the eastern North Atlantic is not on a drift and appears to be a case where the flux from above matches the accumulation (based on $^{230}Th_{excess}$ analyses [*McManus et al.*, 1998]). Thus it is a good reference core for deep ocean IRD characteristics in the IRD belt. In contrast to V28-82, in western North Atlantic core V23-14, Heinrich layers are at minima in >63 μm fraction and number of lithic grains per gram (see Figure 5). V23-14 has a very low sedimentation rate between Heinrich layers of approximately 3 cm kyr^{-1} [*Hemming and Hajdas*, 2003], and it is likely that bottom currents are robbing the fine fraction from this site. Eastern North Atlantic core V23-81 from the Feni Drift is a place where extra fine fraction is added by bottom current processes. V23-81 has a sedimentation rate of approximately 12 cm kyr^{-1}, and Heinrich layers are strong maxima in numbers of lithic grains per gram (see Figure 10). However,
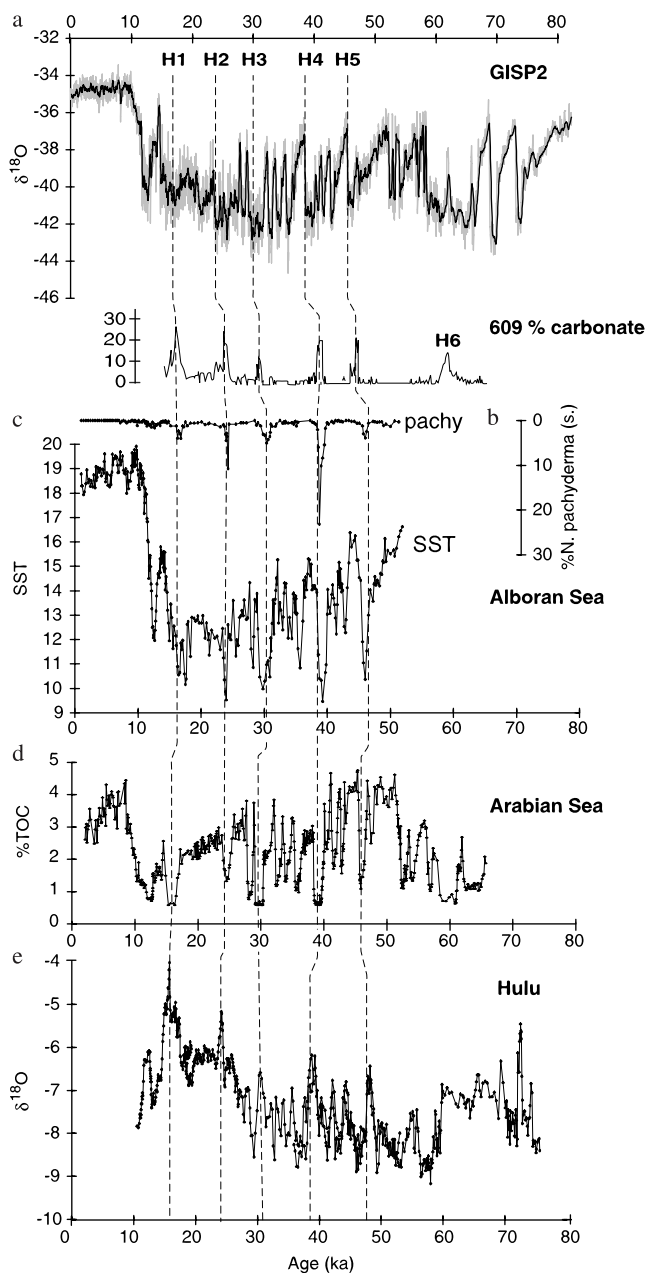
Figure 4. Correlation of some high-resolution, Northern Hemisphere records. (a) GISP2 data [*Meese et al.*, 1997; *Stuiver and Grootes*, 2000; data from http://depts.washington. edu/qil/datasets/gisp2_main.html]. All data are shown with shading, and a 10-point running average is shown as the solid line. (b) Percentage of detrital carbonate from DSDP609 [*Bond et al.*, 1999]. (c) Percentage of *Neogloboquadrina pachyderma* (s.) from an Alboran Sea record [*Cacho et al.*, 1999]. (d) $U_{37}^{K'}$ sea surface temperature estimates from the same Alboran Sea record [*Cacho et al.*, 1999]. (e) Estimated total organic carbon (TOC) (a percentage) from an Arabian Sea core [*Schulz et al.*, 1998]. (f) The $\delta^{18}O$ of speleothem calcite from Hulu Cave, China, dated with high-precision U series methods [*Wang et al.*, 2001].

the maximum is only about 1500 grains per gram [*Bond and Lotti*, 1995; *Bond et al.*, 1999].

2.2. Geochemical Provenance Studies and Potential Source Terranes Around the North Atlantic

[10] Geochemical approaches provide a valuable complement to petrographic provenance studies. Petrographic studies allow identification of major lithological components in the sand fraction, as well as potentially diagnostic minerals and/or rock types. In general, geochemical approaches are applicable to both coarse- and fine-grained fractions. Potential complications exist with using the fine fractions. For example, fine-grained sediments typically represent more homogeneously mixed sources. Additionally, in studies of marine sediment cores, processes other than ice rafting are capable of transporting fine-grained components. However, the fine fraction carries valuable information about sources. Measurements of components that are greatly enriched or depleted in the sedimentary cycle yield information about the degree of chemical alteration of the source and thus provide insights into the contributions from sedimentary sources. In the North Atlantic, geochemical studies of the fine terrigenous fraction include X-ray diffraction (mineralogical) studies, K/Ar ages, Rb-Sr, Sm-Nd, and Pb isotopes, and organic compounds.

[11] Many of the studies of IRD provenance have focused on the sand fraction. The sand fraction is appealing because it must have been rafting on ice (although whether sea ice or icebergs were the rafts is difficult to determine). In the North Atlantic, geochemical studies of the sand fraction include the Sm-Nd and Rb-Sr isotope systems in the bulk sand fraction (after carbonate is removed), Pb isotopes in individual grains or composite samples of feldspar, and $^{40}Ar/^{39}Ar$ ages of individual grains of hornblende.

2.2.1. Sm-Nd Isotope System

[12] The Sm-Nd isotope system provides an average age of crust formation of the sediment's sources [*Taylor and McLennan*, 1985; *Goldstein and Jacobsen*, 1988; *McLennan and Hemming*, 1992]. This is because Sm and Nd are rare earth elements with similar radii, and thus are generally not separated by most sedimentary processes (although there are exceptions). Average post-Archean upper continental crust has a Sm/Nd of 0.173, and average post-Archean shale has a Sm/Nd of 0.175 [*Taylor and McLennan*, 1985]. Evidence from Archean sedimentary rocks indicates a slightly higher Sm/Nd [*Taylor and McLennan*, 1985; *McLennan and Hemming*, 1992], but for the purpose of this application the difference is negligible. Because of the relatively small range of Sm/Nd of continental sources the Nd isotope composition of a sediment provides a rough estimate of the average continental age of its sources (there is approximately a 1 epsilon unit decrease per 100 million years, so a sample with ε_{Nd} of -27 can be inferred to have been derived from a late Archean source or, alternatively, from a mix of early Archean source with a younger source). In the North Atlantic, Iceland can be a significant sediment contributor, with a higher Sm/Nd [*Farmer et al.*, 2003] and ε_{Nd} ranging

TABLE 1. Cores That Have Been Studied for Heinrich Layers in and Close to the IRD Belt[a]

Map	Source	Core	Longitude, deg	Latitude, deg	Depth, m	H1 ΔT	H1 C	H2 ΔT	H2 C	H3 ΔT	H3 C	H4 ΔT	H4 C	H5 ΔT	H5 C	H6 ΔT	H6 C
1	Heinrich [1988]	ME69-17	−19.71	47.36	3905	5	23	9	46.5	13	64	20	106	6	133	14	162
1		ME69-19	−19.69	47.32	4350		18		37		44		79		100		140
2	Bond et al. [1992]	HU75-55	−58.65	61.50	2500	40	90	69	210								
3		V27-20	−46.20	54.00	3510					0	125	8	210				
4		V23-14[b]	−45.25	43.40	3177	6	13	24	52	2	86	20	116				
5		V23-16	−45.05	46.00	2813	25	45	35	120	20	205	50	270	8	375	12	550
6		V27-17	−37.30	50.08	4054					2	70	3	95			2	147
7		V30-101k	−32.50	44.10	3504	3	37	8	52	5	80	4	98	5	192		
8		Mo1-32	−28.93	47.58	4070	3	42	7	78	0	105	12	157			0	236
9		V29-179	−24.53	44.02	3331	2	60	3	83	1	120	4	200				
10		DSDP609	−24.23	49.88	3884	1	82	5	113	0	150	10	229	10	296	0	400
11		V28-82[c]	−22.27	49.45	3935	18	60	21	99		131	31	192	30	245	0	305
12		V23-82	−21.93	52.58	3974	1	90	5	152	0	190	4	270	2	340	0	440
13		V23-81	−16.83	54.25	2393	1	220	3	329	0	383	3	495	2	584	0	760
41	Grousset et al. [1993]	CH69-K09	−47.35	41.75	4100	23		62				31		15			
5		V23-16	−45.05	46.00	2813	25		35									
14		SU90-11	−40.27	44.73	3645	28	34	27	81.5	10	110	35	144.5	30	210		279
15		KS79-14	−32.13	45.33	3500	32		54		38		24		14			
16		KS79-15	−30.20	43.22	2875	10		12		8		16		15			
17		SU90-08	−30.40	43.50	3080	16	79	12	130			10		27			
18		KS79-24	−29.00	47.04	3425	9		18		40		38		3			
1		ME69-17	−19.71	47.36	3905	7		9		6		21		22			
19		KS79-18	−27.24	45.47	2815	20		10		30	61	40	106	20	168		230
20		KS79-25	−27.28	46.98	2950			20	35	20		40					
21		KS79-17	−27.17	43.00	3030	7		7		6		17		13			
10		ODP609	−24.23	49.88	3884	6		5		15		18		17			
22		KS79-28	−22.76	45.63	3625	12		12		8		10		12			
23		SU90-39	−23.00	53.00	3955	8		6		3		10		7			
24		SU90-40	−22.50	52.00		1	50	13	83	4				9			
25		SU90-43	−19.30	50.30		3	67	12	136								
26		SU90-44	−17.93	50.10	4255	8	31	4	43	15	182.5	17	243.5	10	293		
27		KS79-29	−15.07	46.30	3499	6				3	65	12	88	2	118		148
28		SU90-09	−31.08	43.08	3375	13	56.5	10	87	7	110.5	10	147	10	191		

TABLE 1. (continued)

Map	Source	Core	Longitude, deg	Latitude, deg	Depth, m	H1 ΔT	H1 C	H2 ΔT	H2 C	H3 ΔT	H3 C	H4 ΔT	H4 C	H5 ΔT	H5 C	H6 ΔT	H6 C
29	*Francois and Bacon* [1994]	CHN82 31 11PC	−31.80	42.38	3209	5	53.5	7	83.5								
30	*Bond and Lotti* [1995]	GGC31	−46.35	50.57		16	45	15	104.5								
31	*Manighetti et al.* [1995]	BOFS 5K	−21.87	50.68	3547		72		109				226		175		212
32		BOFS 6K	−21.20	51.12	2865		34		60				136		103		125
33		BOFS 7K	−22.54	51.76	2327		32		42				83				
34		BOFS 8K	−22.07	52.50	4045		76		126				234				
35		BOFS 17K	−16.50	58.00	1150		62		90				150		188		230
36	*Thomson et al.* [1995]	CD63#9K	−12.55	46.40	3849	11	36	10	98.5	5	135	15	630				
37	*Vidal et al.* [1997]	NA87-22	−14.70	55.50	2161	17.5	348.3	22.5	494	15	555	10	205				
17		SU90-08	−30.04	43.05	3080	11	68.5	11	123.5				195	10	249		
38	*Chapman and Shackleton* [1998]	SU90-03	−32.00	40.05	2475		77		132								
39	*Stoner et al.* [1998]	HU91-045-094P	−45.69	50.20	3448	20	237	15	375		470		570		680		835
39	*Veiga-Pires and Hillaire-Marcel* [1999]	HU91-045-094P	−45.69	50.20	3448		238		372.5								
40	*Zahn et al.* [1997]	SO75-26KL	−9.50	37.82	1099	8	136	10	272			28	568				
46	*Cortijo et al.* [1997]	SU90-12	−39.78	51.87	2950								109				
17		SU90-08	−30.40	43.50	3080							18	201				
41		CH69-K09	−47.35	41.75	4100							15	482				
45		SU90-05	−32.25	41.63	3285								493				
36	*Snoeckx et al.* [1999]	CD63#9K	−12.55	46.40	3849						137		175				
48		KS01	−17.03	46.00	4730						109		141				
50		D11957P											125				
1		ME69196									68		109				
24		SU90-40	−22.50	52.00	4255						110		160				
26		SU90-44	−17.93	50.10	997						180		240				
49		SU92-28	−9.47	37.09									493				
47	*Thomson et al.* [1999]	MD95-2039	−10.35	40.69	3381	11	225	3	550			18	1020	5	1220		
41	*Labeyrie et al.* [1999]	CH69-K09	−47.35	41.75	4100		294.5		344.5	8	384		481		617.5		
42	*Grousset et al.* [2000]	MD95-2002	−8.53	47.45	2174		~330										
43	*Bard et al.* [2000]	SU81-18	−11.18	37.77	3135												
44	*van Kreveld et al.* [1996]	T88-9P	−25.08	48.38	3193												

[a] ΔT is thickness, and C is core depth at center of layer, both in centimeters.
[b] Value is corrected according to *Hemming and Hajdas* [2003].
[c] Value is corrected according to *McManus et al.* [1998].
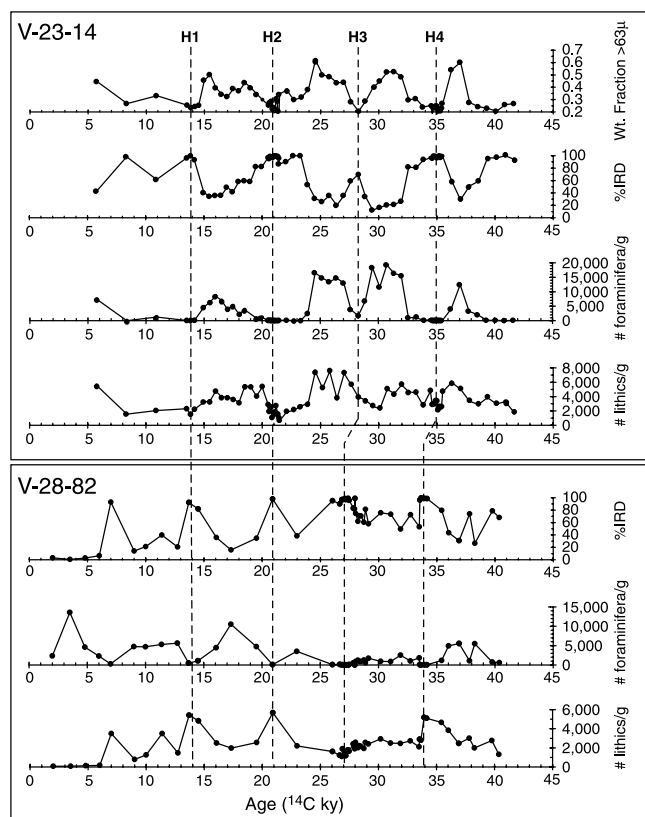
Figure 5. Comparison of IRD and foraminifera data from V28-82 [*Gwiazda et al.*, 1996a; *McManus et al.*, 1998; *Hemming et al.*, 1998] and V23-14 [*Hemming and Hajdas*, 2003]. Age scales were developed using the ages of the Heinrich layers (discussed in section 4.6). Weight percent data for the <63 μm fraction are not available for V28-82. Note that in both cores the number of foraminifera per gram is minima at Heinrich layers and that the percentage of IRD is maxima. However, in contrast to core V28-82 the numbers of lithic grains per gram in Heinrich layers in V23-14 are at relatively low values compared to the rest of the core. Additionally, the weight fractions >63 μm are distinct minima at Heinrich intervals in V23-14.

up to near depleted mantle compositions [*Grousset et al.*, 1993; *Farmer et al.*, 2003].

2.2.2. Rb-Sr Isotope System

[13] The Rb-Sr isotope system may be disturbed by many geological processes [*Dasch*, 1969; *Goldstein and Jacobsen*, 1988]. This is because of the large geochemical difference between Rb (alkali metal) and Sr (alkaline earth element) as well as their mineralogical hosts. Rb tends to follow K and is enriched in K-feldspar and micas, whereas Sr tends to follow Ca and is enriched in plagioclase and pyroxene. Plagioclase and pyroxene are generally susceptible to chemical attack during weathering, and Sr is removed to the aqueous system. Rubidium's hosts have greater resistance to chemical weathering, and, additionally, Rb released during weathering tends to follow Al and thus to be retained in the solid system. In addition to the sedimentary alteration of the Rb-Sr system, metamorphism tends to break down and reform the mineral hosts of these

elements, and thus metamorphic resetting of the Rb-Sr isotope system is common. Accordingly, the Rb-Sr isotope system provides a large signal compared to our ability to measure the Sr isotope composition, but the interpretation of the geological source is complicated by the wide array of processes that disturb or reset its clock.

2.2.3. Pb Isotope System

[14] The Pb isotope system is a powerful provenance tool because of its formation from two isotopes of U and one of Th. Pb is composed of four stable isotopes, ^{204}Pb, ^{206}Pb, ^{207}Pb, and ^{208}Pb. Of these isotopes, only ^{204}Pb is non-changing. Isotopes ^{206}Pb and ^{207}Pb are the final products from decay of ^{238}U and ^{235}U, respectively. Owing to the much longer half-life of ^{238}U (~4.5 b.y.) compared to ^{235}U (~700 m.y.) the Pb isotope system is particularly sensitive to detection of ancient (particularly Archean) sources. Although some published Pb isotope data exist from bulk samples of Heinrich layers and potential sources [*Hemming et al.*, 1998; *Farmer et al.*, 2003], they are still too scarce to determine how sensitively they can be used to discriminate sources in the North Atlantic region. However, the Pb isotope composition of feldspar provides important insights into basement sources to sediments. Feldspars have high Pb abundance and very low U and Th abundance, and thus the Pb isotope composition of feldspar approximates the initial Pb isotope composition of its source [e.g., *Hemming et al.*, 1994, 1996, 2000b].

2.2.4. K/Ar Isotope System

[15] The K/Ar isotope system is reset as easily as the Rb-Sr system, perhaps even more easily [*Hurley et al.*, 1963; *Hurley and Rand*, 1969]. Accordingly, the K/Ar ages of sedimentary components are likely to record the approximate time of the last disturbance of the system. In the case of the North Atlantic the K/Ar age of ambient pelagic sediments is about 400 Ma [*Hurley et al.*, 1963; *Jantschik and Huon*, 1992], consistent with a dominant derivation from Paleozoic shale sources. As mentioned in section 4.4, K/Ar ages of fine-sediment fractions from the Heinrich layers are approximately 1 Ga [*Jantschik and Huon*, 1992], and this age is most likely derived from a mixture of clay minerals from Paleozoic sediments and glacially powdered minerals from older terranes [*Hemming et al.*, 2002]. The ^{40}Ar/^{39}Ar age range of feldspar grains from Heinrich layers is large, but the average is about 1.4 Ga [*Hemming and Rasbury*, 2000; *Hemming et al.*, 2002]. Although the ^{40}Ar/^{39}Ar age range of hornblende is smaller and older, hornblende is a minor rock-forming mineral, and it has a low K concentration, and thus it has little impact on the bulk K/Ar age of North Atlantic sediments.

2.2.5. Continents Around the North Atlantic

[16] The continents around the North Atlantic have experienced a similar set of thermal pulses: ~3.8 Ga, ~2.5 Ga, ~1.8 Ga, ~1 Ga, ~0.6 Ga, ~0.4 Ga, and <0.06 Ga (summarized by *Hemming et al.* [1998], see geological provinces shown in Figure 1). It is not expected that any 3.8 Ga terrains have ^{40}Ar/^{39}Ar hornblende ages any older than ~2.6 Ga because of thermal overprinting. Hornblende has a blocking temperature to diffusion of Ar of

about 450°C [e.g., *Harrison*, 1981]. Thus amphibolite and higher-grade metamorphic events will reset or disturb the ages of hornblende. The Churchill province has an Archean (∼2.7 Ga) heritage, and it experienced an intense metamorphic event in the Paleoproterozoic (∼1.8 Ga). The reader is referred to a review by *Hoffman* [1989] for an overview of the geological history of continents surrounding the North Atlantic.

[17] Although there is substantial overlap in the geologic history of continental sources around the North Atlantic, Nordic Seas, and Arctic regions, the detailed combination of rock types (igneous, metamorphic, and sedimentary and more specific types within these) and geologic ages allows some specific conclusions to be drawn about IRD sources. Generally, it is easier to eliminate sources than it is to demonstrate that a source is the most likely candidate for a particular component. In addition to the specific details that may allow "fingerprinting" a particular source (e.g., Campanian chalk from Europe [*Scourse et al.*, 2000]), the geographic arrangement of the terranes on the continents may yield useful constraints. For example, *Hemming et al.* [2000a] and *Hemming and Hajdas* [2003] used the general trend from old to young basement terranes from north to south along the North American margin to constrain the maximum position of the Laurentide ice sheet during the last glacial cycle. With this approach it is possible to determine when the ice sheet had extended far enough south to contribute hornblende grains with Paleozoic and Mesoproterozoic $^{40}Ar/^{39}Ar$ ages to the IRD.

2.2.6. Geochemical Evidence for Sedimentary Sources

[18] Geochemical evidence for sedimentary sources may provide unique insights into ice rafting. This appears to be particularly true of organic compounds where the combination of depositional environment and burial/diagenesis creates specific groups of compounds that are only found in limited places. Organic compounds are greatly enriched in sedimentary sources compared to igneous and metamorphic terranes. The Heinrich layers again provide a good example of the application of this approach. While preparing samples for sea surface temperature estimates by separating the alkenones, *Rosell-Melé et al.* [1997] found some unusual organometalic compounds that require sedimentary sources from a very specific depositional environment and a very specific diagenetic history. J. Sachs (personal communication, 2000) has found similar compounds in one sample from the Hudson Strait.

2.3. Sediment Flux Estimates by the $^{230}Th_{excess}$ Method

[19] As a result of the long residence time of uranium in seawater the ^{230}Th production rate by the radioactive decay of dissolved ^{234}U within the entire water column above any particular seafloor location is a simple function of water depth. The ^{230}Th is extremely particle reactive and is rapidly removed from the water column and buried after adsorption by settling particles. Once buried, this excess ^{230}Th, combined with independently derived ages and the assumption of constant $^{230}Th_{excess}$ burial rate, may be used to measure instantaneous sediment rates. The method only normalizes the vertical flux of sediment, and lateral movement of sediment along the seafloor (focusing) can only be estimated by comparing the ^{230}Th accumulation with that predicted for the water column depth of the core. The reader is referred to articles that summarize the methods and assumptions [*Bacon*, 1984; *Suman and Bacon*, 1989; *Francois et al.*, 1990] and to the articles that specifically deal with Heinrich events [*Francois and Bacon*, 1994; *Thomson et al.*, 1995; *McManus et al.*, 1998; *Veiga-Pires and Hillaire-Marcel*, 1999]. The high percentage of IRD that characterizes Heinrich layers (Figure 1) could theoretically be a product of two end-member scenarios: very low flux of foraminifera or, alternatively, very high flux of IRD. In fact, four of the six Heinrich layers from the last 60 kyr, H1, H2, H4, and H5, have very high IRD flux in cores within the IRD belt, whereas two of the layers, H3 and H6, only show a modest increase in flux (Figure 20) or in the number of lithic grains per gram (see comparison of percentage of IRD and number of lithic grains per gram in core V28-82 in Figure 5).

## 3. ICE-RAFTED DETRITUS IN THE GLACIAL NORTH ATLANTIC: PATTERN OF DEPOSITION

[20] *Ruddiman* [1977] mapped the flux of lithic grains (mg cm^{-2} kyr^{-1}) in the 63 μm to 2 mm (i.e., sand) fraction in seven time slices between 125 and 13 kyr. He found two distinct patterns of variation in North Atlantic IRD (refer to section 2.1 for a working definition of IRD), loosely corresponding to interglacial and glacial conditions. The interglacial pattern is characterized by a depocenter along the 50° latitude "locus of melting" approximating the North Atlantic Drift (Figure 6a). During glacial time the flux is much greater, and the maximum IRD concentration is shifted to the south by a few degrees (Figures 6b and 6c). The 250 mg cm^{-2} kyr^{-1} contours from the 25–13 kyr slice (Figure 6c) are used extensively throughout this paper as the reference position of the IRD belt. This pattern of IRD deposition requires a significant drift of icebergs from west to east across the North Atlantic during glacial times [*Ruddiman*, 1977; *Robinson et al.*, 1995; *Matsumoto*, 1997].

4. CHARACTER OF HEINRICH LAYERS

4.1. Definition, Identification, and Correlation

[21] As noted in section 1, Heinrich measured the percentage of lithic grains to total entities (percentage of IRD) in the 180 μm to 3 mm size fraction of marine sediment samples from the Dreizack seamounts. Within the last glacial cycle he found six layers with a high percentage of IRD. Four of these six layers, specifically H1, H2, H4, and H5 were termed "cemented marls" [*Heinrich*, 1988; *Huon and Jantschik*, 1993; *Jantschik and Huon*, 1992] (these works refer to internal German theses in which many of the original core descriptions appear to be reported). The three sediment types that were defined for these cores are "foraminiferal
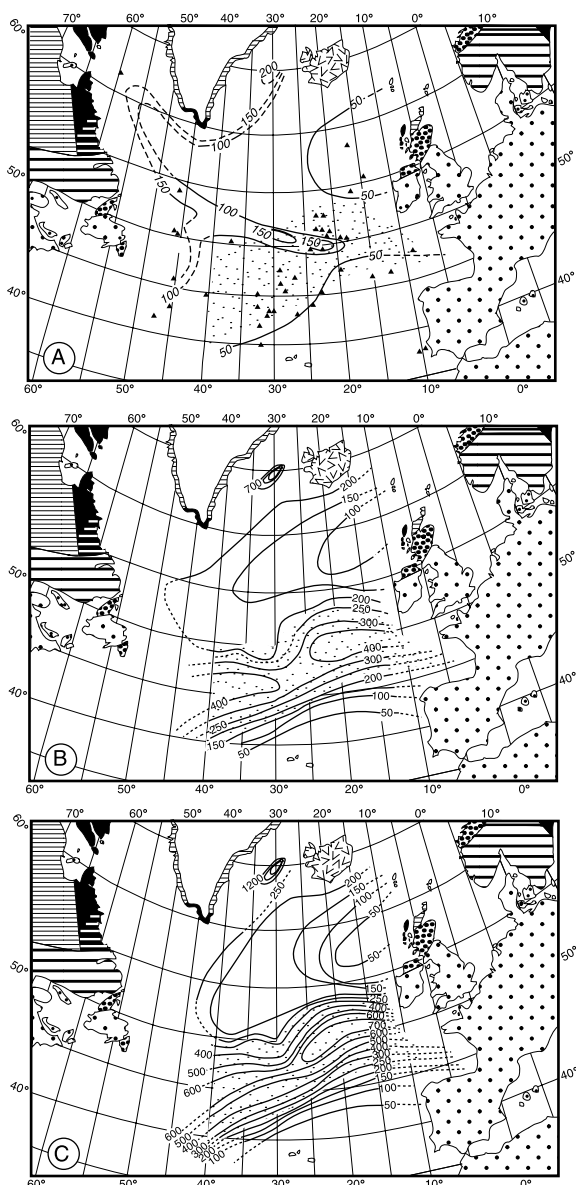
Figure 6. Maps of IRD flux to the North Atlantic from *Ruddiman* [1977] for (a) 125–115, (b) 40–25, and (c) 25–13 kyr. Geologic provinces and zone with flux >250 mg cm^{-2} kyr^{-1} (stippled area) from 25 to 13 kyr interval are shown for reference.

ooze" (interglacial), "diamicton" (glacial), and "cemented marl" (Heinrich layers H1, H2, H4, and H5). Although they have high percentage of IRD and lithic counts, these measures do not uniquely separate H1, H2, H4, and H5 from other IRD-rich layers. Several types of measurements of bulk samples have been shown to be diagnostic of these four Heinrich layers: high detrital carbonate concentration, flux as measured by ^{230}Th$_{excess}$, high magnetic susceptibility, 1 Ga K/Ar ages, and ε_{Nd} of approximately −27. As discussed in section 4.4, these characters are all consistent with the inference that they were derived from Hudson Strait [*Hemming et al.*, 1998]. Thus, for practical purposes, I will define a subgroup of Heinrich's layers (H1, H2, H4, and H5) as Hudson Strait (HS) Heinrich events H1, H2, H4, and H5. The distinction is important for attempting to refine the

correlations and assumptions about events in the North Atlantic and Nordic Seas. It is a troubling issue that needs attention because (1) different researchers naturally choose different definitions that depend on the tools applied and the regions of study and (2) it is important to agree on (or at least to understand differences in) definitions in order to assess the relations among disparate observations in time and space.

[22] *Heinrich*'s [1988] original percentage of IRD assessment works well for identifying the approximate positions of Heinrich layers in the IRD belt; however, the layers of high-IRD content are composites of different provenance and possibly different sea surface conditions [e.g., *Bond et al.*, 1992, 1993, 1997, 1999; *Bond and Lotti*, 1995; *Grousset et al.*, 2001; *Huon et al.*, 2002]. Accordingly, even within the IRD belt, there is a clear need for refinement of the definition in order to understand Heinrich layers. Heinrich layers are most clearly identifiable in the IRD belt of *Ruddiman* [1977] and have been mapped (Figure 7) based on anomalously high magnetic susceptibility [e.g., *Grousset et al.*, 1993] and IRD content [e.g., *Bond et al.*, 1992]. *Grousset et al.* [1993] and *Robinson et al.* [1995] showed the correspondence between IRD measures and magnetic susceptibility in some North Atlantic cores within the IRD belt, and *Grousset*'s correlations for core SU90-08 are shown in Figure 8. *Stoner et al.* [1996] have used multiple magnetic measurements to quantify the magnetic character of IRD in Labrador Sea sediments, and this shows promise as a provenance tracer [see also *Stoner and Andrews*, 1999]. However, although H1, H2, H4, and H5 have strong magnetic susceptibility peaks in core V28-82, they are not entirely coincident with the IRD layers and peaks in deposition rate (Figure 9), so even in the IRD belt more refinement is needed. *Grousset et al.* [1993] showed the contrast between the magnetic susceptibility character of cores within and outside of the IRD belt (Figure 8).

[23] Outside the IRD belt, identification of the Heinrich events is trickier and relies on different types of observations. IRD peaks are found for virtually every cold interval in cores north of the IRD belt [e.g., *Bauman et al.*, 1995; *Fronval et al.*, 1995; *Dokken and Hald*, 1996; *McManus et al.*, 1996; *Rasmussen et al.*, 1997; *Andrews et al.*, 1998; *Elliot et al.*, 1998; *Lackschewitz et al.*, 1998; *Mangerud et al.*, 1998; *Voelker et al.*, 1998; *Dokken and Jansen*, 1999; *van Kreveld et al.*, 2000; *Hald et al.*, 2001; *Knies et al.*, 2001]; however, their provenance is clearly different. The inability to track a single IRD source north of the IRD belt hinders correlations between HS Heinrich events and the numerous IRD peaks documented out of the belt. Furthermore, no estimates of IRD flux, based on constant flux proxies, have been reported outside of the IRD belt.

4.2. Anatomy of Heinrich Layers

[24] On the basis of ^{230}Th$_{excess}$ measurements [e.g., *McManus et al.*, 1998] the high percentage of IRD of Heinrich layers (Figure 1) is attributable to a high IRD flux in four of the six Heinrich layers from the last 60 kyr, namely, H1, H2, H4, and H5 (Figure 9). These big four, HS Heinrich layers (also called cemented marl layers by
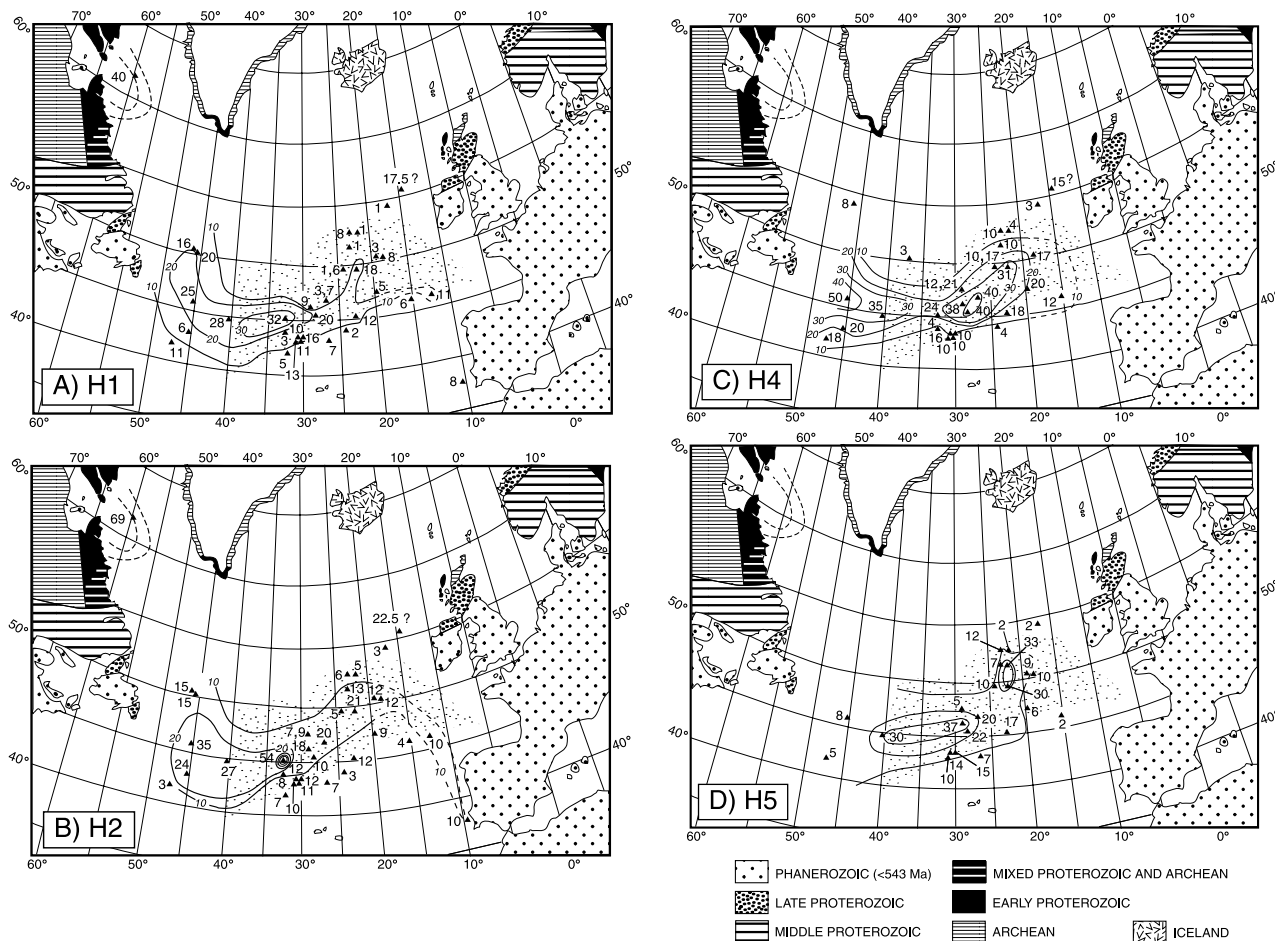
Figure 7. Isopach maps of the Heinrich layers in the North Atlantic: (a) H1, (b) H2, (c) H4, and (d) H5. Contour intervals are 10 cm. Data and data sources are given in Table 1.

Heinrich [1988] and colleagues studying Dreizack seamounts cores) also have large fractions of detrital carbonate [*Bond et al.*, 1992]. Carbonate-bearing Heinrich layers appear to require a series of repeated, anomalous, glacialogical processes within the northern portion of the Laurentide ice sheet. They have razor-sharp bases and thus must have had extremely rapid onsets [*Bond et al.*, 1992; *Broecker et al.*, 1992]. *Bond et al.* [1992] and *Broecker et al.* [1993] made a detailed assessment of H1 and H2 from DSDP core 609. Their results emphasize the decline in numbers of foraminifera during the Heinrich events within the IRD belt and the change in the slope of the ^{14}C age versus depth across these intervals. *Bond et al.* [1992] emphasized that the detrital carbonate peaks do not coincide with the entire cold intervals. Although foraminifera abundance is low in DSDP609, the shells that are found are in good shape in H1, H2, H4, and H5 [*Bond et al.*, 1992], so it does not appear to be a preservation problem. Because the abundance of foraminifera is so low in DSDP609 Heinrich layers, it is difficult to interpret the relative timing of decrease in percent of *Neogloboquadrina pachyderma* (sinistral (s.)). In V23-81 the detrital carbonate maxima occur within coldest part of the record, and except for H6 they are abruptly followed by warming [*Bond et al.*, 1999].

[25] Heinrich layers H3 and H6 are different from the other Heinrich layers. Although H1, H2, H4, and H5 have very high IRD flux in cores within the IRD belt, H3 and H6 show only a modest increase in flux and in the number of lithic grains per gram despite their high percentage of IRD (Figures 1, 9, and 10). *Gwiazda et al.* [1996b] concluded that H3 and H6 were not really ice rafting events but instead were low foraminifera intervals, which would account for the high percentage of IRD. *Bond et al.* [1992] reported evidence for foraminiferal dissolution in H3 from DSDP609. Further study of H6 would be useful, particularly in comparison to H3. H6 has not been studied as much as the others. It is not clear what the reasons are, but possibly it is because it is in a rather difficult time interval for high-quality chronology. Additionally, the IRD abundance appears generally high across much of stage 4, perhaps analogous to the Last Glacial Maximum (LGM) rather than an abrupt event. In any case, more attention needs to be directed at both H3 and H6, especially at H6.

4.2.1. Heinrich Layer H4

[26] Cores can be correlated with particular confidence near Heinrich layer H4 because the event occurred shortly after the Laschamp geomagnetic excursion [*Kissel et al.*, 1999; *Laj et al.*, 2000; *Stoner et al.*, 2000]. Additionally, H4
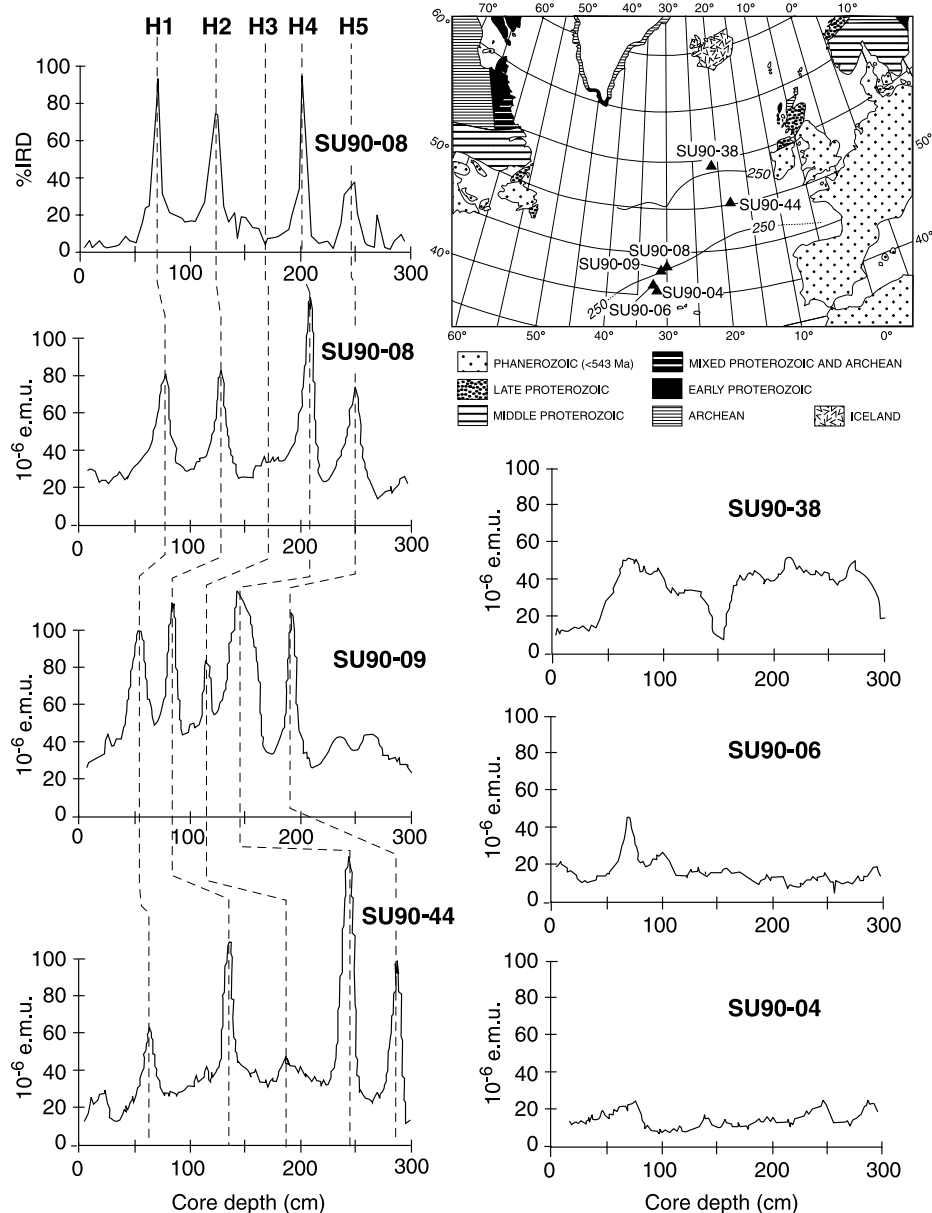
Figure 8. Magnetic susceptibility measurements from North Atlantic cores [*Grousset et al.*, 1993]. (left) Four cores from within the *Ruddiman* [1977] IRD belt. (top right) Map showing the locations of the cores in Figure 8. (right) Three cores from outside the IRD belt. Note that H1, H2, H4, and H5 stand out as prominent spikes in magnetic susceptibility and that H3 and H6 are less prominent or not visible.

is the largest of the six events during the last glacial period. Several studies have focused on H4 [*Cortijo et al.*, 1997; *Vidal et al.*, 1997; *Snoeckx et al.*, 1999; *Elliot et al.*, 2002], so it is possible to examine the geographic pattern of IRD (Figure 11a), $\delta^{18}O$ of surface water (Figure 11b), and Sr and Nd isotopes (Figures 11c and 11d). Radiogenic isotopes including Sr and Nd are discussed more thoroughly in the section on geochemical provenance studies (section 2.2), but two things are clear from these maps. The detritus in Heinrich layers was derived from very ancient sources. Additionally, there are no apparent geographic trends in these radiogenic isotopes, except that the two cores outside the IRD belt have distinctly different compositions. Both surface $\delta^{18}O$ and benthic $\delta^{13}C$ show dramatic decreases

during H4, consistent with a large iceberg-derived freshwater flux and associated retardation of North Atlantic Deep Water (NADW) formation [*Cortijo et al.*, 1997; *Vidal et al.*, 1997; *Elliot et al.*, 2002].

4.2.2. Heinrich Layers in Previous Glacial Stages?

[27] Little published information is available to address the question of whether Heinrich layers occur in previous glacial stages. I have found four tidbits of information pertaining to this question. (1) In ODP core 980 on the Feni Drift, *McManus et al.* [1999; see also *Oppo et al.*, 1998] have shown that millennial-scale variation in IRD persists in glacial intervals for the last 500 kyr, but no indication of provenance or flux is given. (2) *Grousset et al.* [1993] presented a magnetic susceptibility record, interpreted to
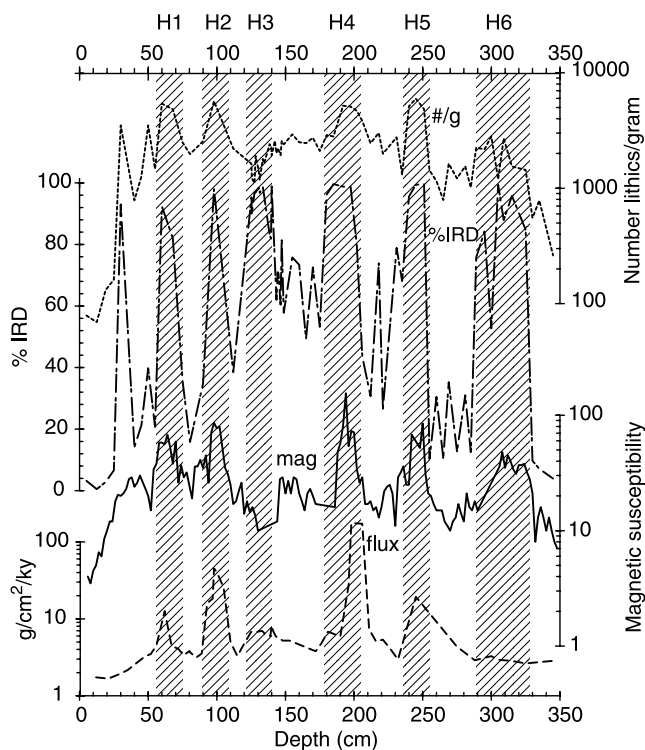
Figure 9. Different measures of IRD in V28-82. Note that the Heinrich intervals defined by number of grains per gram do not appear to be precisely correlated with those defined by percentage of IRD. Additionally, the intervals of high flux measured by ^{230}Th excess are smaller than those defined by counts. The intervals of high magnetic susceptibility are also smaller and appear to be offset from the flux peaks. These records reflect at least four independent samplings of the core, so partly the apparent offsets could be related to that. However, they are too large to be entirely explained in this way. Data sources are percentage of IRD and number of lithic grains per gram [*Gwiazda et al.*, 1996a; *McManus et al.*, 1998; *Hemming et al.*, 1998], flux [*McManus et al.*, 1998], and magnetic susceptibility (G. Downing, unpublished data, 2003).

extend through stage 7, for SU90-08. No large magnetic susceptibility peaks are found outside of the last glacial, HS Heinrich layers. (3) *Van Kreveld et al.* [1996] claim to have found 13 Heinrich layers in stages 7 to 2; however, the IRD layers, other than the four HS Heinrich layers discussed in section 4.2, have very different character, including low detrital carbonate percentage. (4) *Huon and Jantschik* [1993] reported ~1 Ga K/Ar ages for a "cemented marl" layer in each of stages 8 and 12. From the published information it appears that the IRD events in older parts of the record (except the layers from stages 8 and 12 mentioned above) have different sources, or they are not as prominent.

[28] If there were major IRD events in stage 6, their provenance seems to be different. It appears that SU90-08 had a much lower sediment accumulation rate in stage 6 than stages 2−4 [*Grousset et al.*, 1993]. In either case the magnetic susceptibility signal, which is so prominent in the Heinrich layers of the last glacial interval, seems much less pronounced in stage 6. An ongoing survey of cores at

Lamont-Doherty Earth Observatory of Columbia University (G. Downing, unpublished data, 2003) indicates that the prominent magnetic signature of HS Heinrich layers is absent through stage 6. However, *Rasmussen et al.* [2003] have found 12 IRD peaks in a sediment core off the Newfoundland margin, with up to 10% detrital carbonate, through the last 130 kyr (i.e., through H11 at termination 2). More work is needed to characterize the flux and provenance of IRD in this interval, as well as in previous glacial intervals. Although the provenance appears to be different based on magnetic susceptibility [*Grousset et al.*, 1993; G. Downing, unpublished data, 2003) as well as composite feldspar Pb isotope compositions [*Gwiazda et al.*, 1996b], an increased flux of IRD is indicated for termination II [*McManus et al.*, 1998], and each glacial termination appears to be characterized by a prominent IRD event [*McManus et al.*, 1999].

4.3. Detrital Carbonate Contents of the Heinrich Layers

[29] Several observations have led to the conclusion that the elevated detrital carbonate contents of Heinrich layers [e.g., *Bond et al.*, 1992] are derived from a Hudson Strait source [e.g., *Andrews and Tedesco*, 1992]. Paleozoic carbonate deposits occur in many places surrounding the North Atlantic (major locations compiled by *Bond et al.* [1992]); however, the thickness of Heinrich layers increases toward the Canadian margin, and the Hudson Strait and Hudson Bay are floored by Paleozoic carbonate. The thickest deposits of the detrital carbonate occur in the Labrador Sea, just off the Hudson Strait [*Andrews and Tedesco*, 1992]. *Andrews* [1998] credits *Clough* [1978] as the first to identify a series of carbonate facies in northwestern Labrador Sea cores that are now known to correlate with Heinrich events [*Andrews and Tedesco*, 1992; *Bond et al.*, 1992] (see also *Andrews*' [1998] review paper). In an even earlier paper by *Pastouret et al.* [1972] on a study of Newfoundland margin sediments, Heinrich layers are apparent although the authors did not recognize their significance (F. Grousset, personal communication, 2003). A recent paper by *Rasmussen et al.* [2003] further documents the presence of detrital carbonate-rich IRD peaks off Newfoundland, with many more layers than seen in the IRD belt. Figure 12 shows the correlation among Heinrich layers with the various methods that have been used to detect the detrital carbonate contribution. A map of the distribution of cores where detrital carbonate estimations within the Heinrich layers are published is shown in Figure 13. It is clear from this map that a more systematic study of detrital carbonate contents is in order. Cores DSDP609, V23-81, SU90-24 (on a volcanic-free basis), EW93-GGC31, and V28-82 were all counted by G. Bond [*Bond et al.*, 1992, 1999; *Bond and Lotti*, 1995; *Hemming et al.*, 1998], and yet there are some puzzling features of the pattern. Core V28-82 is in the heart of the thickest Heinrich layer deposits, whereas nearby DSDP609 shows uniformly thinner layers (Table 1 and Figure 7). Additionally, V28-82 shows much more pronounced magnetic susceptibility maxima than DSDP609 (G. Downing, unpublished data, 2003). Thus
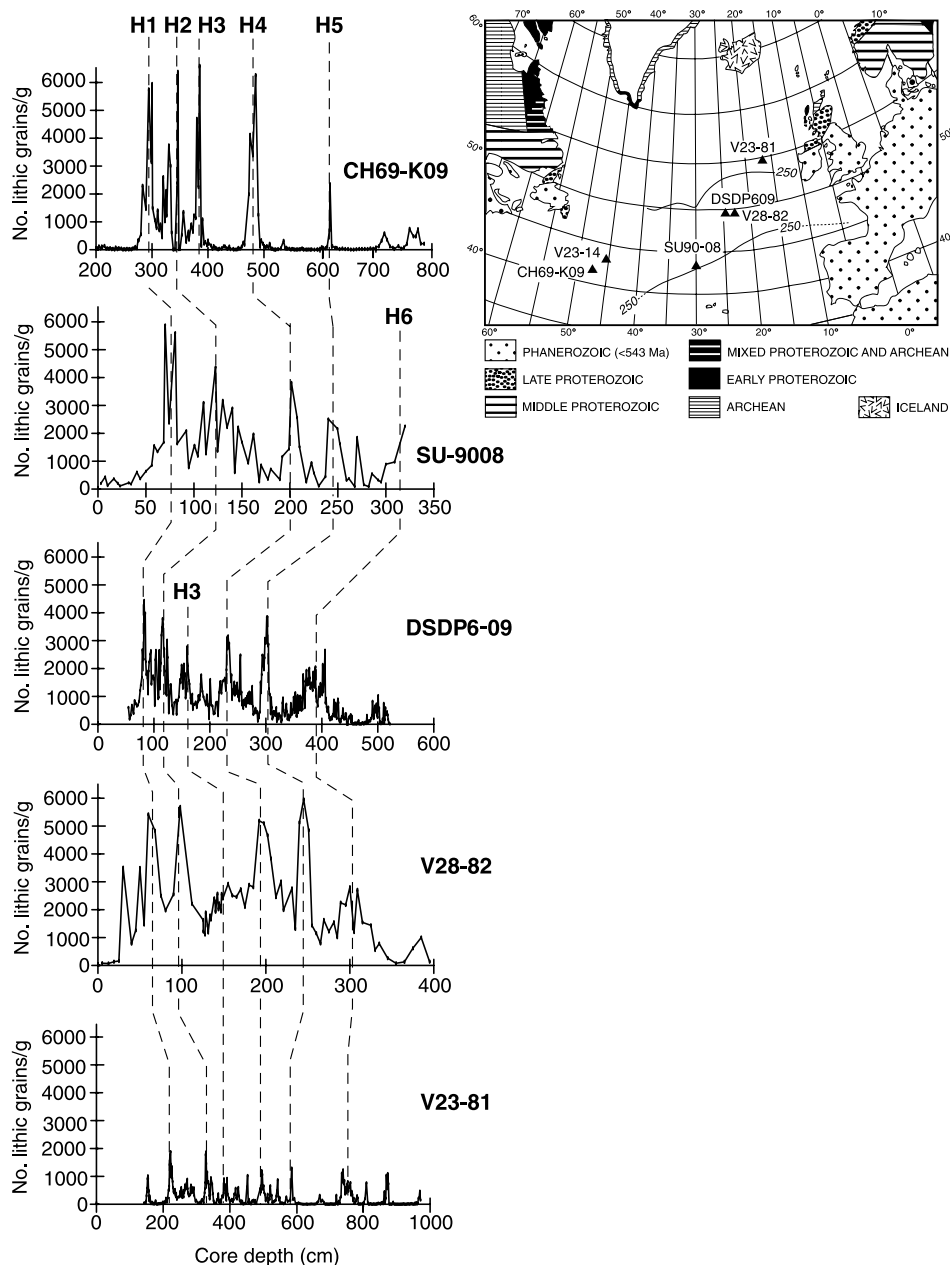
Figure 10. Number of lithic grains per gram in the >150 μm fraction from North Atlantic cores. Note all *y* axes have the same range. Map shows the locations of cores. Data sources are CH69-K09 [*Labeyrie et al.*, 1999], SU90-08 [*Grousset et al.*, 1993], DSDP609 [*Bond et al.*, 1999], V28-82 [*Gwiazda et al.*, 1996a; *McManus et al.*, 1998; *Hemming et al.*, 1998], and V23-81 [*Bond et al.*, 1999].

the Heinrich layers from V28-82 should record a more pure Heinrich signal. However, the detrital carbonate contents at the maximum IRD peaks in V28-82 are approximately half those in DSDP609. An additional complication is that Heinrich events near the Hudson Strait are quite different than they are in the open ocean, as discussed in section 4.5.

[30] The dolomite component of some detrital carbonate layers has also been used to detect Heinrich layers H1, H2, H4, and H5 [e.g., *Andrews and Tedesco*, 1992]. To identify the dolomite, *Francois and Bacon* [1994] measured Mg/Ca ratios of 6N-HCl-leachable fraction, and *Thomson et al.* [1995] measured the Mg/Al ratio of totally dissolved sediment (Figure 12). Stoichiometric dolomite has molar

Mg/Ca of 1, so highest Mg/Ca ratios occur where contemporaneous biogenic carbonate contents are low and dolomite is a significant part of the detrital carbonate. Although Ca is a large part of the detrital carbonate, it also occurs in the biogenic fraction, so the Mg/Al is a proxy for the carbonate/silicate in the detrital fraction.

4.4. Geochemical Provenance

[31] The provenance of Heinrich layers H1, H2, H4, and H5 within the IRD belt is very distinctive and hence can be mapped by any number of geochemical measurements (as well as magnetic susceptibility and detrital carbonate content as reviewed in sections 4.1 and 4.3). In particular,
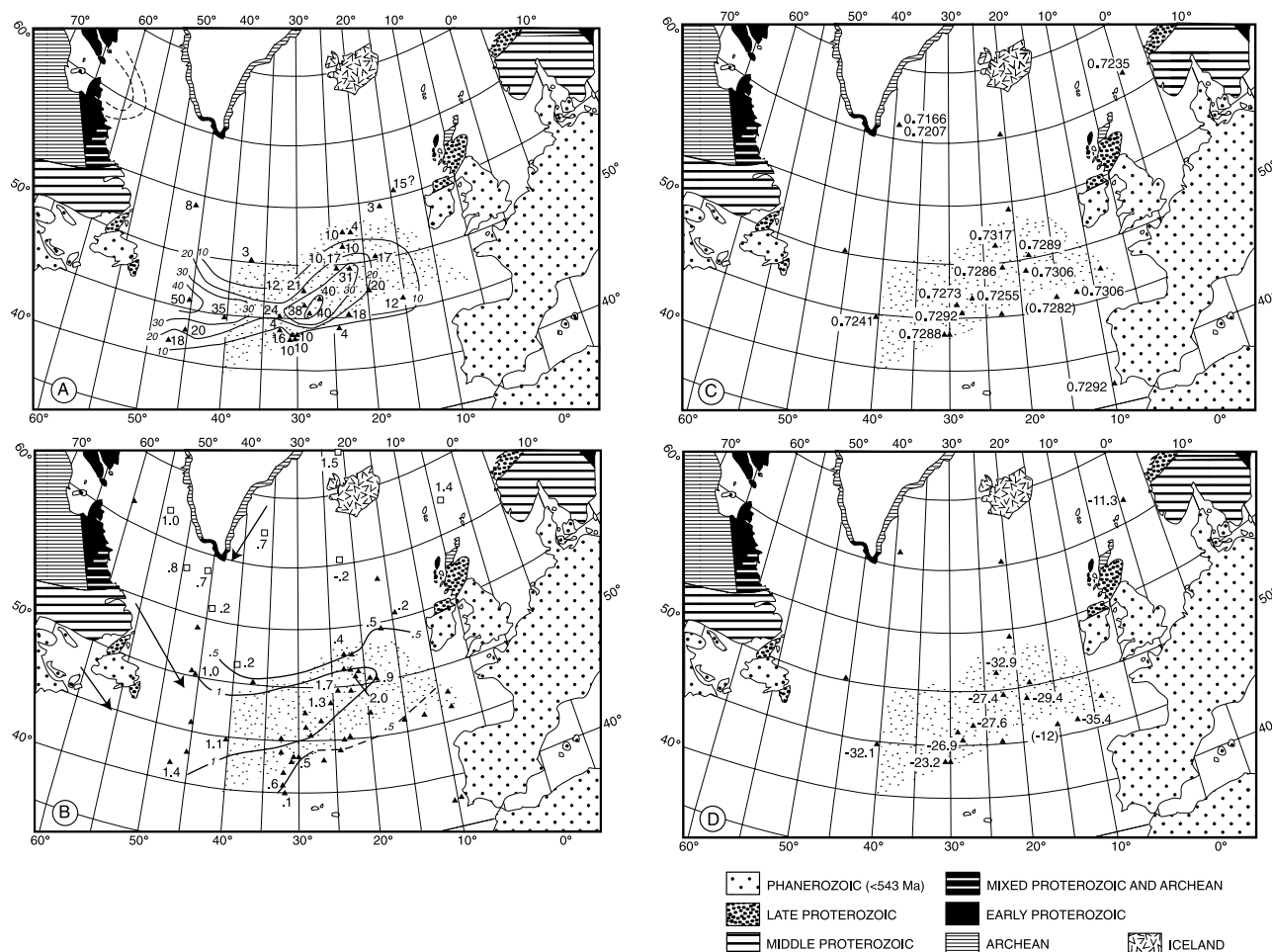
Figure 11. Maps of Heinrich layer H4. The stippled area is the region with greater than 250 mg cm^{-2} kyr^{-1} sediment flux between 25 and 13 kyr [*Ruddiman*, 1977]. (a) Isopach with 10 cm contour intervals (from Figure 7). (b) Map of difference between δ^{18}O before and during H4. Data are from *Cortijo et al.* [1997]. (c) The ^{87}Sr/^{86}Sr composition of the terrigenous fraction within H4. Data are from *Snoeckx et al.* [1999], *Hemming et al.* [1998], *Grousset et al.* [1993, 2001], and *Revel et al.* [1996]. (d) The ε_{Nd} composition of the terrigenous fraction within H4. Data are from *Snoeckx et al.* [1999], *Hemming et al.* [1998], *Grousset et al.* [1993, 2001], and *Revel et al.* [1996].

studies to date have examined Heinrich layer provenance using K/Ar, Nd, Sr, and Pb isotopic techniques as well as organic geochemical measures. Refer to section 2.2 for a brief overview of geochemical provenance approaches.

4.4.1. K/Ar Ages

[32] The first geochemical provenance measurement of the Heinrich layers was the K/Ar apparent age of the fine fractions <2 μm and 2–16 μm [*Jantschik and Huon*, 1992]. Ambient North Atlantic sediments have apparent K/Ar ages of approximately 400 Ma [*Hurley et al.*, 1963; *Huon and Ruch*, 1992; *Jantschik and Huon*, 1992], whereas the sediments from Heinrich layers H1, H2, H4, and H5 yielded apparent ages of approximately 1 Ga (Figure 14). Variation in the K concentration is small, and thus the K/Ar age signal is a product of the radiogenic ^{40}Ar* concentration [*Hemming et al.*, 2002]. *Hemming et al.* [2002] showed that the ^{40}Ar* is quite uniform in eastern North Atlantic cores (Figure 14) and that the K/Ar age and ^{40}Ar/^{39}Ar spectra of <2 μm terrigenous sediment from Heinrich layer H2 in the eastern North Atlantic and from Orphan Knoll (southern Labrador Sea/

western Atlantic) are indistinguishable (Figure 15). Taken together these results imply the entire fine fraction of Heinrich layer H2 was derived from sources bordering the Labrador Sea, presumably the Hudson Strait. The same pattern most likely characterizes H1, H4, and H5, because their K/Ar ages and ^{40}Ar* concentrations are similar to H2 in eastern North Atlantic cores.

4.4.2. Nd-Sr-Pb Isotope Composition of Terrigenous Sediments

[33] *Grousset et al.* [1993] reported Nd and Sr isotope compositions of Heinrich layers from core SU90-08 (Figures 1 and 2). Although the Sr isotope composition is not particularly diagnostic, the Nd isotope composition is consistent with derivation from a source with Archean heritage, and *Grousset et al.* [1993] suggested sources surrounding the Labrador Sea or Baffin Bay (Figure 16). Nd and Sr isotope compositions for various grain size fractions from North Atlantic sediments suggest that the total terrigenous sediment load within these Heinrich layers in the IRD belt may derive from the same limited range of
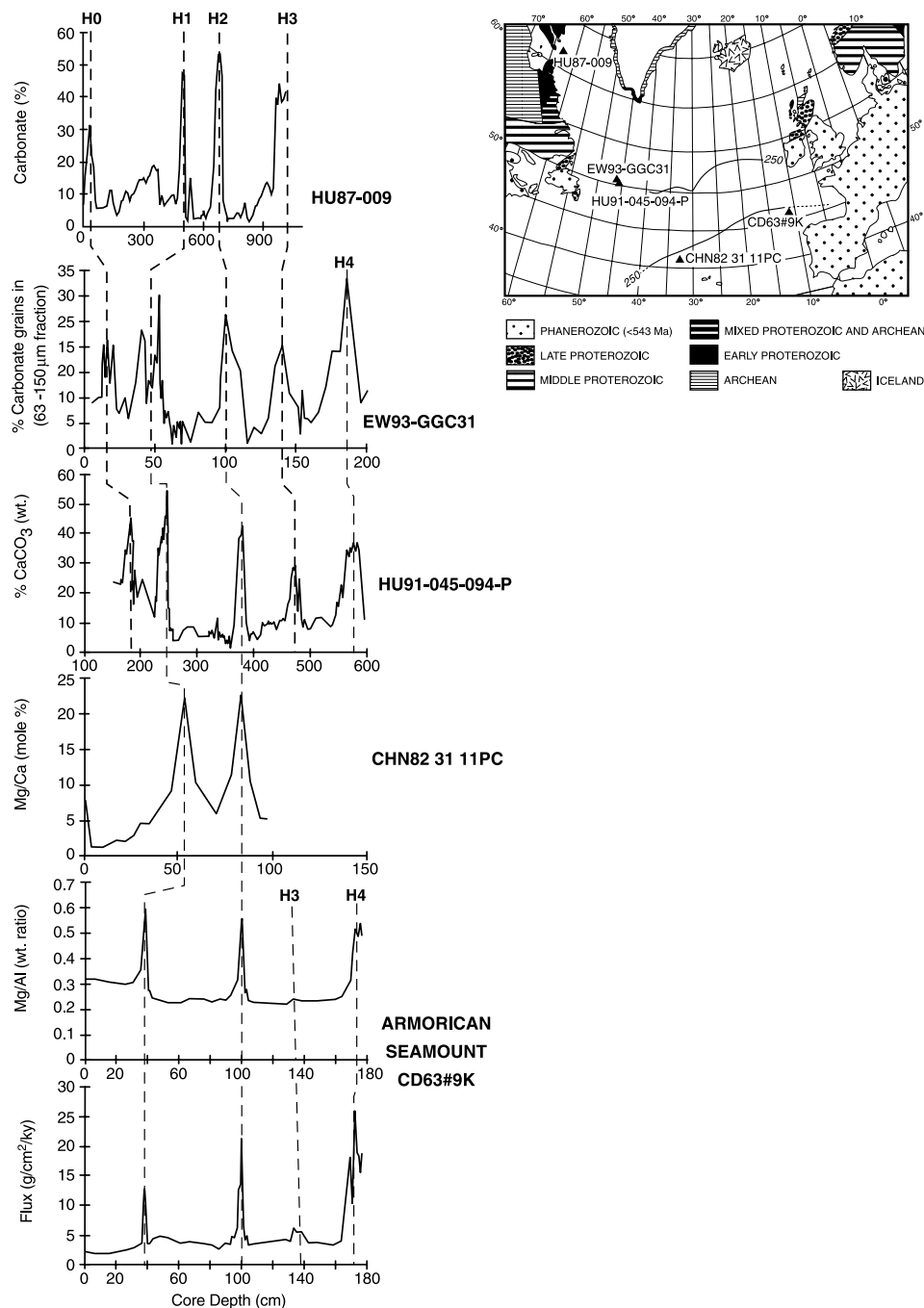
Figure 12. Different measures of detrital carbonate that have been used in Labrador Sea and North Atlantic sediment cores. Data sources are HU87-009 [*Andrews et al.*, 1994b], HU91-045-094-P (wt % CaCO$_3$ [*Hillaire-Marcel et al.*, 1994]), EW93-GGC31 (percentage of carbonate grains in 63–150 μm fraction [*Bond and Lotti*, 1995]), CHN82 31 11PC (Mg/Ca weight fraction [*Francois and Bacon*, 1994]), and CD63#9K (Mg/Al weight fraction [*Thomson et al.*, 1995]). Also shown for reference is the estimated sediment flux from CD63#9K based on excess ^{230}Th [*Thomson et al.*, 1995].

sources [*Revel et al.*, 1996; *Hemming et al.*, 1998; *Snoeckx et al.*, 1999; *Grousset et al.*, 2000, 2001]. The University of Colorado group has extensively characterized the composition of potential source areas in the vicinity of the Hudson Strait as well as Baffin Bay [*Barber*, 2001; *Farmer et al.*, 2003] and other regions along the western Labrador coast and the Gulf of St. Lawrence [*Farmer et al.*, 2003]. Their data are consistent with the interpretation

of a Hudson Strait provenance for Heinrich layers H1, H2, H4, and H5 and demonstrate an absence of substantial southeastern Laurentide ice sheet sources within pure Heinrich intervals.

[34] The Pb isotope composition of the fine terrigenous fraction of Heinrich layers is also distinctive [*Hemming et al.*, 1998] and consistent with derivation from the Hudson Strait region [*Barber*, 2001]. New results from *Farmer et al.*
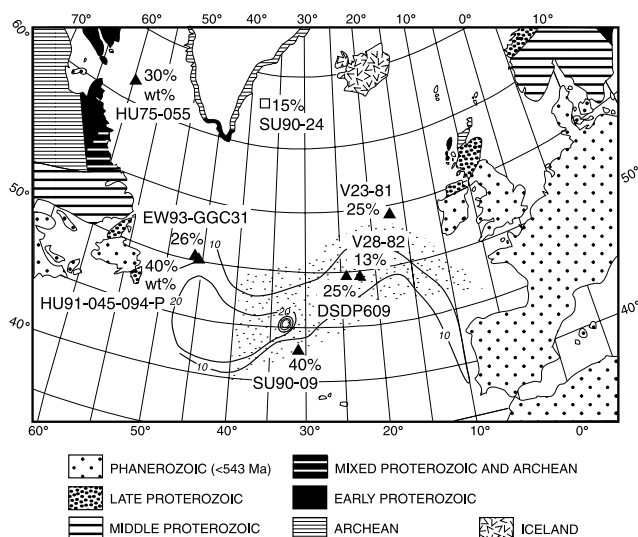
Figure 13. Locations of cores where detrital carbonate contents have been estimated for H2. Isopach for H2 and stippled area representing *Ruddiman*'s [1977] IRD belt are shown for reference. Data sources are HU75-055 (wt % CaCO$_3$ [*Andrews et al.*, 1994b]), HU91-045-094-P (wt % CaCO$_3$ [*Hillaire-Marcel et al.*, 1994]), EW93-GGC31 (percentage of carbonate grains in 63–150 μm fraction [*Bond and Lotti*, 1995]), SU90-09 (percentage of carbonate grains in >150 μm fraction [*Grousset et al.*, 2001]), DSDP609 (percentage of carbonate grains in 63–150 μm fraction [*Bond et al.*, 1992, 1999]), V28-82 (percentage of carbonate grains in >150 μm fraction [*Hemming et al.*, 1998]), SU90-24 (percentage of carbonate grains in 63–150 μm fraction on a nonvolcanic basis [*Bond et al.*, 1999]).

[2003] may allow further distinction of fine-grained sediment sources with Pb isotopes.

4.4.3. Isotopic and Geochronologic Measurements on Individual Grains

[35] In addition to the bulk geochemical methods several studies have examined individual grains or composite samples of feldspar grains for their Pb isotope compositions [*Gwiazda et al.*, 1996a, 1996b; *Hemming et al.*, 1998] or individual grains of hornblende for their ^{40}Ar/^{39}Ar ages [*Gwiazda et al.*, 1996c; *Hemming et al.*, 1998, 2000a; *Hemming and Hajdas*, 2003]. These studies provide remarkable insights into the geologic history of Heinrich layers that allow further refinement of the interpretations based on bulk isotopic analyses. Feldspars have high Pb abundance and very low U and Th abundance, and thus the Pb isotope composition of feldspar approximates the initial Pb isotope composition of its source [e.g., *Hemming et al.*, 1994, 1996, 2000b]. Pb isotope data from Heinrich layer H1, H2, H4, H5 feldspar grains form a linear trend that indicates an Archean (∼2.7 Ga) heritage and a Paleoproterozoic (∼1.8 Ga) metamorphic event (Figure 17b). Heinrich layer grains are similar in composition to H2 from Hudson Strait proximal core HU87-009 and to feldspar grains from Baffin Island till. However, they are distinctly different from feldspar grains from Gulf of St. Lawrence core V17-203 where Appalachian (Paleo-

zoic) and Grenville (∼1 Ga) sources are found. The ^{40}Ar/^{39}Ar ages of individual hornblende grains from Heinrich layers H1, H2, H4, and H5 cluster around the implied Paleoproterozoic metamorphic events from the feldspar Pb isotope data [*Gwiazda et al.*, 1996c; *Hemming et al.*, 1998, 2000a; *Hemming and Hajdas*, 2003] and are consistent with hornblende grains from Baffin Island tills [*Hemming et al.*, 2000b].

4.4.4. Organic Carbon Compounds

[36] Organic compounds are important provenance tools because they emphasize sedimentary contributions to IRD, and they are sufficiently diverse in different sedimentary basins with different sedimentary and diagenetic conditions that they may prove to be very sensitive monitors of provenance components. Several studies have examined organic carbon compounds through Heinrich intervals [*Madureira et al.*, 1997; *Rosell-Melé et al.*, 1997; *Huon et al.*, 2002] and have found evidence that a large fraction of terrestrial organic carbon contributed to the layers. *Madureira et al.* [1997] found enhanced concentrations of total terrigenous lipids during glacial intervals, which they attributed to a combination of eolian and IRD sources. Heinrich events H1, H2, H4, and H5 have low concentrations of organic carbon and terrigenous lipids [*Madureira et al.*, 1997; *Huon et al.*, 2002]; however, they have very high terrigenous flux [e.g., *Francois and Bacon*, 1994; *Thomson et al.*, 1995; *McManus et al.*, 1998], and the carbon is almost exclusively from terrestrial sources [*Huon et al.*, 2002]. *Rosell-Melé et al.* [1997] found vanadyl porphyrins and carotenoid-derived aromatic hydrocarbon compounds within Heinrich layers and found specific compounds that originated from green sulphur bacteria that must have been derived from an ancient sedimentary source that was deposited in anoxic conditions. A survey of potential source areas has found one sample from the Hudson Strait region with appropriate compositions to match Rosell-Melé's results (J. Sachs, personal communication, 2000). A. Rosell-Melé (personal communication, 2002) is also in the process of surveying potential source areas around the North Atlantic region.

4.4.5. Geologic History of Heinrich Layers' Source

[37] The data that have been collected on Heinrich layer provenance reveal a remarkably complete story of the geological history of the Heinrich layers' source (Table 2). The entire spectrum of provenance observations is consistent with derivation from near the Hudson Strait.

4.4.6. Contrasting Provenance of H3 and H6

[38] Events H3 and H6 do not appear to be derived from the same sources as H1, H2, H4, and H5 (Figures 17c and 18). Using Pb isotope compositions of composite feldspar samples, *Gwiazda et al.* [1996b] found that H3 and H6 resemble ambient sediment in V28-82, suggesting a large contribution from European sources, which agrees with the conclusion of *Grousset et al.* [1993]. Pb isotope data from composites of 75 to 300 grains from *Gwiazda et al.* [1996b] are shown in Figure 17c. As mentioned in section 4.4.6, H3 and H6 seem to be low-foraminifera intervals rather than ice-rafting events. These conclusions
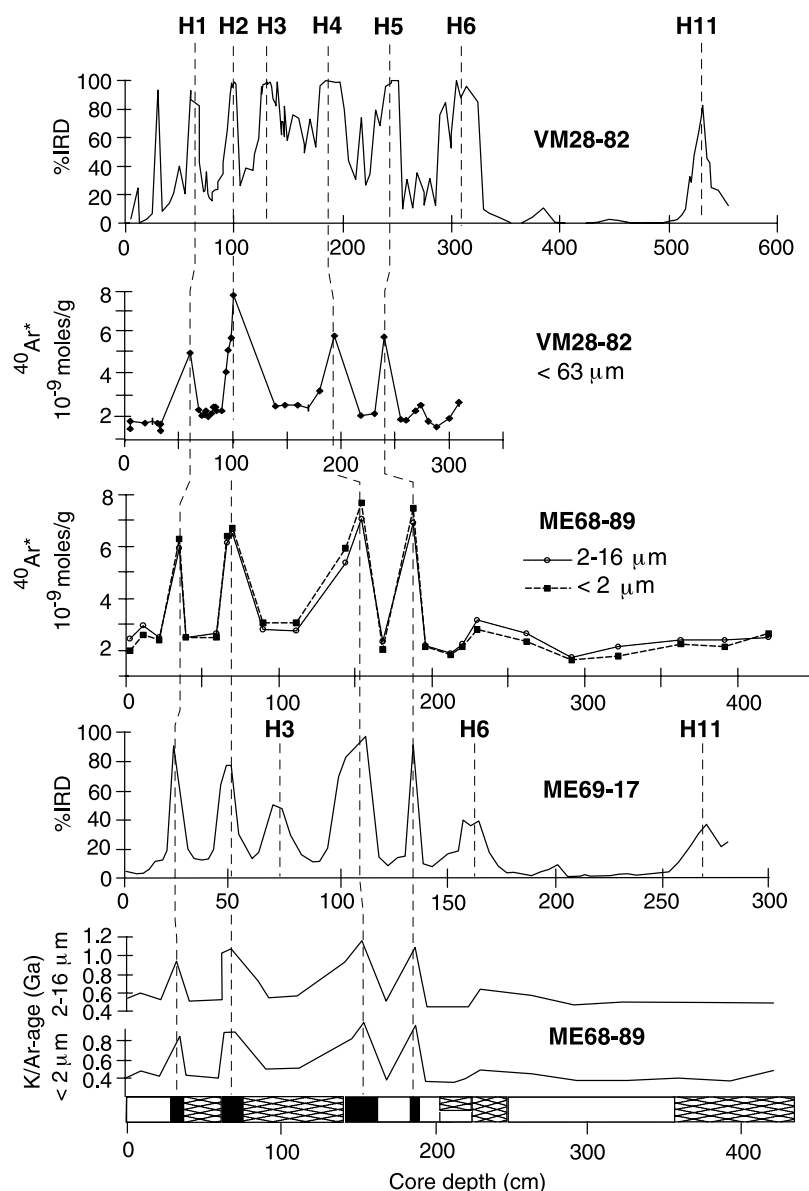
Figure 14. Ice-rafted detritus data from V28-82 [*Gwiazda et al.*, 1996a; *McManus et al.*, 1998; *Hemming et al.*, 1998] and ME69-17 [*Heinrich*, 1988] and K/Ar ages of the <2 and 2–16 μm fractions from Dreizack seamount core ME68-89 [*Jantschik and Huon*, 1992]. Also shown are the ^{40}Ar* (radiogenic Ar) concentrations from the same samples from ME68-89 [*Jantschik and Huon*, 1992] and from the <63 μm (decarbonated) fraction from V28-82 [*Hemming et al.*, 2002]. Reprinted from *Hemming et al.* [2002] with permission from Elsevier.

are consistent with other observations around the North Atlantic. Although Heinrich layer H3 appears to be a Hudson Strait event [*Grousset et al.*, 1993; *Bond and Lotti*, 1995; *Rashid et al.*, 2003a; S. R. Hemming, unpublished Pb isotope and ^{40}Ar/^{39}Ar hornblende data from Orphan Knoll, 2003], it does not spread Hudson Strait-derived IRD as far to the east as the other Heinrich events [*Grousset et al.*, 1993] (Figure 19). *Rasmussen et al.* [2003] report detrital carbonate peaks at approximately the times of both H3 and H6, as well as many other additional peaks, in a core from the Newfoundland margin. Additionally, *Kirby and Andrews* [1999] proposed that H3 (and the Younger Dryas) represent across-Strait (also modeled by *Pfeffer et al.* [1997]) rather than along-Strait flow as inferred for the larger events. The

map pattern of Sr isotope data from H3 shows a striking pattern of decrease in ^{87}Sr/^{86}Sr nearly perpendicular to the IRD belt (Figure 19b), consistent with a mixture of sediments from the Labrador Sea icebergs with those derived from icebergs from eastern Greenland, Iceland, and Europe. H6 has not been studied, but the organic composition of H3 does not stand out prominently in the studies mentioned above [*Madureira et al.*, 1997; *Rosell-Melé et al.*, 1997; *Huon et al.*, 2002].

### 4.4.7. Summary of Geochemical Provenance Analysis of Heinrich Layers

[39] Heinrich layers H1, H2, H4, and H5 have several distinctive characteristics that distinguish them from ambient IRD, and they are derived from a mix of provenance
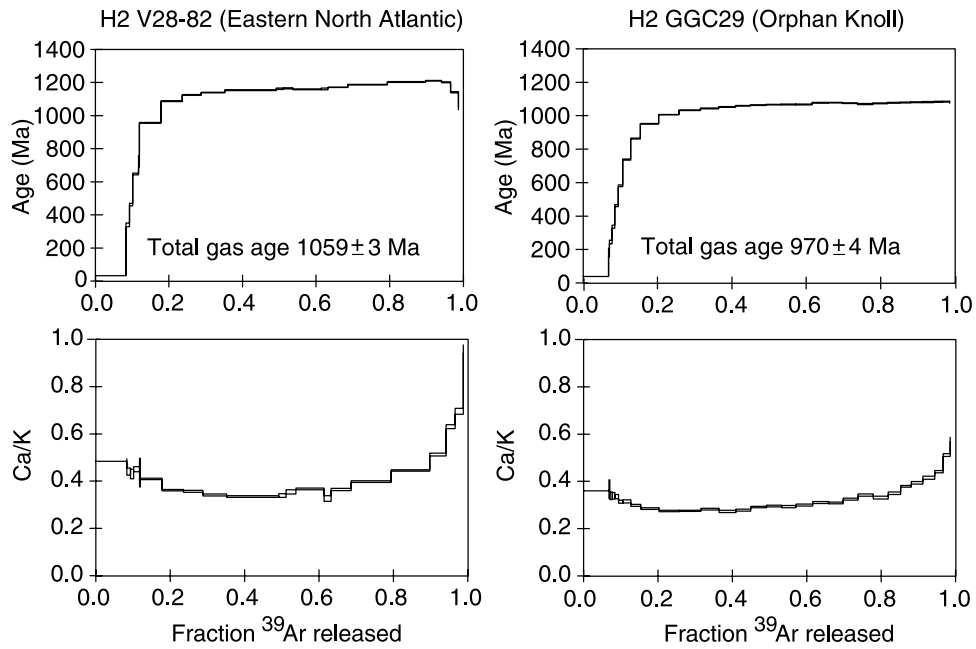
Figure 15. Comparison of $^{40}Ar/^{39}Ar$ laser step-heated spectra from Heinrich layer H2 from V28-82 and from Orphan Knoll core EW93-GGC29. Note that both the total gas age and the Ca/K systematics are very similar and consistent with a dominant (solely?) Labrador Sea source for H2 at V28-82. Data are from *Hemming et al.* [2002].

components that are all consistent with derivation from a small region near Hudson Strait. Heinrich layers H3 and H6 have different sources, at least in the eastern North Atlantic. These events appear to have a Hudson Strait source in the southern Labrador Sea and western Atlantic, consistent with a similar but weaker event compared to the big four. Important related questions are as follows: How many types (provenance, flux, etc.) of Heinrich layers are there? Are
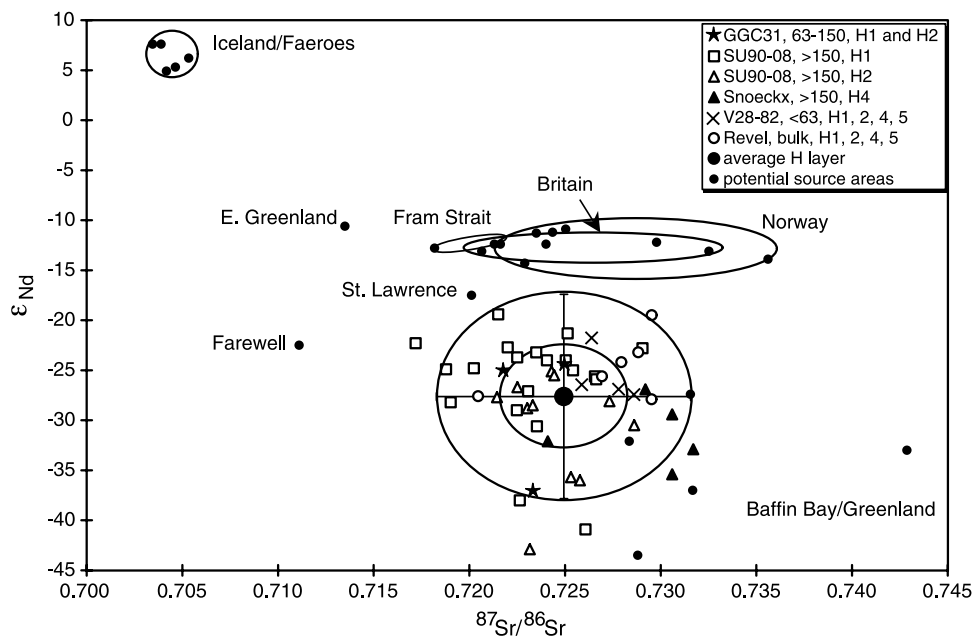
Figure 16. Nd-Sr isotope compositions of terrigneous clastic components of Heinrich layers H1, H2, H4, and H5. Shown for reference are the average and 1- and 2-sigma range for the data published on these Heinrich layers and reported compositions of potential source areas of ice-rafted detritus [*Grousset et al.*, 2001, and references therein]. Note that the data are from different size fractions in different publications, but there is not evidence that there is a substantial bias even in the $^{87}Sr/^{86}Sr$ where one might be expected. This is most likely due to the large fraction of glacial flour with approximately the same composition in the fine as the coarse fraction.
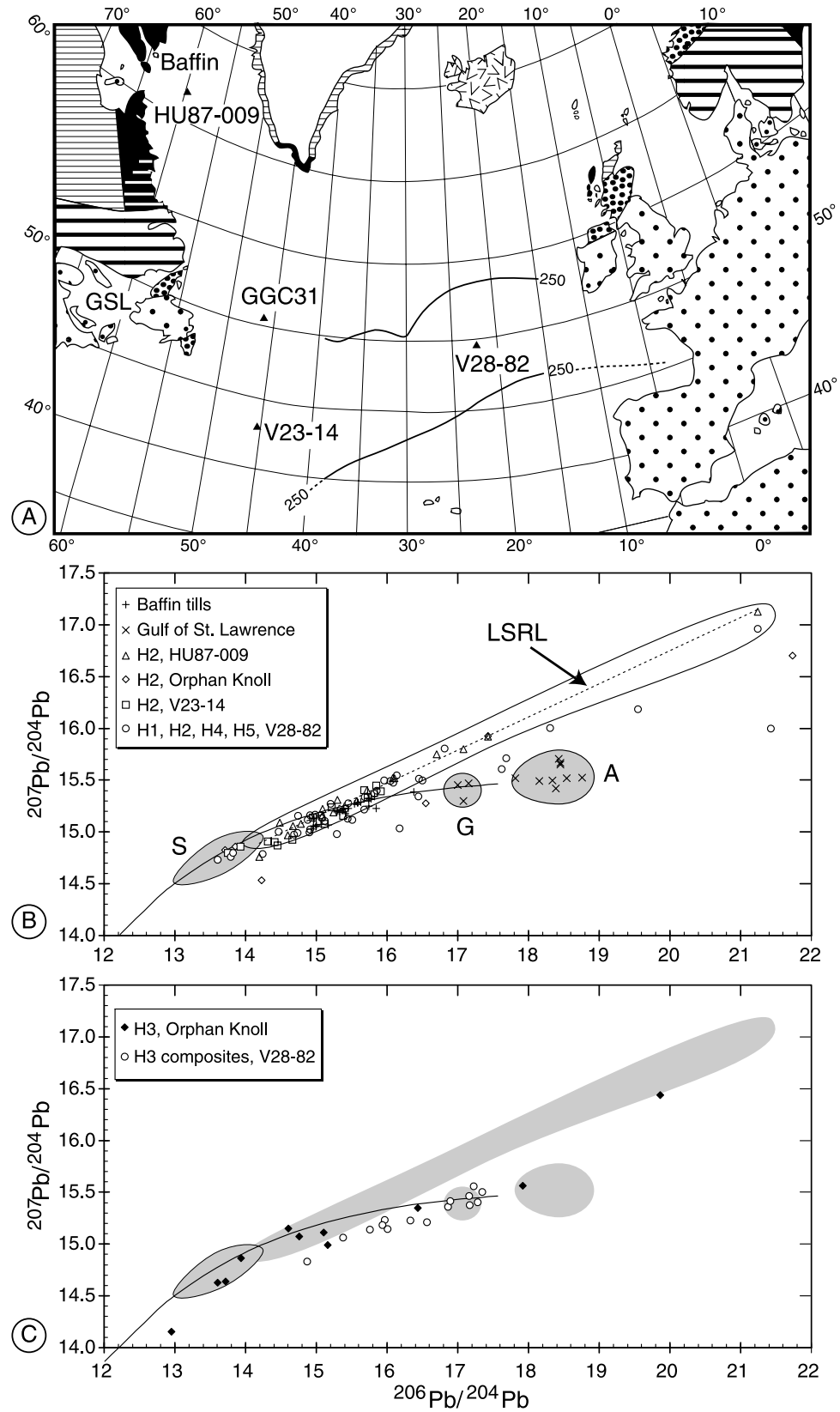
Figure 17

TABLE 2.   Geologic History of Heinrich Layers' Source

Provenance Character	Evidence
Archean heritage	Nd isotopes of bulk sediments and Pb isotopes in feldspar grains
Paleoproterozoic orogeny	Pb isotopes in feldspar grains and ^{40}Ar/^{39}Ar hornblende ages of hornblende grains
Paleozoic sedimentary cover	detrital carbonate, K/Ar, and Rb/Sr ages of fine fraction, ^{40}Ar/^{39}Ar ages of pelitic fragments, chemical (inorganic and organic), and mineralogical composition

IRD events in previous glacial intervals akin to the six in the last glacial period?

4.5. "Precursor Events" and the Placement of Heinrich Events in D-O Cycles

[40] *Bond and Lotti* [1995] showed that in addition to the variation of detrital carbonate, other petrological changes could be quantified in the IRD fraction. Specifically, percentages of fresh basaltic glass and hematite-stained grains, counted at high resolution in several North Atlantic cores, vary on a 1 to 2 kyr interval [*Bond et al.*, 1999]. The pacing of petrological changes in IRD appears to be similar to that of δ^{18}O changes in Greenland ice [*Bond and Lotti*, 1995; *Bond et al.*, 1997, 1999]. *Bond and Lotti* [1995] showed that Icelandic glass and hematite-stained grains peak within the broad lithic peaks that encompass Heinrich layers and that they precede the detrital carbonate peaks for Heinrich layers H1, H2, H3, and H4 in cores DSDP609 and V23-81 [see also *Bond et al.*, 1999].

[41] *Grousset et al.* [2001] showed a series of provenance changes consistent with these observations. They found that during Heinrich layers H1 and H2, there appear to be sequential increases in volcanic grains, quartz grains, and carbonate grains at core SU90-09 in the south central part of the IRD belt. This observation of a precursor of increased concentration of lithic grains with a non-Hudson Strait source suggested that the Laurentide ice sheet was not always responding to the same climate forcing as the D-O cycles or was doing so later than other ice sheets.

[42] *Grousset et al.* [2000] showed that the Nd and Sr isotope composition of the coarse IRD fraction from core MD95-2002 in the Bay of Biscay recorded values close to the end-member composition of Labrador sources during the peak of Heinrich events but showed much different compositions in the precursory interval. The compositions of Sr and Nd measured in the precursory interval of this core and core SU90-09 are similar to those documented from European sources [*Grousset et al.*, 2000], although they are also similar to values that would be expected from the southeastern Laurentide ice sheet [*Farmer et al.*, 2003].

Furthermore, *Vance and Archer* [2002] have found that the provenance of precursory intervals to H4 and H2 are not similar based on radiogenic isotope studies of DSDP609 sediments. It will be important to find a combination of tracers that allows distinction between Gulf of St. Lawrence and European sources. Perhaps tracing the geographic pattern of distribution of the precursory tracers will yield the answer. The provenance of the precursor intervals may become clearer with studies close to glaciated margins [e.g., *Darby and Bischof*, 1996; *Bischof and Darby*, 1999; *Grousset et al.*, 2001; *Hemming et al.*, 2000b, 2002; *Hemming and Hajdas*, 2003; *Farmer et al.*, 2003].

[43] *Scourse et al.* [2000] documented the presence of H1 and H2 based on magnetic susceptibility and dolomite concentrations in cores from the southwest of the British Isles. The magnetic susceptibility signal is similar to that found in the IRD belt, but the dolomite concentrations of ∼20% are anomalously high for Heinrich layers and may be derived from more than one source (this may also be a counting artifact, and "dolomite" is really Paleozoic carbonate including both limestone and dolostone (I. N. McCave, personal communication, 2002)). *Scourse et al.* [2000] reported an increase in Celtic shelf detritus, characterized by up to 3% Campanian chalk and 8% mica, prior to the H2 event; however, they do not see a similar pattern prior to the H1 event. While it is conceivable that there is a cause and effect relation between the British ice sheet and Heinrich events, given the proximity to Britain and the absence of the source before the H1 event, more data would be required if a convincing case is to be made.

[44] One view of precursors is that they are simply the IRD signals of D-O cool phases in the North Atlantic [*Bond et al.*, 1999; G. Bond, personal communication, 2002], and their occurrence before the Hudson Strait-derived detritus means that the sea surface cooled prior to the input of Heinrich layers. Icelandic glass is an important component of the Iceland Sea [*Voelker et al.*, 1998] and Irminger Basin [*Elliot et al.*, 1998; *van Kreveld et al.*, 2000], and East Greenland may be a significant source of hematite-stained grains [*Bond et al.*, 1999; *van Kreveld et al.*, 2000]. Several

Figure 17.   Pb isotopes in feldspar grains from Heinrich layers. (a) Map showing locations of cores analyzed with geology and IRD belt for reference. (b) Data from Heinrich layers H1, H2, H4, and H5 from several North Atlantic and Labrador Sea cores. Also shown are data from Gulf of St. Lawrence core V17-203 (S. R. Hemming, unpublished data, 2003) and from Baffin Island tills [*Hemming et al.*, 2000b]. Reference fields are Superior province (S) [*Gariépy and Allègre*, 1985], Labrador Sea reference line (LSRL) [*Gwiazda et al.*, 1996a]), Grenville (G) [*DeWolf and Mezger*, 1994] and Appalachian (A) [*Ayuso and Bevier*, 1991]. Data sources are H2 from HU87-009, V23-14, and V28-82 [*Gwiazda et al.*, 1996a], Orphan Knoll core GGC31 (S. R. Hemming, unpublished, 2003), and H1, H4, and H5 from V28-82 [*Hemming et al.*, 1998]. (c) Data from Heinrich layer H3 with reference fields from Figure 17b. Data sources are H3 from V28-82 [*Gwiazda et al.*, 1996b] and H3 from Orphan Knoll core GGC31 (S. R. Hemming, unpublished data, 2003).
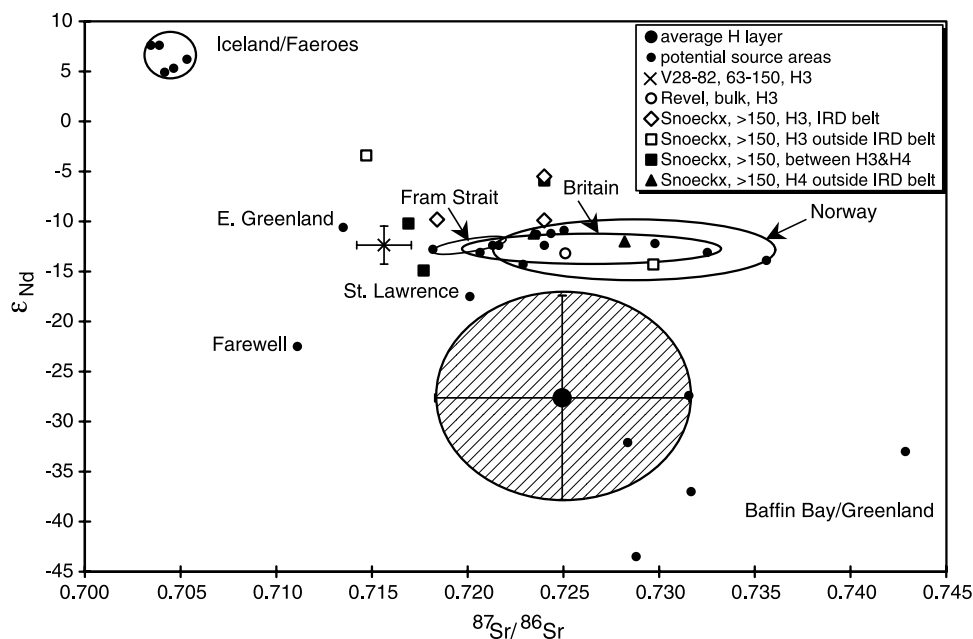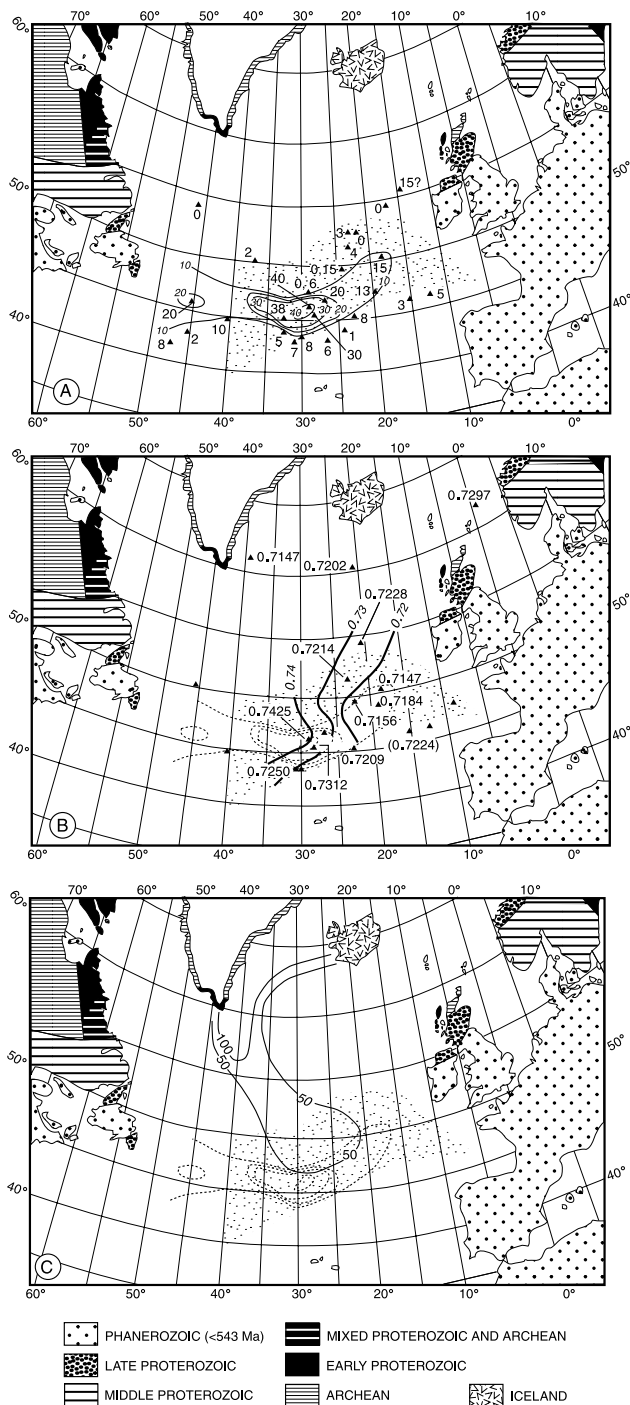
Figure 18. Nd-Sr isotope compositions of terrigneous clastic components of Heinrich layer H3. Shown for reference are the average and 2-sigma range for the data published on Heinrich layers H1, H2, H4, and H5 and reported compositions of potential source areas of ice-rafted detritus [*Grousset et al.*, 2001, and references therein]. Data sources are *Grousset et al.* [1993], *Revel et al.* [1996] and *Snoeckx et al.* [1999]. Also included is the average of five unpublished analyses across H3 from V28-82, where the error bars represent the range of values measured (A. Jost and S. Hemming, unpublished data, 1999).

studies have reported IRD contents at high resolution in the Nordic Seas and North Atlantic sites north of the IRD belt, and in these locations the IRD contents and other indicators of climate change appear to closely follow the pattern of $\delta^{18}O$ change in Greenland ice [*Bauman et al.*, 1995; *Fronval et al.*, 1995; *Dokken and Hald*, 1996; *McManus et al.*, 1996; *Rasmussen et al.*, 1997; *Andrews et al.*, 1998; *Elliot et al.*, 1998; *Lackschewitz et al.*, 1998; *Mangerud et al.*, 1998; *Voelker et al.*, 1998; *Dokken and Jansen*, 1999; *van Kreveld et al.*, 2000; *Hald et al.*, 2001; *Knies et al.*, 2001].

[45] Although there is contention about whether Heinrich layers have correlatives in the Nordic Seas (e.g., *Fronval et al.* [1995] and *Elliot et al.* [2002] versus *Dowdeswell et al.* [1999]), it is clear that the pattern is different. In the IRD belt, Heinrich layers are outstanding IRD events, while events in between are modest, although apparently correlative with Greenland cooling events [*Bond et al.*, 1993, 1999; *Bond and Lotti*, 1995]. In contrast, there is apparently an IRD event of equal magnitude for each of the Greenland cooling events, although there is a larger flux in general during the Last Glacial Maximum. This Greenland pattern also appears in the Barra Fan record of British glacial activity [*Knutz et al.*, 2001]. However, *Darby et al.* [2002] report evidence for four Arctic iceberg export events through Fram Strait, approximately coincident with Heinrich events H1–H4. They consider the Arctic export events to precede Hudson Strait IRD, although both are not found in the core, so the interpreted lead is subject to the vagaries of dating uncertainties.

[46] The key precursory events to Heinrich events may be preserved in Labrador Sea sediment. The recognition that the carbonate-rich intervals in the Labrador Sea are approximately synchronous with Heinrich events [*Andrews and Tedesco*, 1992; *Bond et al.*, 1992] helped to explain the origin of the Heinrich ice armadas [e.g., *MacAyeal*, 1993] as well as to emphasize the importance of studies proximal to large glacial-marine outlets. A large fraction of the sediment deposited near the Hudson Strait is brought by meltwater not icebergs as is the case in the open ocean. *Hesse and Khodabakhsh* [1998] showed that the carbonate-rich layers near the mouth of Hudson Strait differ in sedimentological character from the Heinrich layers in the open ocean and, in particular, are much finer grained. They described a series of facies: nepheloid layer deposits (or type I Heinrich layers), mud turbidites (or type II Heinrich layers), laminae of IRD (or type III Heinrich layers), and fine suspended sediment and dropstones supplied by ice rafting (type IV Heinrich layers). These facies are generally arranged proximal to distal from the Hudson Strait, with type IV being the character of Heinrich layers in the IRD belt. (Sedimentological details can be found in several other references cited in this paper as well as a new paper by *Rashid et al.* [2003b].) *Hillaire-Marcel et al.* [1994] and *Clarke et al.* [1999] suggest that at Orphan Knoll site HU91-045-094-P (Table 1 and Figures 2, 13, and Figure 20), Heinrich events are separable into two distinct depositional processes. Turbidite sedimentation with high fine-grained carbonate concentrations is followed by a brief interval of increased IRD. Taken collectively, the observations from the Labrador Sea seem to imply an interval of significant subglacial

meltwater-derived sediments to the North Atlantic Mid-Ocean Channel prior to the launching of iceberg armadas to the North Atlantic IRD belt.
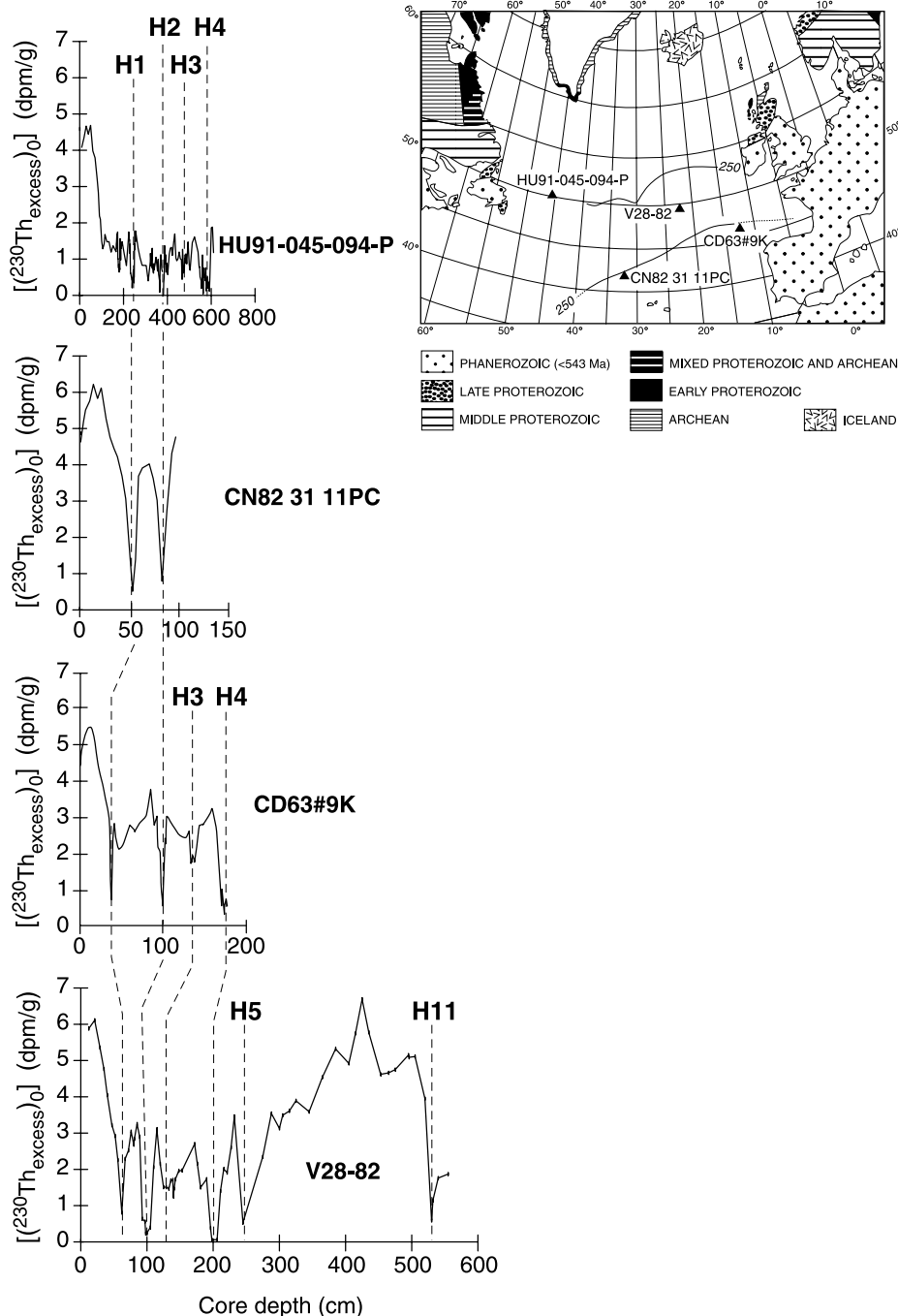
4.6. Chronology and Duration of the Heinrich Layers

[47] Constraining the chronology and duration of the Heinrich layers is critical to understanding their origin as well as their role in global abrupt climate change. There are two chronological objectives: (1) to place the Heinrich events in time, i.e., ^{14}C dates, and (2) to assess their sedimentation rates and hence also their duration. Although radiocarbon is a powerful chronometer, there are issues that limit its applicability to constraining the age and duration of Heinrich layers. There is a relatively large and variable difference between ''^{14}C years'' and ''calendar years.'' This difference is due to a combination of an incorrect decay constant and variability in the ^{14}C content of the reservoir from which the foraminifera precipitate their shells. The ^{14}C content of the seawater reservoir varies because of changes in the cosmogenic production rate as well as the movement of carbon through the ocean-atmosphere-biosphere system, particularly changes in ventilation of the deep water [e.g., *Bard et al.*, 1990, 1998; *Adkins et al.*, 1998; *Wunsch*, 2003]. Today there is about a 400 year reservoir age in surface waters of the North Atlantic, and in most applications of the chronometer to North Atlantic sediments it is generally assumed that this reservoir age was the same in the past. However, recent publications have raised questions about this assumption [e.g., *Voelker et al.*, 2000; *Waelbroeck et al.*, 2001].

[48] The duration of Heinrich layers has been estimated by the difference in ^{14}C ages across Heinrich layers, particularly H1 and H2 [*Bond et al.*, 1992, 1993]. The published radiocarbon measurements of the cores, whose stratigraphy is summarized in this paper, are given in Figure 21. *Heinrich* [1988] did not publish ^{14}C ages but used the planktonic $\delta^{18}O$ record for his age model. Duration estimates have been also made by measurements of sediment flux by the $^{230}Th_{excesss}$ method (see section 2.3 for an overview of the $^{230}Th_{excess}$ method; see Figure 20 for the four published records).

[49] Nonetheless, there are complications in interpreting these ages. The ages of Heinrich layers H1 and H2 are reasonably certain based on radiocarbon measurements (Table 3 and Figure 21), but estimations of their duration are compromised by the events themselves because they represent a large sediment flux increase [*Manighetti et al.*, 1995]. Within the IRD belt the estimated age at the base of the layers is a maximum because of capping of the bioturbated layer by the Heinrich layer (Figure 22). The estimated age at the top is a minimum because of bioturbation after the events. Additionally, the likelihood that Heinrich events are associated with major deep water circulation changes [*Vidal et al.*, 1997; *Kissel et al.*, 1999; *Elliot et al.*, 2001, 2002] and thus changes in the atmospheric radiocarbon content [e.g., *Yokoyama et al.*, 2000], as well as reservoir issues such as mentioned above, means that it is uncertain how to interpret the value of

Figure 19. Maps of data from Heinrich layer H3. Geology and *Ruddiman* [1997] IRD belt for reference. (a) Isopach map with 10 cm contour interval. (b) The $^{87}Sr/^{86}Sr$ values for siliciclastic detritus in H3. Isopachs are shown in dashed lines for reference. (c) The 25-23 kyr 250 mg cm^{-2} kyr^{-1} contours defining the approximately E-W IRD belt [*Ruddiman*, 1977], contours of 10, 50, and 100 sand-sized ash shards per square centimeter defining the approximately N-S trajectory of currents bringing Icelandic detritus into the North Atlantic [*Ruddiman and Glover*, 1982], and dashed lines of 10 cm thickness intervals for H3.

Figure 20. Initial ^{230}Th excess values from the Labrador Sea (HU91-045-094-P [*Veiga-Pires and Hillaire-Marcel*, 1999]) and the North Atlantic (CN82-31-11PC [*Francois and Bacon*, 1994], CD63#9K [*Thomson et al.*, 1995], and V28-82 [*McManus et al.*, 1998]). Heinrich layers H1, H2, H4, and H5 stand out as prominent minima.

the radiocarbon measurements near these events. Data published by *Bond et al.* [1992, 1993] for core V23-81 give the best estimates of the ages (see density of data in Figure 21) but show age plateaus above both H2 and H1 (Figures 23a and 23b). The plateaus could represent an increased sediment flux associated with reinvigorated North Atlantic Deep Water (NADW) convection following the events (G. Bond, personal communication, 1995). Alternatively, they could be consistent with changes in atmospheric radiocarbon content because of the shutdown of NADW during Heinrich events, such as proposed by *Yokoyama et al.* [2000], or large and rapid changes in North Atlantic surface reservoir ages as proposed by *Waelbroeck et al.* [2001].

[50] Detailed correlation of climatic proxies in North Atlantic sediment cores with Greenland ice core records provides the potential for improved chronology of the Heinrich layers and for global climate correlations. Cold sea surface temperatures, as indicated by high *N. pachyderma* (s.) abundance, appear to correlate to
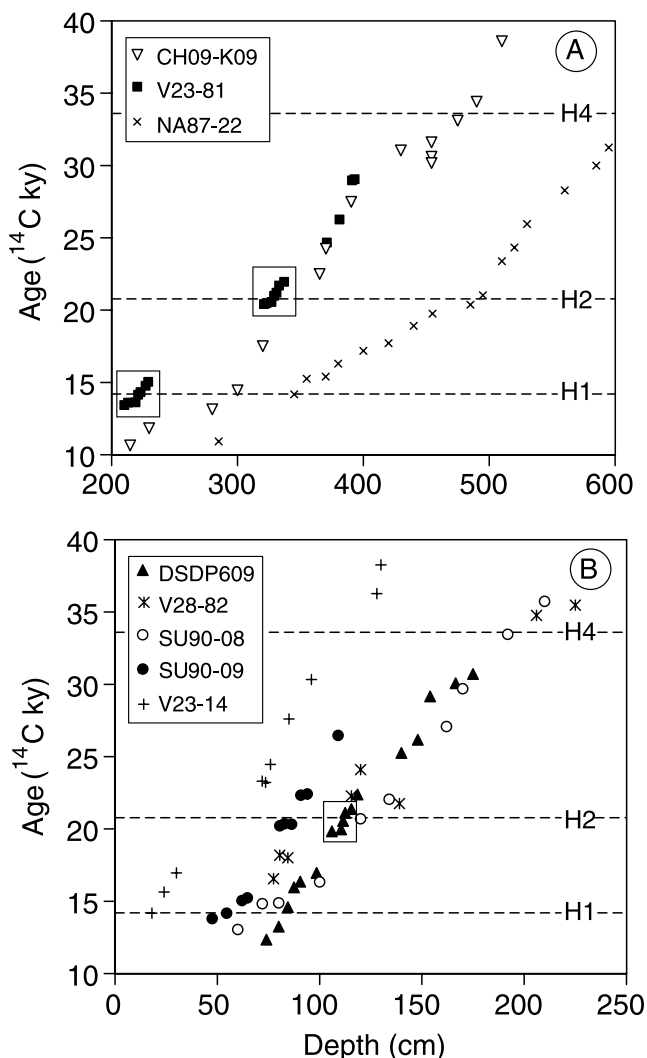
Figure 21. Age versus depth plots for cores used in plots throughout this paper. (a) Cores with high sedimentation rates. Data sources are CH09-K09 [*Labeyrie et al.*, 1999], V23-81 [*Bond et al.*, 1992, 1993], and NA87-22 [*Vidal et al.*, 1997]. The boxes around the data of H1 and H2 indicate the intervals of V23-81 that are shown in Figures 23a and 23b. (b) Cores with low sedimentation rates. Data sources are DSDP609 [*Bond et al.*, 1992, 1993], V28-82 [*Hemming et al.*, 1998], SU90-08 [*Vidal et al.*, 1998], SU90-09 [*Grousset et al.*, 2001], and V23-14 [*Hemming and Hajdas*, 2003]. The box around the data of H1 indicates the interval of DSDP609 that is shown in Figure 23c.

low $\delta^{18}O$ of Greenland ice (Figure 24) [*Bond et al.*, 1993, 1999]. Estimates of the calendar ages of Heinrich events, using this approach for H3–H6, are provided in Table 4. However, in detail, there are some substantial differences among the patterns that introduce uncertainty in the correlations and thus ice core-based chronologies. In particular, the Heinrich events do not stand out as more extreme temperatures in the Greenland ice cores, although they do appear to be located within longer-duration cold spells (Figure 24). Additionally, this correlation method appears to work best during stage 3 (i.e., between H5 and

H3) and is not particularly sensitive within stages 2 and 4. Radiocarbon dating provides a good alternative (with caveats stated above) within stage 2, but stage 4 remains problematic. The approach of correlating to the Greenland ice cores with detailed speleothem records that can be precisely dated using U series methods shows promise for improving ice core chronology [e.g., *Wang et al.*, 2001], but this depends on the accuracy of correlation, as discussed section 5.2.

[51] Published estimates of Heinrich layer duration are given in Table 3, and they range from 208 to 2280 years. In the Labrador Sea data, where the focusing factor is very large and its value is uncontrolled during Heinrich layers [*Veiga-Pires and Hillaire-Marcel*, 1999], the apparent duration is almost twice as long as for other North Atlantic $^{230}Th_{excess}$ estimates. This core is located in a sediment drift, and it is uncertain what changes may have happened to bottom currents during Heinrich events. The Labrador Sea data are more similar to open Atlantic data, with the assumption of similar focusing during Heinrich events as the ambient conditions (minimum estimates of *Veiga-Pires and Hillaire-Marcel* [1999]). Taking the best estimates (that is open ocean $^{230}Th_{excess}$ and V23-81 and DSDP609 ^{14}C data from H1 and H2), the average duration is 495 years, and the standard deviation in this duration is 255 years.

5. PROCESSES THAT MAY PRODUCE HEINRICH LAYERS

[52] As summarized above, Heinrich layers record profound and catastrophic events, likely armadas of icebergs launched from Hudson Strait. In this section I review the constraints on volume of water discharged based on the area covered by Hudson Strait IRD and the $\delta^{18}O$ composition of planktonic foraminifera. I then review the mechanisms that have been proposed for their origin, the implied water volumes that would be produced by each, and the concentration of IRD that the ice would have contained in each. Finally, I conclude that it should be possible to resolve their origin by a combination of local sedimentological synthesis near Hudson Strait, further quantification of hydrographic impacts in the North Atlantic, further quantification of ice and sediment flux using ^{10}Be and ^{3}He, and possibly quantification of global sea level rises that accompanied them.

5.1. Size of the Discharge

[53] *Alley and MacAyeal* [1994] estimated the mass and volume of a typical Heinrich IRD layer to be $1.0 \pm 0.3 \times 10^{15}$ kg or 370 ± 120 km^3. Their estimate was based on combining the total glacial IRD flux estimate of 9.8×10^{15} kg from *Ruddiman* [1977] with the area fractions under the SU90-08 magnetic susceptibility curve that are Heinrich fluxes as opposed to background glacial values [*Grousset et al.*, 1993]. A consistent estimate of $100–400$ km^3 is derived from simple mapping of the layer thickness across the North Atlantic (Figures 7 and 25 and Table 5), but more importantly the mapping of Heinrich layer area allows assessment

TABLE 3.   Timing and Duration of Heinrich Layers

| Core	Top, cm	Base, cm	Top,[a] yr	Base,[a] yr	ΔT, yr	Interval, cm	Sedimentation Rate, cm kyr^{-1}	Flux, g cm^{-2}kyr^{-1}	Source
HU75 − 55									*Andrews et al.* [1994b]
H1	81	116	13190	14560	1370	35	26		
H2	181	250	19410	21050	1640	69	42		
H2 to H1	116	181	14560	19410	4850	65	13		
NA87−22									*Vidal et al.* [1997]
H1	340	358	13200	14400	1200	18	15		
H2	482	505	21200	22800	1600	23	14		
H2 to H1	358	482	14400	21200	6800	124	18		
SU90-08									*Vidal et al.* [1997] and *Cortijo et al.* [1997]
H1	70	74				4	4		
H2	118	128	20700			10	10		
H2 to H1	74	118				44	7		
H4	192	210	33450	35730	2280	18			
H4 to H2	128	192					25		
SU90-09									*Grousset et al.* [2001]
H1	50	62	13860	14960	1100	12	11		
H2	82	92	20160			10			
H2 to H1			14960	20160	5200	20	4		
GGC31									*Bond and Lotti* [1995]
H1	35	53		14998		18	18		
H2	97	112	20443			15	15		
H2 to H1			14998	20443	5445	44	8		
V23-81									*Bond et al.* [1992, 1993]
H1	219	223	13630	14330	700	4	6		
H2	327	329	20570	20990	420	2	5		
H2 to H1			14330	20570	6240	104	17		
DSDP609									*Bond et al.* [1992, 1993]
H1	82	84.5		14588		2.5			
H2	112	117	21110	21875	765	5	7		
H2 to H1			14588	21110	6522	27.5	4		
V28-82									*McManus et al.* [1998]
H1	57	68			589	11		14	
H2	92	104			450	12		20	
H2 to H1	69	92			5750	23		3	
H3	128	144			1500	16		8	
H4	188	202			525	14		20	
H4 to H2	104	188			12600	84		5	
H5	241	252			434	11		19	
H6	300	328			7000	28		3	
CN82 31 11PC									*Francois and Bacon* [1994]
H1	51	56			208	5		18	
H2	80	87			477	7		11	
between H2 and H1					9000	24		2	
CD63#9K									*Thomson et al.* [1995][b]
H1	35	40			288	5		13	
H2	98	102			143	4		21	
H2 to H1	40	98			10875	58		4	
H3	135	139			600	4		5	
H4	170	177			210	7		25	
H4 to H2	102	170			12750	68		4	
91-045-094									*Veiga-Pires and Hillaire-Marcel* [1999]
H1	228	247			1410	19	13		
H2	365	380			1310	15	11		
H2 to H1						118	20		
H3	458	475			1480	17	11		
H4	561	590			2140	29	14		

[a]Ages are uncalibrated ^{14}C results.
[b]Dry bulk density is 0.75 g cm^{-3}.

of water volumes derived from the icebergs. The area covered by Heinrich layers, with average thickness of ~10–15 cm, is 1×10^6 (H1) to 2.4×10^6 km^2 (H4). Accordingly, the volume (V_{IRD} (km^3)) is estimated by

$$V_{\mathrm{IRD}} = A \times t \times 10^{-5},$$

where A is the area covered by HS Heinrich layer debris (km^2), t is the average thickness (cm), and 10^{-5} is the conversion factor for centimeters to kilometers. This is smaller than the estimate of *Dowdeswell et al.* [1995] of 3.4×10^6, where the thickness of H1 and H2 north of the IRD belt appears to be overestimated.
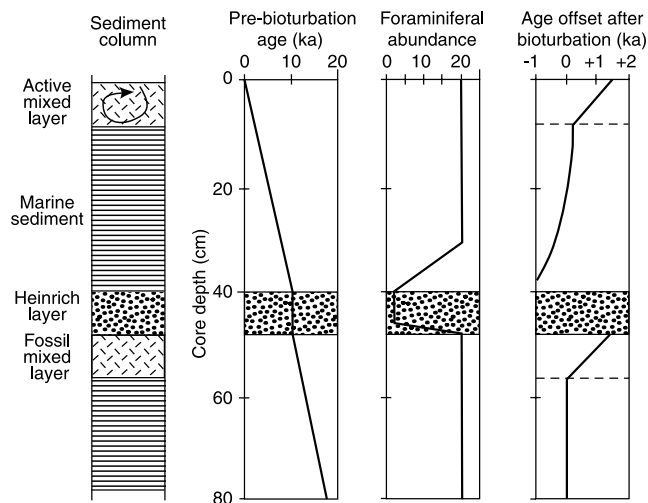
Figure 22. Cartoon showing the effect of rapid deposition of a layer such as Heinrich layers [from *Manighetti et al.*, 1995]. The age prior to Heinrich layers is a maximum due to the layers' capping bioturbation, and the age after Heinrich layers is a minimum due to downward bioturbation of young foraminifera. Heinrich layers are virtually devoid of foraminifera.

[54] Estimates of the volume of water released during Heinrich events can be made using the assumptions provided in Table 6. The minimum volume of water (V_{wat}(min) (km^3), i.e., a one-shot instantaneous addition) diluted by fresh water during a Heinrich event is

$$V_{wat}(min) = A \times t_{ml},$$

where A is the same area as defined above and t_{ml} is the ocean mixed layer thickness in kilometers. The fraction of water derived from the melting of Heinrich event icebergs can then be calculated from this volume using the fraction of meltwater, calculated from the corrected $\delta^{18}O$ excursion (Table 6), and an assumed average $\delta^{18}O$ of ice of approximately -31. This is probably an extreme estimation of the ice composition for the Laurentide ice sheet (D. P. Schrag, personal communication, 2003), and thus the meltwater fraction calculated this way is a minimum.

[55] The minimum estimate described above does not take into account the strong flows within the sea, which would have tended to dissipate the low-salinity lens. This flow requires that the actual glacially derived water volume depends on the duration of the event. It is clear from the pattern of distribution of Heinrich layer IRD with the distinctive Hudson Strait provenance that a strong eastward flow existed along the latitude of about 45°N (Figures 6 and 7), consistent with an iceberg transport rate close to that of today and/or a lower melting rate resulting from reduction of water temperatures in the North Atlantic [*Matsumoto*, 1997]. *Lynch-Stieglitz et al.* [1999] estimated that the flow of the Gulf Stream was reduced by about 30% to between 14 and 21 Sv (1 Sv = 10^6 m^3 s^{-1}) in the LGM. It appears that today a large fraction of the Gulf Stream goes to form the North Atlantic Current [e.g., *Schmitz and*

McCartney, 1993; *Schmitz*, 1996]. Input values ranging from 4.5% glacial water and 14 Sv Gulf Stream contribution to 9% glacial water and 21 Sv Gulf Stream contribution require a flux of 0.6–1.9 Sv of glacial water (Table 6).

[56] The amount of ice required to maintain the dilution implied by the $\delta^{18}O$ values depends on the duration of the event and the fraction of the North Atlantic Current flow that is contaminated by the ice-derived water (approximately the mixed layer thickness). The volume of water (V_{wat}(flow) (km^3)) is

$$V_{wat}(flow) = F \times t \times 10^{-9},$$

where F is the ice-water flux (m^3 s^{-1}), t is time (seconds), and 10^{-9} is the conversion from cubic meters to cubic kilometers (a longer version with more normal units is presented in Table 6). For 1 year and a fully contaminated flow the volume is similar to the minimum limit (Table 6). For 1000 years, $\sim 4 \times 10^7$ m^3 would be required. Under these conditions, if the average ice thickness from which the bergs were derived is 1 km, the areas occupied by the ice that produced the layers are between 3×10^4 km^2 and 4×10^7 km^2. This maximum number is very large. For
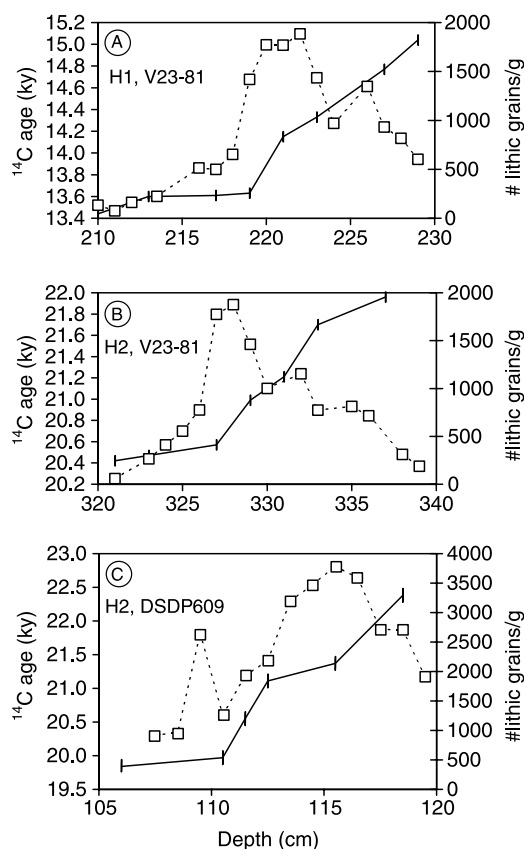
Figure 23. Age versus depth (left axis, solid lines) and number of lithic grains per gram (right axis, dashed lines) for intervals with high-resolution ^{14}C measurements across Heinrich layers: (a) H1 core V23-81, (b) H2 core V23-81, and (c) H2 core DSDP609. These are the best, published estimates of the ages and durations of H2 and H1. Data are from *Bond et al.* [1992, 1993].
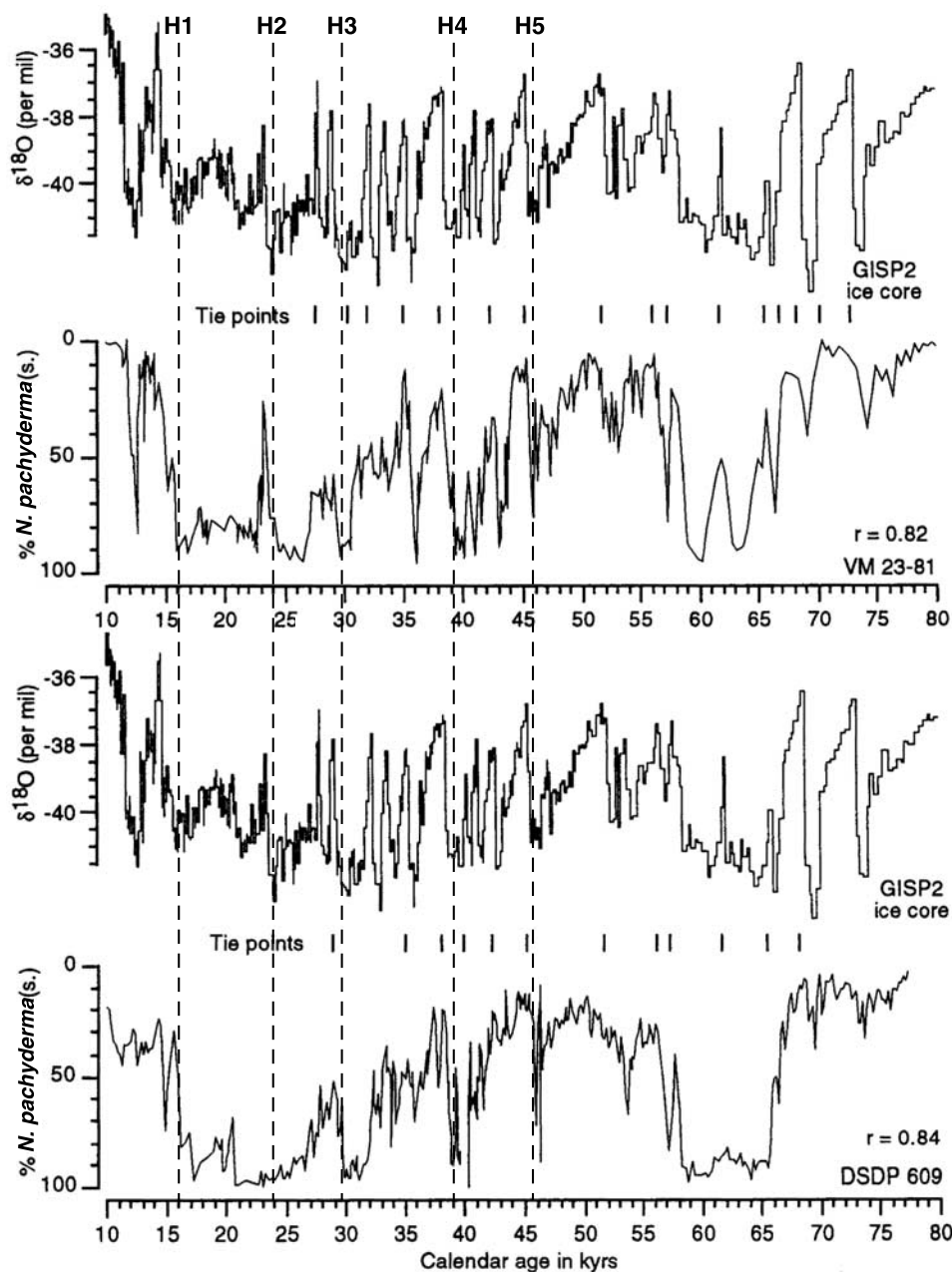
Figure 24. Correlations of sea surface temperatures in the North Atlantic, as estimated by the abundance of *N. pachyderma* (s.), and Greenland ice core temperatures, as estimated by the $\delta^{18}O$ of ice. Figure 24 is from *Bond et al.* [1999].

reference, the area occupied by Hudson Bay is about 8×10^5 km², and *MacAyeal* [1993] and *Matsumoto* [1997] estimated the area of the Hudson Strait catchment to be about 1×10^6 and 2×10^6 km², respectively. A best estimate area for a possible Hudson Bay catchment of 1.66×10^6 km² results from the following input values: the duration estimate discussed above of about 500 years, a 14 Sv Gulf Stream contribution, 4.5% glacial water, a 50 m mixed layer, and a 1.5 km ice thickness. (I have assumed here that reducing the thickness of the mixed layer reduces the volume required linearly, but this ignores a decrease in rate with depth.) Accordingly, it appears that a mechanism to add 3×10^4 to $>5 \times 10^6$ km³ of ice must be invoked to

account for the $\delta^{18}O$ recorded in the Heinrich layers. The range in estimated ice volume corresponds to a range of scenarios for its entry to the ocean. At the fastest the entry would last about 1 year and imply about 0.1 m of sea level rise and 1 Sv of freshwater flux (or 0.025 m and 0.25 Sv for 50 m mixed layer). At the slowest the entry would last about 500 years and imply 10–20 m of sea level rise and 0.15–0.3 Sv of freshwater flux (for 50 and 100 m mixed layer). These estimates are comparable to those of *Alley and MacAyeal* [1993], who used a similar strategy to estimate ~0.01 m yr^{-1} sea level rise and a 200–300 year duration (2–3 m total rise, if duration was 500 years, then their estimate would be a 5 m sea level rise). On the basis of

TABLE 4.   Ages of Heinrich Layers[a]

Heinrich Layer	Calendar Age, years	Basis	Source
H1	16800	[14]C(14200 + 2600)	Bond et al. [1992, 1993]
H2	24000	[14]C (20500 + 3500)	Bond et al. [1992, 1993]
H3	~31000	correlation to Greenland[a]	GISP2 [Meese et al., 1997]
H4	38000	correlation to Greenland[a]	GISP2 [Meese et al., 1997]
H5	45000	correlation to Greenland[a]	GISP2 [Meese et al., 1997]
H6	~60000	correlation to Greenland[a]	GISP2 [Meese et al., 1997]

[a]Bond et al. [1993] set the basis for making correlations between North Atlantic records and Greenland ice core $\delta^{18}O$. The ages from H3 through H5 are based on this strategy, but the ages are different and are based on current age estimates. The ages for H1 through H4 are compatible with those derived from U-Th of dated carbonate correlated to GISP2 based on $\delta^{18}O$ pattern matching the Hulu (China) speleothem record [Wang et al., 2001]. That for H5 would be 47,000 with the correlation to the Hulu speleothem record [Wang et al., 2001]. The position of H3 is more difficult to discern, and thus the age is uncertain but probably is within ±1000 years. The age of H6 is very poorly constrained and could be different by at least ±5000 years.

estimates of IRD concentration in the ice and glaciological processes, and using their mapped volume of H1 and H2, *Dowdeswell et al.* [1995] suggested 1.4×10^5 to 1.4×10^6 km^3 of water released over 250–1250 years (0.39–3.9 m sea level rise).

5.2.   What Caused the Heinrich Layers?

[57] A successful Heinrich layer model, that is, specifically for the Hudson Strait Heinrich layers, must produce sufficient IRD and distribute it across the North Atlantic [*Hulbe*, 1997]. It must explain the limited source region for the terrigenous sediments and the presence of abundant detrital carbonate only within the Heinrich layers. It must account for the apparent association with the cold phases of the D-O cycles, with the dramatic ocean circulation changes, and with the rapid warming that directly follows them. Finally, if Hudson Strait Heinrich events accompanied global mountain glacier advances [e.g., *Denton et al.*, 1999], then they must be interpreted in the context of global climate change. Three proposed mechanisms to model the IRD and freshwater delivery of Hudson Strait Heinrich layers are reviewed here: catastrophic ice sheet purging, jökulhlaup activity, and ice shelf buildup/collapse. An additional model that involves a sea ice switch to trigger the abrupt warming (Y. Kaspi et al., A 'triple sea-ice state' mechanism for the abrupt warming and synchronous ice sheet collapses during Heinrich events, submitted to *Nature*, 2003, hereinafter referred to as Kaspi et al., submitted manuscript, 2003) is described briefly after the discussion of glaciological mechanisms.

[58] *MacAyeal* [1993] formulated an internally driven "binge-purge" model. The premise of a binge-purge model is that a large ice sheet will build up gradually during the binge stage, dependent on air temperature and moisture supply. Some combination of geothermal heat, advection of heat from the upper surface, and internal friction in the bottom boundary zone at the base of the ice sheet will act to eventually destabilize the ice sheet, resulting in a rapid purge phase, also known as Heinrich events. *MacAyeal* [1993] assumed geothermal heating is the driving force for purging the interior of the ice sheet, while *Verbitsky and Saltzman* [1995] found friction and heat advection from the surface to be more important parameters. *Marshall and Clarke* [1997] provided a continuum mixture model be-

tween sheet ice, which deforms by viscous creep, and stream ice with fluxes dictated by basal sliding and sediment deformation. They used this model to test the sensitivity of a Hudson Strait ice stream and concluded that it is unlikely for an ice stream in Hudson Strait to drain the interior portions of the ice sheet. *Clarke et al.* [1999] concluded that it is likely that the onset of a Heinrich event occurs when glacier flow instability is triggered, and they favor episodic surging of an ice stream in Hudson Strait. An alternative purge mechanism was proposed by *Hunt and Malin* [1998], that is, that ice-load-induced earthquakes may have destabilized the Laurentide ice sheet (although they call for successively shorter intervals between the Heinrich events, whereas my reassessment of the timing (Table 4) suggests a nonchanging, 7 kyr spacing).

[59] The volume *MacAyeal* [1993] estimated is 1.25×10^6 km^3 of fresh water (he estimated an area of 1×10^6 km^2 with an average thickness of 1250 m), introduced into the North Atlantic over about 250–500 years, implying a 0.16–0.08 Sv flux. Dividing the volume by the area of the world ocean, 3.61×10^8 km^2, MacAyeal estimated a sea level rise of about 3.5 m. If the Heinrich events represent a purging of a very large part of the Laurentide ice sheet, then it would take an interval considerably longer than a single D-O cycle to rebuild the ice sheet and create the conditions necessary to trigger a purge. The binge interval estimated from MacAyeal's model was about 7 kyr (remarkably close to the recurrence time of Heinrich layers, see Table 4). The water volumes and event durations calculated by *MacAyeal* [1993] abide by the maximum constraints discussed above. *Marshall and Clarke* [1997] modeled the behavior of an ice stream in Hudson Strait using mixed bed conditions, and they were able to produce a maximum flux of 0.03 Sv of icebergs, which is about 10 times lower than that implied by the $\delta^{18}O$-based calculations given above. One possible explanation they proposed is that their ice streams do not tap deep enough into the core of the ice sheet. However, because the maximum ice stream velocity in their simulations is 900 m yr^{-1}, ice originating at the head (750 km in) takes 833 years to get to the outlet. Accordingly, *Marshall and Clarke* [1997] concluded that it is unlikely for an ice stream in Hudson Strait to drain the interior portions of the ice sheet. They left open the possibility that their omission of hydrological conditions under the ice sheet may have led
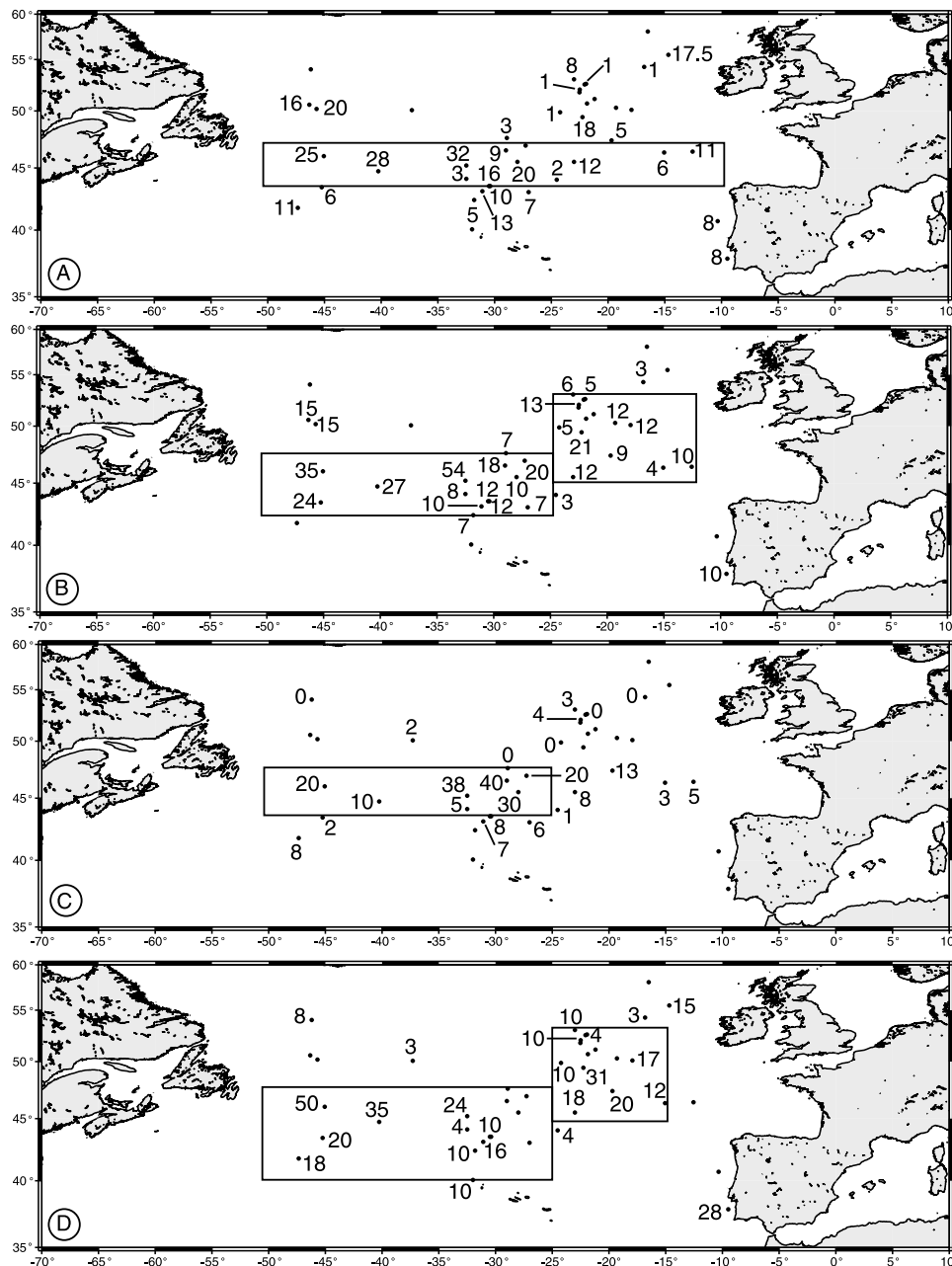
Figure 25. Equal area maps of H1–H4 used to estimate area covered by Hudson Strait-derived IRD: (a) H1, (b) H2, (c) H3, and (d) H4. Data sources are reported in Table 1. Numbers are estimated thickness for each location. Values of "0" are used where the position where the layer would be is understood but the layer was not identified. Rectangles surround the areas estimated for the layers, and the results are reported in Table 5.

to an underestimation, and this theme was extended by *Clarke et al.* [1999]. The *Verbitsky and Saltzman* [1995] model implies that the formation of the Heinrich events depends on climate; however, *Marshall and Clarke* [1997] concluded that the response time of the Laurentide ice sheet to climate change is quite long. Large ice streams tend to take on oscillatory behavior without the need for climate forcing [*Marshall and Clarke*, 1997], and rapid climate change is integrated into the buildup of the ice sheet (S. J. Marshall, personal communication, 2002). However, hydrologically controlled ice streams might have a more direct

influence from climate change [*Marshall and Clarke*, 1997], and *Clarke et al.* [1999] speculated that during the buildup to a Heinrich event, phase locking between an atmospheric forcing applied to the ice surface and subglacial meltwater production can be achieved if the ice bed contact is at the melting temperature and strain heating is appreciable. The apparent interhemispheric symmetry of mountain glacier advances and their coincidence in timing with Heinrich events [e.g., *Lowell et al.*, 1995; *Denton et al.*, 1999] favors a climate control on the Heinrich layers but does not eliminate the binge-purge behavior.

TABLE 5.   Area and Volume Estimates of Heinrich Layer IRD

H Layer	Area Covered, km²	Average Thickness, cm	Volume Detritus, km³
1	1.0×10^6	10	100
2	2.0×10^6	15	300
3	0.7×10^6	15	99
4	2.4×10^6	15	350

[60] *Johnson and Lauritzen* [1995] proposed an alternative hypothesis for Heinrich layers: Repetitive jökulhlaups from a Hudson Bay lake may have produced major freshwater pulses into the North Atlantic when the ice dams at the mouth of the Hudson Strait failed. A jökulhlaup is a massive flood that occurs when the height of the dam is exceeded by lake level because of rising lake level or reduced flow of glacial ice into the dam [*Johnson and Lauritzen*, 1995]. As noted in section 5.1, the area of Hudson Bay is about 8×10^5 km², and if it was overfilled by 100 m, the amount of water that would spill into the ocean in this process is around 8×10^4 km³, about twice the minimum estimate based on the area occupied by H4 and assuming a 200 m mixed layer. The *Johnson and Lauritzen* [1995] mechanism would be very rapid, and thus a number approaching the minimum estimate is reasonable based on the volume constraints alone. It is clear that a large fraction of the precursor fine carbonate sediment deposited near the Hudson Strait is brought by meltwater not icebergs [e.g., *Hesse and Khodabakhsh*, 1998; *Rashid et al.*, 2003b]. This model could produce a sea level change of only ~0.2 m or

less, and it would be virtually instantaneous. In the distribution of continental ice proposed by the *Johnson and Lauritzen* [1995] mechanism, Hudson Bay is filled with water and surrounded by glacial ice flowing into it rather than being a glacial dome itself. During early phases of the ice sheet buildup (stage 5) and possibly for H3, an ice-damned lake in Hudson Bay is possible; however, during the LGM it is unlikely that a lake occupied Hudson Bay (J. Andrews, personal communication, 2003). J. Andrews (personal communication, 2003) is considering the possibility of large, subglacial lakes under the Laurentide ice sheet. If large subglacial lakes existed under the Laurentide ice sheet, this would provide scope for large bursts of meltwater, accompanied by dramatic destabilization of the ice sheet.

[61] *Hulbe* [1997] proposed a model for Heinrich events in which the Hudson Strait ice stream flows into the Labrador Sea from a Hudson Bay dome and forms an ice shelf in the Labrador Sea, in other words with an ice sheet configuration similar to that assumed by *MacAyeal* [1993]. The ice shelf model proposed by *Hulbe* [1997] would operate under extreme cold conditions, consistent with the observations of Heinrich layers in DSDP609 and V23-81 [e.g., *Bond et al.*, 1992; *Broecker et al.*, 1992]. Ice shelves form where grounded ice flows into the sea and floats on the surface. In this model, sediment would be enriched in the basal zone of the ice shelf by basal freezing due to large slopes in the basal topography. *Hulbe*'s [1997] model appears to produce an acceptable volume of ice of 800×1200 km, with ~500 m average thickness (4.8×10^5 km³ of ice). However, there is not a Heinrich event for every cold interval in Greenland, and the $\delta^{18}O$ excursions coincident

TABLE 6.   Parameters Used to Calculate Water Volumes From Hudson Strait Heinrich Events

Parameter Used	Value	Source or Calculation
$\delta^{18}O$ of ice	-28 to -34‰	*Duplessy et al.* [2002] and *Schrag et al.* [2002] (note that the Laurentide is likely heavier, so this yields minimum volumes (D. P. Schrag, personal communication, 2003))
Magnitude of $\delta^{18}O$ excursion ($\delta^{18}O_{Heinrich} - {}^{18}O_{ambient}$)	-1 to -2‰	*Cortijo et al.* [1997]
Temperature lowering (ΔT)	$3°$ to $4°C$	*Cortijo et al.* [1997]
$\delta^{18}O$ excursion of water	-1.7 to -2.9‰	$(\delta^{18}O_{Heinrich} - \delta^{18}O_{ambient}) - (\Delta_{Heinrich} - \Delta_{ambient})^a$
Area of Heinrich layers A	0.7 to 2.3×10^6 km²	Table 3 and Figure 24
Mixed layer depth (MLD)	0.02 to 0.1 km	*Kara et al.* [2003]
Volume of water (minimum)[b]	1.4×10^4 to 2.3×10^5 km³	from A times mixed layer depth
Duration t	1 to 500 years	timing and duration section
Replenishment of NAC	14 to 21 Sv	*Lynch-Stieglitz et al.* [1999] and *Schmitz and McCartney* [1993]
Flux of water to maintain dilution F	0.6 to 1.9 Sv	(4.5% of 14 Sv) to (9% of 21 Sv)[c]
Volume of water[d]	1.9×10^4 to 3×10^7 km[e]	$V_{water}(km^3) = F(Sv) \times 1 \times 10^6 (m^3 \ s^{-1} \ Sv^{-1}) \times t(years) \times 3.15 \times 10^7 (s \ yr^{-1}) \times 10^{-9} \ (km^3 \ m^{-3})$

[a]Temperature-$\delta^{18}O$ relationship [*Shackleton*, 1967] is shown: $(T°C - 16.9)/(-4.28) = \Delta$ (Δ is CaCO$_3$ minus water difference; in the case presented here, $\Delta_{Heinrich} - \Delta_{ambient}$ is taken from the $3°-4°C$ temperature lowering and is $-3/(-4.28)$ or $-4/(-4.28)$ or an extra $0.7-0.9$‰ added to the measured excursion).

[b]Value assumes a volume the area of the Heinrich layers, and the thickness of the mixed layer is mixed one time with enough ice and water to make the $\delta^{18}O$ excursion.

[c]Here 4.5% and 9% are the range in $\delta^{18}O$ excursion as deduced from information provided in Table 6 on measured values, assumed ice values, and the temperature-$\delta^{18}O$ relationship.

[d]The range of estimates from 1 to 500 years is used to estimate the volume of water with the equation in the third column. For the minimum a 1 year duration and 0.6 Sv flow are assumed. For the maximum a 500 year duration and 1.9 Sv flow are assumed.

[e]The estimate 3×10^7 km³ is probably beyond what is reasonable, as discussed in text. In Table 7 and the text I suggest possible modifications of the "maximum" estimate.

TABLE 7.   Vital Statistics of Heinrich Layers

| *Duration*	*495 ± 255 years* (1σ)
Freshwater flux	$\sim 3 \times 10^4$ km³(1 year, 200 m mixed layer)
	$\sim 1 \times 10^7$ km³ (500 years, 4.5% ice water, and 14 Sv flow); if assumption of 100 (or 50) m mixed layer halves (quarters) volume,then 5 (or 2.5) $\times 10^6$ km³
Sea level rise	0 m (ice shelf)
	0.2 m (jökulhaup)
	3−15 m (Laurentide ice sheet purge)
Size of Hudson Strait catchment	1.66×10^6 km² (for 5×10^6 km³ volume and 3 km ice thickness or for 2.5×10^6 km³ volume and 1.5 km thickness)
Average ice thickness for 500 year duration	≥1.5 km
Volume of over-deepened Hudson Strait	$\sim 2 \times 10^3$ km³
Volume of IRD	100−350 km³
Concentration of IRD in ice	0.01−10%

with Heinrich events do not stand out in magnitude (Figure 24). Nonetheless, Heinrich events do appear to occupy relatively long cold intervals, and the model shelf needs about a thousand years of cooling to build up the ice shelf volume noted above [*Hulbe*, 1997]. Hulbe's model should predict detrital carbonate events for every cold phase of the D-O cycles in the vicinity of Hudson Strait. Indeed, it appears that there might be such events [*Andrews and Barber*, 2002], although the greatly reduced amplitudes that are implied are puzzling unless the freezing-on process in the ice shelf model operates effectively only when the shelf is fully developed. Sea level should not rise because of ice shelf collapse because the ice is already floating in the Labrador Sea prior to its release. However, perhaps small sea level rise from surges of other ice sheets could be a trigger for Hudson Strait collapse. Additionally, the collapse of the ice shelf could allow enhanced ice stream activity in Hudson Strait (although this does not appear to provide appropriate amounts of ice in the required time interval according to the work of *Marshall and Clarke* [1997]).

[62]   *Hulbe et al.* [2004] suggest a revision of the ice shelf hypothesis. In the new scenario the ice shelf is fringing the Laurentide ice sheet margin rather than extending across the Labrador Sea, and the events are formed by explosive disintegration of the ice shelf such as recently witnessed along the Antarctic Peninsula. The proposed ice shelf was fed by several ice streams, which have been identified by geomorphic studies. Each of the suggested ice streams is underlain by dominantly Churchill Province basement, consistent with the provenance constraints. The ice-derived water volume estimated in this study is 2.8×10^4 to 2×10^5 km³, consistent with volume constraints shown in Table 6 as long as the duration is very short.

[63]   The three mechanisms described above, (1) purging of the Laurentide ice sheet [*MacAyeal*, 1993; *Verbitsky and Saltzman*, 1995; *Hunt and Malin*, 1998; *Clarke et al.*, 1999] or episodic activity of an ice stream in Hudson Strait [*Marshall and Clarke*, 1997], (2) jökulhlaup activity [*Johnson and Lauritzen*, 1995], and (3) ice shelf buildup/ collapse [*Hulbe*, 1997; *Hulbe et al.*, 2004], all appear to be capable of producing the first-order features of the Heinrich layers, including the large injection of fresh water into the

North Atlantic Current (with volume depending on duration, see Table 7) and the large volume of sediment deposited rapidly in these events. In the purging and jökulhlaup scenarios the best way to get IRD-enriched icebergs appears to be a glaciohydraulic supercooling mechanism [e.g., *Alley et al.*, 1997, 1998; *Lawson et al.*, 1998; *Roberts et al.*, 2002], which would allow the limited sediment provenance of Heinrich layer sediments [*Bond et al.*, 1992; *Gwiazda et al.*, 1996a; *Hemming et al.*, 1998, 2002]. In this mechanism, ice accretes to the bottom of the glacier ice from water that is supercooled due to flowing up large topographic features such as the Hudson Strait sill. In the case of binge-purge behavior, basal debris entrainment mechanisms described by *Alley and MacAyeal* [1994] will also yield appropriate sediment loads. Glaciohydraulic supercooling may not apply to the ice shelf model. According to R. Alley (personal communication, 2003) the detritus from the mouth of Hudson Strait is most likely melted out. This is because the ice shelf is likely to be thickest in the mouth of Hudson Strait where the bed is deep. Freeze-on would be expected down flow, where the ice shelf is thinner, but after the debris has melted out. Alternatively, the freeze-on could be transverse to flow, which would tend to preserve sediment incorporated in the slower moving ice from the sides of the strait rather than in the main ice coming out of the strait (or other ice streams in the modified ice shelf model of *Hulbe et al.* [2004]). Additionally, it is likely that warming, rather than sea level rise, drives the retreat of the ice shelf [e.g., *Parizek et al.*, 2002; *Hulbe et al.*, 2004], although the revised ice shelf model may not require very substantial warming [*Hulbe et al.*, 2004].

[64]   Taking everything together, glacialogical instability (episodic purging) seems to be the most likely explanation for the Hudson Strait Heinrich layers unless it can be demonstrated that these events are substantially shorter than the apparent 500 year duration or that the mixed layer is extremely thin ($\sim 0.5-1$ m). Such a thin mixed layer seems unlikely given the (probably) more vigorous atmospheric circulation that accompanies Heinrich events. Interestingly, a scenario that involves components of all three proposed end-members may have some appeal. Buttressing by an ice shelf during cold periods could lock up the Hudson Strait
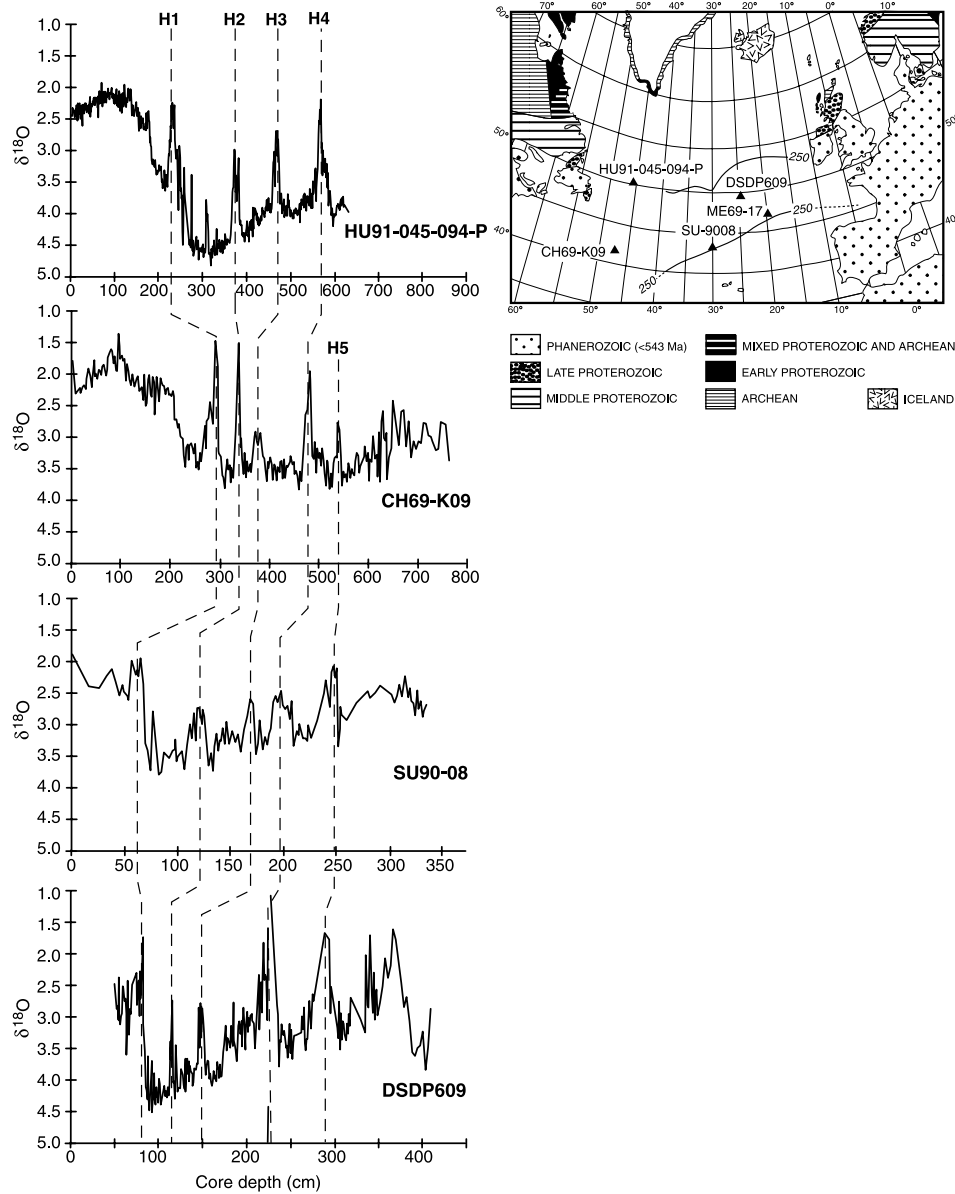
Figure 26. Evidence for large meltwater flux to the North Atlantic during Heinrich events from the $\delta^{18}O$ of *N. pachyderma* (s.). Map shows the locations of the cores. Data sources are HU91-045-094-P [*Hillaire-Marcel et al.*, 1994], CH69-K09 [*Labeyrie et al.*, 1999], SU90-08 [*Cortijo et al.*, 1997], and DSDP609 [*Bond et al.*, 1992].

ice stream. If the low area of Hudson Bay contains subglacial water, release of the ice shelf could set off a chain of events, ending in a massive purging of the Laurentide ice sheet. Kaspi et al. (submitted manuscript, 2003) have modeled a triple sea-ice state to produce the pattern of variability found in North Atlantic records. In their model, phase locking ties the behavior of Northern Hemisphere ice sheets together. I am not convinced that this locking is necessary, but it is an interesting theory that can presumably be tested if paleoceanographers can come to better understand the meaning of changes in the content of IRD in marine sediment cores (see section 2.1 for a discussion of defining IRD). In addition to the phase locking mechanism, Kaspi et al. (submitted manuscript, 2003) propose that rapid melting of sea ice following a Heinrich event is what leads

to the abrupt warming recorded in sediment cores, inferred to be the product of ice-albedo feedback.

[65] Further examination of hydrographic changes in the North Atlantic (reviewed in section 6) may provide additional constraints on the ice-derived water volume by documenting the mixed layer thickness. The combined application of $^{230}Th_{excess}$ with ^{3}He from interplanetary dust particles and ^{10}Be offers promise for constraining the volume of ice involved in the events [*Higgins*, 2001]. However, to achieve this promise, significant development work is necessary, as well as mapping of the intervals in space and time with these methods. Additionally, further examination of detailed sedimentology and hydrography proxies in the Labrador Sea provides constructive ways to decide among the proposed possibilities. It may be that

much of the hydrographic and sedimentological data from Labrador Sea cores are available [e.g., *Andrews and Tedesco*, 1992; *Andrews et al.*, 1994a, 1994b, 1998; *Hillaire-Marcel et al.*, 1994; *Jennings et al.*, 1996; *Hesse and Khodabakhsh*, 1998; *Hillaire-Marcel and Bilodeau*, 2000; *de Vernal and Hillaire-Marcel*, 2000; *de Vernal et al.*, 2000; *Rashid et al.*, 2003b], and a synthesis with the goal of testing the alternative hypotheses for Heinrich events could be what is most needed.

6. IMPACTS AND CORRELATIVES

6.1. Surface and Deep Water Changes in the North Atlantic

[66] *Maslin et al.* [1995] used foraminiferal assemblages combined with $\delta^{18}O$ measurements of planktonic foraminifera to estimate temperature and salinity at the sea surface and found dramatic reduction in both temperature and salinity during Heinrich events. During Heinrich events, there is a dip in the $\delta^{18}O$ of up to 2‰ in *N. pachyderma* (s.) within the IRD belt, which reveals the change in temperature and salinity attributable to the large amount of ice melting (Figure 26). $U_{37}^{K'}$-based sea surface temperature estimates indicate that sea surface temperatures were reduced in eastern Atlantic cores during these events [*Madureira et al.*, 1997; *Rosell-Melé et al.*, 1997; *Bard et al.*, 2000], consistent with faunal evidence [e.g., *Bond et al.*, 1993; *Cortijo et al.*, 1997]. Other biomarkers are consistent with a dramatic salinity reduction during these events [*Bard et al.*, 2000]. *de Vernal and Hillaire-Marcel* [2000] and *de Vernal et al.* [2000] found evidence from dinoflagellate cyst assemblages for low-salinity conditions, accompanied by extensive sea ice, around the margins of the North Atlantic during the LGM. However, they find evidence for largely sea ice-free conditions in the eastern Nordic Seas. During Heinrich events, sea ice cover increased to 10 months per year, and the sea surface salinity was reduced even further. The lower $\delta^{18}O$ of surface water during Heinrich events was transferred to the deep ocean, and this has been interpreted to be a signal of brine rejection [*Vidal et al.*, 1998].

[67] *Paillard and Cortijo* [1999] have made simple modeling experiments using the planktonic $\delta^{18}O$ and faunal data from H4 [*Cortijo et al.*, 1997] (shown in Figure 11b) to show that such a change in temperature and salinity during glacial conditions is predicted to result in complete shutdown of NADW formation. Dramatic NADW reduction during Heinrich events has been proposed based on observations of dramatically lowered benthic $\delta^{13}C$ [e.g., *Keigwin and Lehman*, 1994; *Vidal et al.*, 1997, 1998; *Zahn et al.*, 1997; *Willamowski and Zahn*, 2000; *Elliot et al.*, 2002]. This dramatic reduction of NADW formation is further supported by excess Pa/Th ratios from Bermuda Rise sediments [*McManus et al.*, 2002; J. F. McManus et al., Rapid deglacial changes in the Atlantic meridional circulation recorded in sedimentary $^{231}Pa/^{230}Th$, submitted to *Nature*, 2002].

[68] Such changes in the thermohaline circulation could be triggers for abrupt climate change [e.g., *Broecker*, 1994;

Clark et al., 2002; *Rahmstorf*, 2002], and hints that they may be mirrored by deep water changes in the northeastern Pacific suggest the possibility of globally propagated signals by deep water circulation changes [e.g., *Lund and Mix*, 1998]. Alternatively, they could be responses to abrupt climate change [e.g., *Boyle*, 2000; *Wunch*, 2003; Kaspi et al., submitted manuscript, 2003]. The estimated flux of glacial meltwater ranges from 3×10^4 km^3 (and 1.6 Sv in 1 year) to 5×10^6 km^3 (0.3 Sv over 500 year interval), derived in section 5 on origin of the Heinrich layers. Model studies have shown a dramatic decrease of NADW turnover when a sudden flux of fresh water is injected into the North Atlantic [e.g., *Manabe and Stouffer*, 1995; *Paillard*, 1995; *Seidov and Maslin*, 1999; *Alley et al.*, 2001; *Ganopolski and Rahmstorf*, 2002] (see recent review articles by *Clark et al.* [2002] and *Rahmstorf* [2002]). These models differ in detail but have in common the sensitivity of Atlantic overturning to freshwater injections. They also produce a cooling of air and sea surface temperatures in the eastern North Atlantic when overturning is slowed or halted.

[69] Global climate changes may have triggered the Heinrich layers [e.g., *Denton et al.*, 1999], but certainly the Laurentide response during Heinrich events must have made a significant impact on regional climate. *Schmittner et al.* [2002] suggested that the presence of large continental ice sheets in the Northern Hemisphere may lead to increased instability in climate. Even if NADW shutdown was not the trigger for global climate change, the imprint it left in the benthic marine record should provide important correlation ties [e.g., *Charles et al.*, 1996].

6.2. Global Signals

[70] High-resolution records around the globe show evidence for millennial-scale climate variability, particularly pronounced during stage 3 of the last glacial interval [e.g., *Broecker*, 1994, 2000; *Lund and Mix*, 1998; *Bond et al.*, 1999; *Mix et al.*, 2001; *Clark et al.*, 2002; *Voelker*, 2002; *Rahmstorf*, 2002; *Siddall et al.*, 2003]. As discussed below, several Northern Hemisphere records resemble the pattern of the Greenland ice cores, and some have extremes that occur approximately synchronous to Heinrich events with little evidence of the other millennial variations. Two important precautions should be kept in mind in interpreting these records: (1) the achievable accuracy of the chronology and of correlations at high resolution (e.g., as discussed by *Boyle* [2000]) and (2) the sensitivity of the proxy and/or the region to the changes that accompany the abrupt climate changes in Greenland and the North Atlantic.

[71] *Voelker* [2002] provides a review of records with high-resolution analyses through stage 3. Within the limits of dating many Northern Hemisphere records show a strong resemblance to $\delta^{18}O$ in the Greenland ice core [*Boyle*, 2000]. This is particularly true of cores within the polar North Atlantic and Nordic Seas [e.g., *Elliot et al.*, 1998; *Rasmussen et al.*, 1997; *Voelker et al.*, 1998; *Dokken and Jansen*, 1999; *van Kreveld et al.*, 2000]. Examples from outside the polar seas are the alkenone sea surface temperature records from the Bermuda Rise [*Sachs and Lehman*,

1999] and Alboran Sea [*Cacho et al.*, 1999], bioturbation and planktonic and benthic $\delta^{18}O$ and $\delta^{13}C$ and total organic carbon records from the Santa Barbara Basin [*Behl and Kennett*, 1996; *Kennett et al.*, 2000], terrigenous runoff records in the Cariaco Basin [*Peterson et al.*, 2000], and total organic carbon and $\delta^{15}N$ records in Arabian Sea [*Schulz et al.*, 1998; *Altabet et al.*, 2002] sediments.

[72] Although Heinrich events do not stand out in the Greenland ice core (Figure 24) or in the Santa Barbara and Cariaco Basins, they do appear as extremes in the Arabian and Alboran Seas (Figures 3 and 4) and Gulf of Lions [*Rohling et al.*, 1998]. In at least two records outside the North Atlantic IRD belt, only the Heinrich pattern is seen (Figure 3). One is the pollen record from Florida's Lake Tulane where pine pollen replaces oak pollen at times corresponding to the Heinrich events [*Grimm et al.*, 1993]. A second is the continental margin sediment record off Brazil where high $CaCO_3$ sedimentation is interrupted by pulses of continental debris at the times of each Heinrich event [*Arz et al.*, 1998]. A third record that appears to capture only Heinrich events is the average grain size of Chinese loess, where Heinrich intervals are seen as having larger average grain size, presumably related to stronger winds [*Porter and An*, 1995] (however, the resolution of this record is too low to identify D-O cycles).

[73] If there are some areas that have climate variability following the pacing of D-O cycles and others that only feel Heinrich events, then the geographic pattern of where they do and do not stand out should provide important clues about the behavior of the climate system [*Leuschner and Sirocko*, 2000; *Broecker and Hemming*, 2001]. However, an alternative explanation is that different aspects of climate are recorded by the different proxies and/or in the different settings. Accordingly, it is possible that the records in which only Heinrich events are seen would show the other millennial events with different proxies. Additionally, it is possible that records where Heinrich events are not seen as clear extremes could contain proxies that do emphasize these events over the others.

[74] Examples of both scenarios come from the North Atlantic itself. Notably, the Greenland ice core does not record greater light $\delta^{18}O$ excursions during Heinrich events than in other cold intervals (Figure 24), although they do appear to be of longer duration. Heinrich events left a dramatic IRD signal in the North Atlantic IRD belt, and there they are clearly related to extreme climate conditions and very different deep water composition and thus presumably collapse of NADW formation. However, Heinrich events are not distinct in every measure of IRD, even in the IRD belt. Although they are dramatically displayed in $^{230}Th_{excess}$ flux estimates, detrital carbonate concentration, and most radiogenic isotope compositions, they are invisible in records of hematite-stained grains and volcanic glass counts, where a quasiperiodic 1500 year variability is seen instead [*Bond et al.*, 1997, 1999].

[75] Different sensitivity is one explanation, and another possible explanation is that biases in the ability to distinguish Heinrich events from other millennial events may be produced if the proxies are at the limits of their range. For example, Heinrich events stand out as having an extremely high percentage of *N. pachyderma* (s.), indicating low sea surface temperatures during stage 3 in the North Atlantic's DSDP609 (Figure 24). However, in stage 2 this species makes up close to 100% in DSDP609, and thus H2 does not stand out at all in the *N. pachyderma* (s.) of this core. Furthermore, H1 is marked only by the abrupt reduction in *N. pachyderma* (s.) that follows it (Figure 24), possibly in the transition to interglacial conditions. In core V23-81 the tops of H1 through H5 are all marked by the abrupt reduction in percentage of *N. pachyderma* (s.) (Figure 24). The two cooling events between H5 and H4 in the ice core show up with approximately the same scaling in V23-81, but this is generally not true between H4 and H2. Even high-resolution North Atlantic records of sea surface temperature variability, as measured by the abundance of *N. pachyderma* (s.), do not necessarily highlight the prominence of the Heinrich events (Figure 24), although some measures do clearly distinguish them from all other events in the IRD belt as discussed throughout this paper.

[76] By analogy, records outside the IRD zone may contain proxies that are sensitive to different aspects of the climate system or are near the limits of their sensitivity. For example, the median grain size of loess from China appears to only distinguish Heinrich events, while other measures show more of the millennial-scale variability [*Porter and An*, 1995]. Additionally, in a speleothem $\delta^{18}O$ record from Hulu Cave, located within the same monsoon-sensitive region, a reasonably certain correlation to the Greenland ice core can be made within the stage 3 interval, and the Heinrich events appear as more prominent maxima than the other cold events [*Wang et al.*, 2001]. The correlation-based approach for Hulu gives comparable ages from H1, H2, H3, and H4 to those from the Greenland Ice Sheet Project 2 (GISP2)/North Atlantic correlations but implies an approximately 2 kyr older age for H5. The pattern of $\delta^{18}O$ variation in Hulu does not appear to be similar to GISP2 beyond this interval. A very large number of papers, reporting records from Chinese loess deposits and nearby marginal seas, include reference to the Heinrich events. However, suggestion of clear pattern matches to Heinrich events is not convincing. There does appear to be evidence for recurrent runoff events from the Selenga River into Lake Baikal that are approximately coincident with Heinrich event timing of H2 through H5, although the chronology appears quite uncertain [*Prokopenko et al.*, 2001].

[77] The records studied by *Arz et al.* [1998], from the Brazil margin, and by *Peterson et al.* [2000], from the Cariaco Basin, are both located near tropical South America, and both are interpreted to reflect variations in rainfall/runoff. However, the Cariaco record shows a pattern of variability similar to Greenland ice and does not distinguish Heinrich events. In contrast, the Brazil margin record only distinguishes Heinrich events. Perhaps this apparent contrast is a real measure of climatic differences at these two sites. The Cariaco Basin variations were interpreted to reflect changes in the position of the Intertropical Conver-

gence Zone (ITCZ) (the core is 10°42.73′N, 65°10.18′W), with rainy intervals correlated to warm intervals in Greenland [*Peterson et al.*, 2000]. Today the ITCZ is north of the equator in July and mostly north of the equator in the Atlantic in January. However, it does dip far south over the South American continent in the winter, and it is considered to have shifted south during the last glacial interval [*Harris and Mix*, 1999]. The *Arz et al.* [1998] location is 3°40.0′S and 37°43.0′W, and the runoff events recorded in this core appear to be reasonably correlated to Heinrich (cold) intervals. Their explanation is that increased trade winds may have led to greater precipitation on the Brazil coast. Arz et al. showed data at a recent miniconference (reviewed by *Broecker and Hemming* [2001]) from beneath the bulge of Africa where Heinrich events appear to be dry spells, which would also be consistent with increased trade winds. Alternatively, perhaps only extreme southward shifts of the ITCZ during glacial times resulted in the greater runoff south of the equator, whereas smaller changes resulted in shifts in the Cariaco Basin hydrology. Could there be a position in between these locations for which a wetness proxy would see all the millennial variations, but the Heinrich events would stand out?

[78] The pattern of difference of Heinrich events compared to ambient glacial as well as the geographic distribution of sites that are sensitive to Heinrich events versus D-O events may provide important clues to the driving forces of these abrupt climate changes. For example, there is no strong evidence in the North Atlantic for large changes in NADW production relative to ambient glacial conditions for each of the non-Heinrich cold stadials. However, during the four massive Heinrich events, there is dramatic evidence of deep water change, as evidenced by the extreme $\delta^{13}C$ values of benthic foraminifera in these intervals [e.g., *Vidal et al.*, 1997; *Elliot et al.*, 2002]. As reviewed by *Rahmstorf* [2002], three ocean states are inferred: interglacial (deep NADW formation), glacial (intermediate NADW formation), and Heinrich (no NADW formation) modes. It appears that the earliest suggestion of this three-state ocean can be attributed to *Sarnthein et al.* [1994], and the idea was popularized by *Alley and Clark* [1999]. Presumably, there is an atmospheric component to spreading all these signals around the globe, but perhaps the differences between regular cold snaps and Heinrich cold snaps lie in the specific mechanisms of thermohaline overturning.

[79] *Dokken and Jansen* [1999] reported evidence for contrasting deep water formation mechanisms in the Nordic Seas during warm and cold intervals of the last glacial. They documented $\delta^{18}O$ excursions of benthic foraminifera to light values, coincident with light excursions of planktonic foraminifera and associated with each of the Greenland cooling events. They inferred that deep water was generated fairly continuously in the Nordic Seas but in two different ways: (1) convection in the open ocean in warm intervals and (2) brine rejection during sea ice formation in cold intervals. The most extreme of these events are credibly correlated to Heinrich events. There is a growing literature of high-resolution stable isotope records in the Nordic Seas that I

expect will provide some important constraints on the behavior of the NADW part of the thermohaline circulation in the last 60 kyr [e.g., *Rasmussen et al.*, 1997; *Voelker et al.*, 1998; *Dokken and Jansen*, 1999; *van Kreveld et al.*, 2000].

[80] It is still unclear how climate records in the Southern Hemisphere relate to Northern Hemisphere variability. *Steig and Alley* [2003] have made detailed statistical analyses of the phase relationships between Antarctic (Byrd) and Greenland (GISP2) ice cores and showed that either a maximum positive correlation with an Antarctic lead of about 1000–1600 years or a maximum negative correlation with an Antarctic lag of about 400–800 years best fit the data. They conclude from this treatment of the data that the concepts of antiphase ("seesaw") or phase-shifted ("southern lead") behavior do not adequately describe the real behavior of the climate system at millennial timescales. The ice cores from Antarctica appear to be generally offset in their temperature records from Greenland. An exception is the Taylor Dome core, where the temperature record appears to be positively correlated with Greenland [e.g., *Steig et al.*, 1998; *Grootes et al.*, 2001]. *Grootes et al.* [2001] interpret this to be a product of varying degrees of marine influence around the Antarctic, yielding heterogeneous climate. According to the best available chronologies, relatively warm sea surface temperatures in the eastern South Atlantic [e.g., *Little et al.*, 1997; *Kanfoush et al.*, 2000; *Voelker*, 2002] and in the eastern South Pacific [e.g., *Ninnemann et al.*, 1999] also appear to indicate warmer conditions in the Southern Ocean when Greenland is cold.

[81] However, the apparent synchrony of moraines in Chile and New Zealand with Heinrich events represents a contrasting image of Southern Hemisphere climate. Moraines representing major glacial advances in the Chilean Lake District may correspond to the youngest three layers at 14.5–14.8 (H1), 22.3–22.6 (or 21?) (H2), and ~26.8 (H3) ^{14}C kyr [*Lowell et al.*, 1995; *Denton et al.*, 1999; *Lowell*, 2000]. These advances are correlated to cooling based on expansion of grassland vegetation [*Heusser et al.*, 1999; *Denton et al.*, 1999]. Many glacial advances are recorded in New Zealand [*Denton et al.*, 1999; G. H. Denton, personal communication, 2002], perhaps enough to match one for one with cold oscillations in Greenland. It is clear from the compilation of records of high-resolution climate variability in stage 3 [*Voelker*, 2002] that there needs to be a concerted focus on the Southern Hemisphere. As pointed out by *Denton et al.* [1999], the apparent discrepancy between mountain glacier and marine records in the southern mid-latitudes might be resolved with an Antarctic Circumpolar Transect emphasizing chronology combined with proxies of climate conditions at high resolution.

6.3. Sea Level Variations Linked to Heinrich Events

[82] Dated coral terraces from the Huon Peninsula, Papua New Guinea, and Barbados appear to record substantial millennial fluctuations in sea level [*Yokoyama et al.*, 2001; *Chappell*, 2002; *Cutler et al.*, 2003]. *Chappell* [2002] and *Yokoyama et al.* [2001] infer that these sea level jumps,

interpreted to reflect approximately 10–15 m excursions, are correlated to Heinrich events. Additionally, planktonic $\delta^{18}O$ from a marine sediment core record from the Red Sea appears to reflect rapid and large sea level excursions during stage 3 [*Siddall et al.*, 2003], and high-resolution benthic $\delta^{18}O$ records appear to support these interpretations [e.g., *Waelbroeck et al.*, 2002; *Cutler et al.*, 2003]. I had thought that sea level jumps could constrain the origin of Heinrich events. Indeed, if it were demonstrated that there were no jumps, it would eliminate the binge-purge scenario. However, as the Hudson Strait is not the only outlet of ice into the ocean, sea level rises are necessary but not sufficient to demonstrate a connection. Although not the "smoking gun" I had originally considered it, further evidence concerning rapid sea level changes should have important implications for understanding the system in which HS Heinrich events operated.

7. SUMMARY AND SCOPE FOR FUTURE RESEARCH

[83] Heinrich layers are spectacular IRD deposits in the North Atlantic that resulted from massive discharges of icebergs from the Laurentide ice sheet through the Hudson Strait. They are clearly linked to dramatic climate shifts in the Northern Hemisphere, and they could have global correlations. Detailed studies of the interval containing H1 through H4 in the IRD belt have demonstrated a strong connection between the timing of Heinrich layers and the pace of climate variability in the North Atlantic. More work is needed in the Southern Hemisphere in order to evaluate whether or not there is truly an interhemispheric correlation at the times of the Heinrich events, and the Antarctic Circumpolar Transect proposed by *Denton et al.* [1999] would be a good way to start.

[84] In order to resolve the details of how Heinrich layers formed, it is necessary to consider the predictions that come from the proposed models, that is, purging of the Laurentide ice sheet through the Hudson Strait ice stream, jökulhlaups, and ice shelf. Careful assessment of the sedimentology of the Labrador Sea in the vicinity of the Hudson Strait should provide important clues about the glacial processes that were operating. Additional work is needed at high resolution across the intervals of Heinrich events in the IRD belt, including their "precursors" and combined with further constraints on the composition of potentially contributing sources.

[85] Much effort has gone into characterizing the Heinrich events in the North Atlantic and into identifying potentially correlative climate events globally, and from this effort a picture is emerging about the causes and effects related to them. They occurred during extreme cold periods in the North Atlantic and were abruptly followed by dramatic warming. A large influx of fresh water into the North Atlantic accompanied these events (Figure 26), and it appears that a complete shutdown of NADW production was produced. What remains to be understood better is whether the correlations are global or Northern Hemisphere-wide and what the ultimate driver of these dramatic events was. The existence of the prominent 100 kyr cycle and its

apparent pacing with the insolation in northern latitudes seems to require a magnifier such as the Northern Hemisphere ice sheets and their impact on such things as thermohaline and atmospheric circulation, albedo, greenhouse gases, and so forth. So it is not a big leap of faith to conclude that the rapid and large climate changes that we see during the last glacial might also be related to the presence of the very large ice sheets that existed in the Northern Hemisphere.

REFERENCES

Adkins, S. F., H. Cheng, E. A. Boyle, E. R. M. Druffel, and R. L. Edwards (1998), Deep-sea coral evidence for rapid change in ventilation of the deep North Atlantic 15,400 years ago, *Science*, *280*, 725–728.

Alley, R. B., and P. U. Clark (1999), The deglaciation of the Northern Hemisphere: A global perspective, in *Mechanisms of Global Climate Change at Millennial Time Scales*, *Geophys. Monogr. Ser.*, vol. 112, edited by P. U. Clark, R. S. Webb, and L. D. Keigwin, pp. 142–182, AGU, Washington D. C.

Alley, R. B., and D. R. MacAyeal (1993), West Antarctic ice sheet collapse: Chimera or clear danger?, *Antarct. J. U.S.*, *XXVIII*(5), 59–60.

Alley, R. B., and D. R. MacAyeal (1994), Ice-rafted debris associated with binge purge oscillations of the Laurentide ice sheet, *Paleoceanography*, *9*(4), 503–511.

Alley, R. B., K. M. Cuffey, E. B. Evenson, J. C. Strasser, D. E. Lawson, and G. J. Larson (1997), How glaciers entrain and transport basal sediment: Physical constraints, *Quat. Sci. Rev.*, *16*(9), 1017–1038.

Alley, R. B., D. E. Lawson, E. B. Evenson, J. C. Strasser, and G. J. Larson (1998), Glaciohydraulic supercooling: A freeze-on mechanism to create stratified, debris-rich basal ice: II. Theory, *J. Glaciol.*, *44*, 563–569.

Alley, R., S. Anandakrishnan, and P. Jung (2001), Stochastic resonance in the North Atlantic, *Paleoceanography*, *16*(2), 190–198.

Altabet, M. A., M. J. Higginson, and D. W. Murray (2002), The effect of millennial-scale changes in Arabian Sea denitrification on atmospheric CO_2, *Nature*, *415*, 159–162.

Andrews, J. T. (1998), Abrupt changes (Heinrich events) in late Quaternary North Atlantic marine environments: A history and review of data and concepts, *J. Quat. Sci.*, *13*(1), 3–16.

Andrews, J. T. (2000), Icebergs and iceberg rafted detritus (IRD) in the North Atlantic: Facts and assumptions, *Oceanography*, *13*(3), 100–108.

Andrews, J. T., and D. C. Barber (2002), Dansgaard-Oeschger events: Is there a signal off the Hudson Strait Ice Stream?, *Quat. Sci. Rev.*, 21(1–3), 443–454.

Andrews, J. T., and K. Tedesco (1992), Detrital carbonate-rich sediments, northwestern Labrador Sea: Implications for ice-sheet dynamics and iceberg rafting (Heinrich) events in the North Atlantic, *Geology*, 20(12), 1087–1090.

Andrews, J. T., K. Tedesco, W. M. Briggs, and L. W. Evans (1994a), Sediments, sedimentation rates, and environments, southeast Baffin Shelf and northwest Labrador Sea, 8–26 ka, *Can. J. Earth Sci.*, 31, 90–103.

Andrews, J. T., H. Erlenkeuser, K. Tedesco, A. E. Aksu, and A. J. T. Jull (1994b), Late Quaternary (Stage 2 and 3) melt-water and Heinrich events, northwest Labrador Sea, *Quat. Res.*, 41, 26–34.

Andrews, J. T., T. A. Cooper, A. E. Jennings, A. B. Stein, and H. Erlenkeuser (1998), Late Quaternary iceberg-rafted detritus events on the Denmark Strait-Southeast Greenland continental slope (~65°N): Related to North Atlantic Heinrich events?, *Mar. Geol.*, 149, 211–228.

Arz, H. W., J. Pätzold, and G. Wefer (1998), Correlated millennial-scale changes in surface hydrography and terrigenous sediment yield inferred from last-glacial marine deposits off northeastern Brazil, *Quat. Res.*, 50, 157–166.

Ayuso, R. A., and M. L. Bevier (1991), Regional differences in Pb isotopic compositions of feldspars in plutonic rocks of the northern Appalachian Mountains, U.S.A. and Canada: A geochemical method of terrane correlation, *Tectonics*, 10, 191–212.

Bacon, M. P. (1984), Glacial to interglacial changes in carbonate and clay sedimentation in the Atlantic Ocean estimated from Th-230 measurements, *Isot. Geosci.*, 2(2), 97–111.

Barber, D. C. (2001), Laurentide ice sheet dynamics from 35 to 7 ka: Sr-Nd-Pb isotopic provenance of northwest Atlantic margin sediments, Ph.D. thesis, Univ. of Colorado, Boulder.

Bard, E., B. Hamelin, R. G. Fairbanks, and A. Zindler (1990), Calibration of the ^{14}C timescale over the past 30,000 years using mass spectrometric U-Th ages from Barbados corals, *Nature*, 345, 405–410.

Bard, E., M. Arnold, B. Hamelin, N. Tisnerat-Laborde, and G. Cabioch (1998), Radiocarbon calibration by means of mass spectrometric Th-230/U-234 and C-14 ages of corals: An updated database including samples from Barbados, Mururoa and Tahiti, *Radiocarbon*, 40(3), 1085–1092.

Bard, E., F. Rostek, J.-L. Turon, and S. Gendreau (2000), Hydrological impact of Heinrich events in the subtropical northeast Atlantic, *Science*, 289, 1321–1324.

Baumann, K.-H., K. S. Lackschewitz, J. Mangerud, R. F. Spielhagen, T. C. W. Wolf-Welling, R. Henrich, and H. Kassens (1995), Reflection of Scandinavian ice sheet fluctuations in Norwegian Sea sediments during the past 150,000 years, *Quat. Res.*, 43, 185–197.

Behl, R. J., and J. P. Kennett (1996), Brief interstadial events in the Santa Barbara basin, NE Pacific, during the past 60 kyr, *Nature*, 379, 243–246.

Bischof, J. F., and D. A. Darby (1999), Quaternary ice transport in the Canadian Arctic and extent of the Late Wisconsinian glaciation in the Queen Elizabeth Islands, *Can. J. Earth Sci.*, 36, 2007–2022.

Bond, G. C., and R. Lotti (1995), Iceberg discharges into the North Atlantic on millennial time scales during the last glaciation, *Science*, 267, 1005–1010.

Bond, G., et al. (1992), Evidence for massive discharges of icebergs into the North Atlantic Ocean during the last glacial period, *Nature*, 360, 245–249.

Bond, G. C., W. S. Broecker, S. Johnsen, J. F. McManus, L. Labeyrie, J. Jouzel, and G. Bonani (1993), Correlation between climate records from North Atlantic sediments and Greenland ice, *Nature*, 365, 143–147.

Bond, G., W. Showers, M. Cheseby, R. Lotti, P. Almasi, P.deMenocal, P. Priore, H. Cullen, I. Hajdas, and G. Bonani (1997), A pervasive millennial-scale cycle in North Atlantic Holocene and glacial climates, *Science*, 278, 1257–1266.

Bond, G. C., W. Showers, M. Elliot, M. Evans, R. Lotti, I. Hajdas, G. Bonani, and S. Johnsen (1999), The North Atlantic's 1–2 kyr climate rhythm: Relation to Heinrich events, Dansgaard-Oeschger cycles and the little ice age, in *Mechanisms of Global Climate Change at Millennial Time Scales*, *Geophys. Monogr. Ser.*, vol. 112, edited by P. U. Clark, R. S. Webb, and L. D. Keigwin, pp. 35–68, AGU, Washington D. C.

Boyle, E. A. (2000), Is thermohaline circulation linked to abrupt stadial/interstadial transitions?, *Quat. Sci. Rev.*, 19(1–5), 255–272.

Broecker, W. S. (1994), Massive iceberg discharges as triggers for global climate change, *Nature*, 372, 421–424.

Broecker, W. S. (2000), Abrupt climate change: Causal constraints provided by the paleoclimate record, *Earth Sci. Rev.*, 51, 137–154.

Broecker, W. S., and S. Hemming (2001), Paleoclimate: Climate swings come into focus, *Science*, 294, 2308–2309.

Broecker, W. S., G. C. Bond, M. Klas, E. Clark, and J. F. McManus (1992), Origin of the northern Atlantic's Heinrich events, *Clim. Dyn.*, 6, 265–273.

Broecker, W., G. Bond, and J. McManus (1993), Heinrich events: Triggers of ocean circulation change?, in *Ice in the Climate System*, NATO ASI Ser., Ser. I, vol. 12, edited by W. R. Peltier, pp. 161–166, Springer-Verlag, New York.

Cacho, I., J. O. Grimalt, C. Pelejero, M. Canals, F. J. Sierro, J. A. Flores, and N. Shackleton (1999), Dansgaard-Oeschger and Heinrich event imprints in Alboran Sea paleotemperatures, *Paleoceanography*, 14(6), 698–705.

Chapman, M. R., and N. J. Shackleton (1998), Millennial-scale fluctuations in North Atlantic heat flux during the last 150,000 years, *Earth Planet. Sci. Lett.*, 159, 57–70.

Chappell, J. (2002), Sea level changes forced ice breakouts in the last glacial cycle: New results from coral terraces, *Quat. Sci. Rev.*, 21(10), 1229–1240.

Charles, C. D., J. Lynch-Stieglitz, U. S. Ninnemann, and R. G. Fairbanks (1996), Climate connections between the hemispheres revealed by deep sea sediment core ice core correlations, *Earth Planet. Sci. Lett.*, 142, 19–27.

Clark, P. U., N. G. Pisias, T. F. Stocker, and A. J. Weaver (2002), The role of the thermohaline circulation in abrupt climate change, *Nature*, 415, 863–869.

Clarke, G. K. C., S. J. Marshall, C. Hillaire-Marcel, G. Bilodeau, and C. Veiga-Pires (1999), A glaciological perspective on Heinrich events, in *Mechanisms of Global Climate Change at Millennial Time Scales*, *Geophys. Monogr. Ser.*, vol. 112, edited by P. U. Clark, R. S. Webb, and L. D. Keigwin, pp. 243–262, AGU, Washington D. C.

Clough, S. K. (1978), Morphology, sedimentary facies and processes of the Northwest Atlantic Mid-Ocean Channel between 61 and 54°N, Labrador Sea, Ph.D. thesis, 167 pp., McGill Univ., Montreal, Que., Canada.

Cortijo, E., L. Labeyrie, L. Vidal, M. Vautravers, M. Chapman, J.-C. Duplessy, M. Elliot, M. Arnold, J.-L. Turon, and G. Auffret (1997), Changes in sea surface hydrology associated with Heinrich event 4 in the North Atlantic Ocean between 40° and 60°N, *Earth Planet. Sci. Lett.*, 146, 29–45.

Cutler, K. B., R. L. Edwards, F. W. Taylor, H. Cheng, J. Adkins, C. D. Gallup, P. M. Cutler, G. S. Burr, and A. L. Bloom (2003), Rapid sea-level fall and deep-ocean temperature change since the last interglacial period, *Earth Planet. Sci. Lett.*, 206, 253–271.

Darby, D. A., and J. F. Bischof (1996), A statistical approach to source determination of lithic and Fe oxide grains: An example from the Alpha Ridge, Arctic Ocean, *J. Sediment. Res.*, 66, 599–607.

Darby, D. A., J. F. Bischof, R. F. Spielhagen, S. A. Marshall, and S. W. Herman (2002), Arctic ice export events and their potential impact on global climate during the late Pleistocene, *Paleoceanography*, 17(2), 1025, doi:10.1029/2001PA000639.

Dasch, E. J. (1969), Strontium isotopes in weathering profiles, deep sea sediments, and sedimentary rocks, *Geochim. Cosmochim. Acta*, *33*, 1521–1552.

Denton, G. H., C. J. Heusser, T. V. Lowell, P. I. Moreno, B. G. Andersen, L. E. Heusser, C. Schlüchter, and D. R. Marchant (1999), Interhemispheric linkage of paleoclimate during the last glaciation, *Geogr. Ann., Ser. A*, *81*(2), 107–153.

de Vernal, A., and C. Hillaire-Marcel (2000), Sea-ice cover, sea-surface salinity and halo-/thermocline structure of the northwest North Atlantic: Modern versus full glacial conditions, *Quat. Sci. Rev.*, *19*(1–5), 65–85.

de Vernal, A., C. Hillaire-Marcel, J.-L. Turon, and J. Matthiessen (2000), Reconstruction of sea-surface temperature, salinity, and sea-ice cover in the northern North Atlantic during the Last Glacial Maximum based on dinocyst assemblages, *Can. J. Earth Sci.*, *37*, 725–750.

DeWolf, C. P., and K. Mezger (1994), Lead isotope analyses of leached feldspars—Constraints on the early crustal history of the Grenville Orogen, *Geochim. Cosmochim. Acta*, *58*, 5537–5550.

Dokken, T. M., and M. Hald (1996), Rapid climatic shifts during isotope stages 2–4 in the polar North Atlantic, *Geology*, *24*, 599–602.

Dokken, T. M., and E. Jansen (1999), Rapid changes in the mechanism of ocean convection during the last glacial period, *Nature*, *401*, 458–461.

Dowdeswell, J. A., and E. K. Dowdeswell (1989), Debris in icebergs and rates of glacimarine sedimentation: Observation from Spitsbergen and a simple model, *J. Geol.*, *97*, 221–231.

Dowdeswell, J. A., and T. Murray (1990), Modelling rates of sedimentation from icebergs, in *Glacimarine Environments: Processes and Sediments*, edited by J. A. Dowdeswell and J. D. Scourse, *Geol. Soc. Spec. Publ. London*, *53*, 121–137.

Dowdeswell, J. A., M. A. Maslin, J. T. Andrews, and I. N. McCave (1995), Iceberg production, debris rafting, and the extent and thickness of Heinrich layers (H-1, H-2) in North Atlantic sediments, *Geology*, *23*, 301–304.

Dowdeswell, J. A., A. Elverhoi, and R. Spielhagen (1998), Glacimarine sedimentary processes and facies on the polar North Atlantic margins, *Quat. Sci. Rev.*, *17*(1–3), 243–273.

Dowdeswell, J. A., A. Elverhøi, J. T. Andrews, and D. Hebbeln (1999), Asynchronous deposition of ice-rafted layers in the Nordic Seas and North Atlantic Ocean, *Nature*, *400*, 348–351.

Dreimanis, A. (1976), Tills: Their origin and properties, in *Glacial Till—An Interdisciplinary Study*, *Spec. Publ.*, vol. 12, edited by R. F. Legget, pp. 11–49, R. Soc. of Can., Ottawa, Ont.

Duplessy, J. C., L. Labeyrie, and C. Waelbroeck (2002), Constraints on the ocean oxygen isotopic enrichment between the Last Glacial Maximum and the Holocene: Paleoceanographic implications, *Quat. Sci. Rev.*, *21*(1–3), 315–330.

Elliot, M., L. Labeyrie, G. Bond, E. Cortijo, J.-L. Turon, N. Tisnerat, and J.-C. Duplessy (1998), Millennial-scale iceberg discharges in the Irminger Basin during the last glacial period: Relationship with the Heinrich events and environmental settings, *Paleoceanography*, *13*(5), 433–446.

Elliot, M., L. Labeyrie, T. Dokken, and S. Manthe (2001), Coherent patterns of ice-rafted debris deposits in the Nordic regions during the last glacial (10–60 ka), *Earth Planet. Sci. Lett.*, *194*, 151–163.

Elliot, M., L. Labeyrie, and J. C. Duplessy (2002), Changes in North Atlantic deep-water formation associated with the Dansgaard-Oeschger temperature oscillations (60–10 ka), *Quat. Sci. Rev.*, *21*(10), 1153–1165.

Farmer, G. L., D. C. Barber, and J. T. Andrews (2003), Provenance of late Quaternary ice proximal sediments in the North Atlantic: Nd, Sr and Pb isotopic evidence, *Earth Planet. Sci. Lett.*, *209*, 227–243.

Francois, R., and M. Bacon (1994), Heinrich events in the North Atlantic: Radiochemical evidence, *Deep Sea Res., Part I*, *41*(2), 315–334.

Francois, R., M. P. Bacon, and D. O. Suman (1990), Th-230 profiling in deep-sea sediments: High-resolution records of flux and dissolution of carbonate in the equatorial Atlantic during the last 24,000 years, *Paleoceanography*, *5*(5), 761–787.

Fronval, T., E. Jansen, J. Bloemendal, and S. Johnsen (1995), Oceanic evidence for coherent fluctuations in Fennoscandian and Laurentide ice sheets on millennium timescales, *Nature*, *374*, 443–446.

Ganopolski, A., and S. Rahmstorf (2002), Abrupt glacial climate changes due to stochastic resonance, *Phys. Rev. Lett.*, *88*(3), 038501, doi:10.1103/PhysRevLett.88.038501.

Gariépy, C., and C. J. Allègre (1985), The lead isotope geochemistry and geochronology of late-kinematic intrucives from the Abitibi greenstone belt, and the implications for late Archaean crustal evolution, *Geochim. Cosmochim. Acta*, *49*, 2371–2383.

Goldstein, S. J., and S. B. Jacobsen (1988), Nd and Sr isotope systematic of river water suspended sediment: Implications for crustal evolution, *Earth Planet. Sci. Lett.*, *87*, 249–265.

Grimm, E. C., G. L. Jacobson Jr., W. A. Watts, B. C. S. Hansen, and K. A. Maasch (1993), A 50,000-year record of climate oscillations from Florida and its temporal correlation with the Heinrich events, *Science*, *261*, 198–200.

Grootes, P. M., E. J. Steig, M. Stuiver, E. D. Waddington, and D. L. Morse (2001), The Taylor dome Antarctic O-18 record and globally synchronous changes in climate, *Quat. Res.*, *56*, 289–298.

Grousset, F. E., L. Labeyrie, J. A. Sinko, M. Cremer, G. Bond, J. Duprat, E. Cortijo, and S. Huon (1993), Patterns of ice-rafted detritus in the glacial North Atlantic (40–55°N), *Paleoceanography*, *8*(2), 175–192.

Grousset, F. E., C. Pujol, L. Labeyrie, G. Auffret, and A. Boelaert (2000), Were the North Atlantic Heinrich events triggered by the behavior of the European ice sheets?, *Geology*, *28*, 123–126.

Grousset, F. E., E. Cortijo, S. Huon, L. Hervé, T. Richter, D. Burdloff, J. Duprat, and O. Weber (2001), Zooming in on Heinrich layers, *Paleoceanography*, *16*(3), 240–259.

Gwiazda, R. H., S. R. Hemming, and W. S. Broecker (1996a), Tracking the sources of icebergs with lead isotopes: The provenance of ice-rafted debris in Heinrich layer 2, *Paleoceanography*, *11*(1), 77–93.

Gwiazda, R. H., S. R. Hemming, and W. S. Broecker (1996b), Provenance of icebergs during Heinrich event 3 and the contrast to their sources during other Heinrich episodes, *Paleoceanography*, *11*(4), 371–378.

Gwiazda, R. H., S. R. Hemming, W. S. Broecker, T. Onsttot, and C. Mueller (1996c), Evidence from ^{40}Ar/^{39}Ar ages for a Church-ill Province source of ice-rafted amphiboles in Heinrich layer 2, *J. Glaciol.*, *42*, 440–446.

Hald, M., T. Dokken, and G. Mikalsen (2001), Abrupt climatic change during the last interglacial-glacial cycle in the polar North Atlantic, *Mar. Geol.*, *176*, 121–137.

Harris, S. E., and A. C. Mix (1999), Pleistocene precipitation balance in the Amazon Basin recorded in deep sea sediments, *Quat. Res.*, *51*, 14–26.

Harrison, T. M. (1981), Diffusion of ^{40}Ar in hornblende, *Contrib. Mineral. Petrol.*, *78*, 324–331.

Heinrich, H. (1988), Origin and consequences of cyclic ice rafting in the northeast Atlantic Ocean during the past 130,000 years, *Quat. Res.*, *29*, 142–152.

Hemming, S. R., and I. Hajdas (2003), Ice rafted detritus evidence from ^{40}Ar/^{39}Ar ages of individual hornblende grains for evolution of the southeastern Laurentide ice sheet since 43 ^{14}C ky, *Quat. Int.*, *99–100*, 29–43.

Hemming, S. R., and E. T. Rasbury (2000), Pb isotope measurements of sanidine monitor standards: Implications for provenance analysis and tephrochronology, *Chem. Geology*, *165*, 311–337.

Hemming, S. R., S. M. McLennan, and G. N. Hanson (1994), Pb isotopes as a provenance tool for quartz: Examples from plutons and quartzite, northeastern Minnesota, *Geochim. Cosmochim. Acta*, *58*, 4455–4464.

Hemming, S. R., D. K. McDaniel, S. M. McLennan, and G. N. Hanson (1996), Pb isotope constraints on the provenance and diagenesis of detrital feldspars from the Sudbury Basin, Canada, *Earth Planet. Sci. Lett.*, *142*, 501–512.

Hemming, S. R., W. S. Broecker, W. D. Sharp, G. C. Bond, R. H. Gwiazda, J. F. McManus, M. Klas, and I. Hajdas (1998), Provenance of the Heinrich layers in core V28-82, northeastern Atlantic: ^{40}Ar-^{39}Ar ages of ice-rafted hornblende, Pb isotopes in feldspar grains, and Nd-Sr-Pb isotopes in the fine sediment fraction, *Earth Planet. Sci. Lett.*, *164*, 317–333.

Hemming, S. R., G. C. Bond, W. S. Broecker, W. D. Sharp, and M. Klas-Mendelson (2000a), Evidence from $^{40}Ar/^{39}Ar$ ages of individual hornblende grains for varying Laurentide sources of iceberg discharges 22,000 to 10,500 yr B.P., *Quat. Res.*, *54*, 372–383.

Hemming, S. R., R. H. Gwiazda, J. T. Andrews, W. S. Broecker, A. E. Jennings, and T. C. Onstott (2000b), $^{40}Ar/^{39}Ar$ and Pb-Pb study of individual hornblende and feldspar grains from southeastern Baffin Island glacial sediments: Implications for the provenance of the Heinrich layers, *Can. J. Earth Sci.*, *37*, 879–890.

Hemming, S. R., C. M. Hall, P. E. Biscaye, S. M. Higgins, G. C. Bond, J. F. McManus, D. C. Barber, J. T. Andrews, and W. S. Broecker (2002), $^{40}Ar/^{39}Ar$ ages and $^{40}Ar^*$ concentrations of fine-grained sediment fractions from North Atlantic Heinrich layers, *Chem. Geol.*, *182*, 583–603.

Hesse, R., and S. Khodabakhsh (1998), Depositional facies of late Pleistocene Heinrich events in the Labrador Sea, *Geology*, *26*, 103–106.

Heusser, C. J., L. E. Heusser, and T. V. Lowell (1999), Paleoecology of the southern Chilean Lake District-Isla Grande de Chiloe during middle-late Llanquihue glaciation and deglaciation, *Geogr. Ann., Ser. A*, *81*(2), 231–284.

Higgins, S. M. (2001), Extraterrestrial tracer in the sea: Evaluation and application of ^3He in interplanetary dust particles as a constant flux tracer in marine sediments, Ph.D. thesis, 203 pp., Dep. of Earth and Environ. Sci., Columbia Univ., New York.

Hillaire-Marcel, C., and G. Bilodeau (2000), Instabilities in the Labrador Sea water mass structure during the last climatic cycle, *Can. J. Earth Sci.*, *37*, 795–809.

Hillaire-Marcel, C., A. de Vernal, G. Bilodeau, and G. Wu (1994), Isotope stratigraphy, sedimentation rates, deep circulation, and carbonate events in the Labrador Sea during the last ~200 ka, *Can. J. Earth Sci.*, *31*, 63–89.

Hoffman, P. F. (1989), United plates of America, the birth of a craton—Early Proterozoic assembly and growth of Laurentia, *Annu. Rev. Earth Planet. Sci.*, *16*, 543–603.

Hulbe, C. L. (1997), An ice shelf mechanism for Heinrich layer production, *Paleoceanography*, *12*(5), 711–717.

Hulbe, C. L., D. R. MacAyeal, G. H. Denton, J. Kleman, and T. V. Lowell (2004), Catastrophic ice shelf breakup as the source of Heinrich event icebergs, *Paleoceanography*, *19*, PA1004, doi:10.1029/2003PA000890.

Hunt, A. G., and P. E. Malin (1998), Possible triggering of Heinrich events by ice load-induced earthquakes, *Nature*, *393*, 155–158.

Huon, S., and R. Jantschik (1993), Detrital silicates in northeast Atlantic deep-sea sediments during the late Quaternary: Major element REE and Rb-Sr isotopic data, *Eclogae Geol. Helv.*, *86*, 195–218.

Huon, S., and P. Ruch (1992), Mineralogical, K-Ar and $^{87}Sr/^{86}Sr$ isotope study of Holocene and last glacial sediments in a deep-sea core from the northeast Atlantic Ocean, *Mar. Geol.*, *107*, 275–282.

Huon, S., F. E. Grousset, D. Burdloff, G. Barboux, and A. Mariotti (2002), Sources of fine-sized organic matter in North Atlantic Heinrich layers: $\delta^{13}C$ and $\delta^{15}N$ tracers, *Geochim. Cosmochim. Acta*, *66*, 223–239.

Hurley, P. M., and J. R. Rand (1969), Pre-drift continental nuclei, *Science*, *164*, 1229–1242.

Hurley, P. M., B. C. Heezen, W. H. Pinson, and H. W. Fairbairn (1963), K-Ar age values in pelagic sediments of the North Atlantic, *Geochim. Cosmochim. Acta*, *27*, 393–399.

Jantschik, R., and S. Huon (1992), Detrital silicates in northeast Atlantic deep-sea sediments during the late Quaternary: Mineralogical and K-Ar isotopic data, *Eclogae Geol. Helv.*, *85*, 195–212.

Jennings, A. E., K. A. Tedesco, J. T. Andrews, and M. E. Kirby (1996), Shelf erosion and glacial ice proximity in the Labrador Sea during and after Heinrich events [H-3 or H-4 to H-0] as shown by foraminifera, in *Late Quaternary Palaeoceanography of the North Atlantic Margins*, edited by J. T. Andrews, *Geol. Soc. Spec. Publ.*, *111*, 29–49.

Johnson, R. G., and S.-E. Lauritzen (1995), Hudson Bay-Hudson Strait jökulhlaups and Heinrich events: A hypothesis, *Palaeogeogr. Palaeoclimatol. Palaeoecol.*, *117*, 123–137.

Kanfoush, S. L., D. A. Hodell, C. D. Charles, T. P. Guilderson, P. G. Mortyn, and U. S. Ninnemann (2000), Millennial-scale instability of the Antarctic ice sheet during the last glaciation, *Science*, *288*, 1815–1818.

Kara, A. B., P. A. Rochford, and H. E. Hurlburt (2003), Mixed layer depth variability over the global ocean, *J. Geophys. Res.*, *108*(C3), 3079, doi:10.1029/2000JC000736.

Keigwin, L. D., and S. J. Lehman (1994), Deep circulation change linked to Heinrich event 1 and Younger Dryas in a middepth North Atlantic core, *Paleoceanography*, *9*(2), 185–194.

Kennett, J. P., K. G. Cannariato, I. L. Hendy, and R. J. Behl (2000), Carbon isotopic evidence for methane hydrate instability during quaternary interstadials, *Science*, *288*, 128–133.

Kirby, M. E., and J. T. Andrews (1999), Mid-Wisconsin Laurentide ice sheet growth and decay: Implications for Heinrich events 3 and 4, *Paleoceanography*, *14*(2), 211–223.

Kissel, C., C. Laj, L. Labeyrie, T. Dokken, A. Voelker, and D. Blamart (1999), Rapid climatic variations during marine isotopic stage 3: Magnetic analysis of sediments from Nordic Seas and North Atlantic, *Earth Planet. Sci. Lett.*, *171*, 489–502.

Knies, J., H.-P. Kleiber, J. Matthiessen, C. Muller, and N. Nowaczyk (2001), Marine ice-rafted debris records constrain maximum extent of Saalian and Weichselian ice-sheets along the northern Eurasian margin, *Global Planet. Change*, *31*, 45–64.

Knutz, P. C., W. E. N. Austin, and E. J. W. Jones (2001), Millennial-scale depositional cycles related to British Ice Sheet variability and North Atlantic paleocirculation since 45 kyr B.P., Barra Fan, U. K. margin, *Paleoceanography*, *16*(1), 53–64.

Labeyrie, L., H. Leclaire, C. Waelbroeck, E. Cortijo, J.-C. Duplessy, L. Vidal, M. Elliot, B. Le Coat, and G. Auffret (1999), Temporal variability of the surface and deep waters of the North West Atlantic Ocean at orbital and millennial scales, in *Mechanisms of Global Climate Change at Millennial Time Scales*, *Geophys. Monogr. Ser.*, vol. 112, edited by P. U. Clark, R. S. Webb, and L. D. Keigwin, pp. 77–98, AGU, Washington D. C.

Lackschewitz, K. S., K.-H. Baumann, B. Gehrke, H.-J. Wallrabe-Adams, J. Thiede, G. Bonani, R. Endler, H. Erlenkeuser, and J. Heinemeier (1998), North Atlantic ice sheet fluctuations 10,000–70,000 yr ago as inferred from deposits on the Reykjanes Ridge, southeast of Greenland, *Quat. Res.*, *49*, 171–182.

Laj, C., C. Kissel, A. Mazaud, J. E. T. Channell, and J. Beer (2000), North Atlantic palaeointensity stack since 75 ka (NA-PIS-75) and the duration of the Laschamp event, *Philos. Trans. R. Soc. London, Ser. A*, *358*, 1009–1024.

Lawson, D. E., J. C. Strasser, E. B. Evenson, R. B. Alley, G. J. Larson, and S. A. Arcone (1998), Glaciohydraulic supercooling: A freeze-on mechanism to create stratified, debris-rich basal ice: I. Field evidence, *J. Glaciol.*, *44*, 547–562.

Leuschner, D. C., and F. Sirocko (2000), The low-latitude monsoon climate during Dansgaard-Oeschger cycles and Heinrich events, *Quat. Sci. Rev.*, *19*(1–5), 243–254.

Little, M. G., R. R. Schneider, D. Kroon, B. Price, C. P. Summerhayes, and M. Segl (1997), Trade wind forcing of upwel-

ling, seasonality, and Heinrich events as a response to sub-Milankovitch climate variability, *Paleoceanogrphy*, *12*(4), 568–576.

Lowell, T. V. (2000), As climate changes, so do glaciers, *Proc. Nat. Acad. Sci. U. S. A.*, *97*(4), 1351–1354.

Lowell, T. V., C. J. Heusser, B. G. Andersen, P. I. Moreno, A. Hauser, L. E. Heusser, C. Schlüchter, D. R. Marchant, and G. H. Denton (1995), Interhemispheric correlation of late Pleistocene glacial events, *Science*, *269*, 1541–1549.

Lund, D. C., and A. C. Mix (1998), Millennial-scale deep water oscillations: Reflections of the North Atlantic in the deep Pacific from 10 to 60 ka, *Paleoceanography*, *13*(1), 10–19.

Lynch-Stieglitz, J., W. B. Curry, and N. Slowey (1999), Weaker Gulf Stream in the Florida straits during the Last Glacial Maximum, *Nature*, *402*, 644–648.

MacAyeal, D. R. (1993), Binge/purge oscillations of the Laurentide ice sheet as a cause of the North Atlantic's Heinrich events, *Paleoceanography*, *8*(6), 775–784.

Madureira, L. A. S., S. A. van Kreveld, G. Eglinton, M. Conte, G. Ganssen, J. E. vanHinte, and J. J. Ottens (1997), Late Quaternary high-resolution biomarker and other sedimentary climate proxies in a northeast Atlantic core, *Paleoceanography*, *12*(2), 255–269.

Manabe, S., and R. J. Stouffer (1995), Simulation of abrupt climate change induced by freshwater input to the North Atlantic Ocean, *Nature*, *378*, 165–167.

Mangerud, J., T. Dokken, D. Hebbeln, B. Heggen, O. Ingolfsson, J. Y. Landvik, V. Mejdahl, J. I. Svendsen, and T. O. Vorren (1998), Fluctuations of the Svalbard Barents Sea Ice Sheet during the last 150,000 years, *Quat. Sci. Rev.*, *17*(1–3), 11–42.

Manighetti, B., I. N. McCave, M. Maslin, and N. J. Shackleton (1995), Chronology for climate change: Developing age models for the Biogeochemical Ocean Flux Study cores, *Paleoceanography*, *10*(3), 513–525.

Marshall, S. J., and G. K. C. Clarke (1997), A continuum mixture model of ice stream thermomechanics in the Laurentide ice sheet: 2. Application to the Hudson Strait ice stream, *J. Geophys. Res.*, *102*(B9), 20,615–20,637.

Maslin, M. A., N. J. Shackleton, and U. Pflaumann (1995), Surface water temperature, salinity and density changes in the northeast Atlantic during the last 45,000 years: Heinrich events, deep water formation and climatic rebounds, *Paleoceanography*, *10*(3), 527–544.

Matsumoto, K. (1997), Modeled glacial North Atlantic ice-rafted debris pattern and its sensitivity to various boundary conditions, *Paleoceanography*, *12*(2), 271–280.

McCave, N. (1995), Sedimentary processes and the creation of the stratigraphic record in the late Quaternary North Atlantic Ocean, *Philos. Trans. R. Soc. London, Ser. B*, *348*, 229–240.

McIntyre, A., and B. Molfino (1996), Forcing of Atlantic equatorial and subpolar millennial cycles by precession, *Nature*, *274*, 1867–1870.

McLennan, S. M., and S. Hemming (1992), Samarium/neodymium elemental and isotopic systematics in sedimentary rocks, *Geochim. Cosmochim. Acta*, *56*, 887–898.

McManus, J. F., C. O. Major, B. Flower, and T. Fronval (1996), Variability in sea-surface conditions in the North Atlantic-Arctic gateways during the last 140,000 years, *Proc. Ocean Drill. Program Sci. Results*, *151*, 437–443.

McManus, J. F., R. F. Anderson, W. S. Broecker, M. Q. Fleisher, and S. M. Higgins (1998), Radiometrically determined sedimentary fluxes in the sub-polar North Atlantic during the last 140,000 years, *Earth Planet. Sci. Lett.*, *155*, 29–43.

McManus, J. F., D. W. Oppo, and J. L. Cullen (1999), A 0.5-million-year record of millennial-scale climate variability in the North Atlantic, *Science*, *283*, 971–975.

McManus, J. F., R. Francois, J. M. Gherardi, and J. Nuwer (2002), Variable rates of ocean circulation from sedimentary Pa-231/Th-230 during the last ice age termination, paper presented at 12th Annual V. M. Goldschmidt Conference, Geochem. Soc., Davos, Switzerland.

Meese, D. A., A. J. Gow, R. B. Alley, G. A. Zielinski, P. M. Grootes, M. Ram, K. C. Taylor, P. A. Mayewski, and J. F. Bolzan (1997), The Greenland Ice Sheet Project 2 depth-age scale: Methods and results, *J. Geophys. Res.*, *102*(C12), 26,411–26,423.

Mix, A. C., E. Bard, and R. Schneider (2001), Environmental processes of the ice age: Land, oceans, glaciers (EPILOG), *Quat. Sci. Rev.*, *20*(4), 627–657.

Ninnemann, U. S., C. D. Charles, and D. A. Hodell (1999), Origin of global millennial scale climate events: Constraints from the Southern Ocean deep sea sedimentary record, in *Mechanisms of Global Climate Change at Millennial Time Scales*, *Geophys. Monogr. Ser.*, vol. 112, edited by P. U. Clark, R. S. Webb, and L. D. Keigwin, pp. 99–112, AGU, Washington, D. C.

Oppo, D. W., J. F. McManus, and J. L. Cullen (1998), Abrupt climate events 500,000 to 340,000 years ago: Evidence from subpolar North Atlantic sediments, *Science*, *279*, 1335–1338.

Paillard, D. (1995), The hierarchical structure of glacial climatic oscillations: Interactions between ice-sheet dynamics and climate, *Clim. Dyn.*, *11*, 162–177.

Paillaird, D., and E. Cortijo (1999), A simulation of the Atlantic meridional circulation during Heinrich event 4 using reconstructed sea surface temperatures and salinities, *Paleoceanography*, *14*(6), 716–724.

Parizek, B. R., R. B. Alley, S. Anandakrishnan, and H. Conway (2002), Sub-catchment melt and long-term stability of ice stream D, West Antarctica, *Geophys. Res. Lett.*, *29*(8), 1214, doi:10.1029/2001GL014326.

Pastouret, L., G. Auffret, M. Hoffert, M. Melguen, H. D. Needham, and C. Latouche (1972), Sédimentation sur la ride de Terre-Neuve, *Can. J. Earth Sci.*, *12*, 1019–1035.

Peterson, L. C., G. H. Haug, K. A. Hughen, and U. Rohl (2000), Rapid changes in the hydrologic cycle of the tropical Atlantic during the last glacial, *Science*, *290*, 1947–1951.

Pfeffer, W. T., M. Dyurgerov, M. Kaplan, J. Dwyer, C. Sassolas, A. Jennings, B. Raup, and W. Manley (1997), Numerical modeling of late glacial Laurentide advance of ice across Hudson Strait: Insights into terrestrial and marine geology, mass balance, and claving flux, *Paleoceanography*, *12*(1), 97–110.

Porter, S. C., and Z. S. An (1995), Correlation between climate events in the North Atlantic and China during the last glaciation, *Nature*, *375*, 305–308.

Prokopenko, A. A., D. F. Williams, W. B. Karabanov, and G. K. Khursevich (2001), Continental response to Heinrich events and Bond cycles in sedimentary record of Lake Baikal, Siberia, *Global Planet. Change*, *28*, 217–226.

Rahmstorf, S. (2002), Ocean circulation and climate during the past 120,000 years, *Nature*, *419*, 207–214.

Rashid, H., R. Hesse, and D. J. W. Piper (2003a), Distribution, thickness and origin of Heinrich layer 3 in the Labrador Sea, *Earth Planet. Sci. Lett.*, *205*, 281–293.

Rashid, H., R. Hesse, and D. J. W. Piper (2003b), Origin of unusually thick Heinrich layers in ice-proximal regions of the northwest Labrador Sea, *Earth Planet. Sci. Lett.*, *208*, 319–336.

Rasmussen, T. L., T. C. E. van Weering, and L. Labeyrie (1997), Climatic instability, ice sheets and ocean dynamics at high northern latitudes during the last glacial period (58–10 ka BP), *Quat. Sci. Rev.*, *16*(1), 71–80.

Rasmussen, T. L., D. W. Oppo, E. Thomsen, and S. J. Lehman (2003), Deep sea records from the southeast Labrador Sea: Ocean circulation changes and ice-rafting events during the last 160,000 years, *Paleoceanography*, *18*(1), 1018, doi:10.1029/2001PA000736.

Revel, M., J. A. Sinko, F. E. Grousset, and P. E. Biscaye (1996), Sr and Nd isotopes as tracers of North Atlantic lithic particles: Paleoclimatic implications, *Paleoceanography*, *11*(1), 95–113.

Roberts, M. J., F. S. Tweed, A. J. Russell, O. Knudsen, D. E. Lawson, G. J. Larson, E. B. Evenson, and H. Bjornsson (2002), Glaciohydraulic supercooling in Iceland, *Geology*, *30*, 439–442.

Robinson, S. G., M. A. Maslin, and N. McCave (1995), Magnetic susceptibility variations in upper Pleistocene deep-sea sediments of the NE Atlantic: Implications for ice rafting and paleocirculation at the Last Glacial Maximum, *Paleoceanography*, *10*(2), 221–250.

Rohling, E. J., A. Hayes, S. De Rijk, D. Kroon, W. J. Zachariasse, and D. Eisma (1998), Abrupt cold spells in the northwest Mediterranean, *Paleoceanography*, *13*(4), 316–322.

Rosell-Melé, A., M. A. Maslin, J. R. Maxwell, and P. Schaeffer (1997), Biomarker evidence for 'Heinrich' events, *Geochim. Cosmochim. Acta*, *61*, 1671–1678.

Ruddiman, W. F. (1977), Late Quaternary deposition of ice-rafted sand in the subpolar North Atlantic (lat 40° to 65°N), *Geol. Soc. Am. Bull.*, *88*, 1813–1827.

Ruddiman, W. F., and L. K. Glover (1982), Mixing of volcanic ash zones in subpolar North Atlantic sediments, in *The Ocean Floor, Bruce C. Heezen Memorial Volume*, edited by R. A. Scrutton and M. Talwani, pp. 37–60, John Wiley, Hoboken, N. J.

Sachs, J. P., and S. J. Lehman (1999), Subtropical North Atlantic temperatures 60,000 to 30,000 years ago, *Science*, *286*, 756–759.

Sarnthein, M., K. Winn, S. J. A. Jung, J. C. Duplessy, L. Labeyrie, H. Erlenkeuser, and G. Ganssen (1994), Changes in east Atlantic deep water circulation over the last 30,000 years: Eight time slice reconstructions, *Paleoceanography*, *9*(2), 209–267.

Schmittner, A., M. Yoshimori, and A. J. Weaver (2002), Instability of glacial climate in a model of the ocean-atmosphere-cryosphere system, *Science*, *295*, 1489–1493.

Schmitz, W. J., Jr. (1996), On the world ocean circulation: Volume I some global features/North Atlantic circulation, *Tech Rep. WHOI-96-03*, Woods Hole Oceanogr. Inst., Woods Hole, Mass.

Schmitz, W. J., Jr., and M. S. McCartney (1993), On the North Atlantic circulation, *Rev. Geophys.*, *31*, 24–49.

Schrag, D. P., J. F. Adkins, K. McIntyre, J. L. Alexander, D. A. Hodell, C. D. Charles, and J. F. McManus (2002), The oxygen isotopic composition of seawater during the Last Glacial Maximum, *Quat. Sci. Rev.*, *21*(1–3), 331–342.

Schulz, H., U. von Rad, and H. Erlenkeuser (1998), Correlation between Arabian Sea and Greenland climate oscillations of the past 110,000 years, *Nature*, *393*, 54–57.

Scourse, J. D., I. R. Hall, I. N. McCave, J. R. Young, and C. Sugdon (2000), The origin of Heinrich layers: Evidence from H2 for European precursor events, *Earth Planet. Sci. Lett.*, *182*, 187–195.

Seidov, D., and M. Maslin (1999), North Atlantic deep water circulation collapse during Heinrich events, *Geology*, *27*, 23–26.

Shackleton, N. J. (1967), Oxygen isotope analyses and paleotemperatures reassessed, *Nature*, *215*, 15–17.

Siddall, M., E. J. Rohling, A. Almogi-Labin, C. Hemeleben, D. Meischner, I. Schmelzer, and D. A. Smeed (2003), Sea-level fluctuations during the last glacial cycle, *Nature*, *423*, 853–858.

Snoeckx, H., F. Grousset, M. Revel, and A. Boelaert (1999), European contribution of ice-rafted sand to Heinrich layers H3 and H4, *Mar. Geol.*, *158*, 197–208.

Steig, E. J., and R. B. Alley (2003), Phase relationships between Antarctic and Greenland climate records, *Ann. Glaciol.*, *35*, 451–456.

Steig, E. J., E. J. Brook, J. W. C. White, C. M. Sucher, M. L. Bender, S. J. Lehman, D. L. Morse, E. D. Waddington, and G. D. Clow (1998), Synchronous climate changes in Antarctica and the North Atlantic, *Science*, *282*, 92–95.

Stoner, J. S., and J. T. Andrews (1999), The North Atlantic as a Quaternary magnetic archive, in *Quaternary Climate, Environments and Magnetism*, edited by B. B. Maher and R. Thompson, pp. 49–80, Cambridge Univ. Press, New York.

Stoner, J. S., J. E. T. Channell, and C. Hillaire-Marcel (1996), The magnetic signature of rapidly deposited detrital layers from the deep Labrador Sea: Relationship to North Atlantic Heinrich layers, *Paleoceanography*, *11*(3), 309–325.

Stoner, J. S., J. E. T. Channell, and C. Hillaire-Marcel (1998), A 200 ka geomagnetic chronostratigraphy for the Labrador Sea: Indirect correlation of the sediment record to SPECMAP, *Earth Planet. Sci. Lett.*, *159*, 165–181.

Stoner, J. S., J. E. T. Channell, C. Hillaire-Marcel, and C. Kissel (2000), Geomagnetic paleointensity and environmental record from Labrador Sea core MD95-2024: Global marine sediment and ice core chronostratigraphy for the last 110 kyr, *Earth Planet. Sci. Lett.*, *183*, 161–177.

Stuiver, M., and P. M. Grootes (2000), GISP2 oxygen isotope ratios, *Quat. Res.*, *53*, 277–283.

Suman, D. O., and M. P. Bacon (1989), Variations in Holocene sedimentation in the North American Basin determined from Th-230 measurements, *Deep Sea Res., Part A*, *36*(6), 869–878.

Taylor, S. R., and S. M. McLennan (1985), The continental crust: Its composition and evolution, in *Geoscience Texts*, pp. 312, Blackwell Sci., Malden, Mass.

Thomson, J., N. C. Higgs, and T. Clayton (1995), A geochemical criterion for the recognition of Heinrich events and estimation of their depositional fluxes by the $^{230}Th_{excess}$ profiling method, *Earth Planet. Sci. Lett.*, *135*, 41–56.

Thomson, J., S. Nixon, C. P. Summerhayes, J. Schönfeld, R. Zahn, and P. Grootes (1999), Implications for sedimentation changes on the Iberian margin over the last two glacial/interglacial transitions from $(^{230}Th_{excess})_0$ systematics, *Earth Planet. Sci. Lett.*, *165*, 255–270.

Vance, D., and C. Archer (2002), Isotopic constraints on the origin of Heinrich event precursors, *Geochim. Cosmochim. Acta*, *66*, Suppl. 1, A798.

van Kreveld, S. A., M. Knappertsbusch, J. Ottens, G. M. Ganssen, and J. E. van Hinte (1996), Biogenic carbonate and ice-rafted debris (Heinrich layer) accumulation in deep-sea sediments from a northeast Atlantic piston core, *Mar. Geol.*, *131*, 21–46.

van Kreveld, S., M. Sarnthein, H. Erlenkeuser, P. Grootes, S. Jung, M. J. Nadeau, U. Pflaumann, and A. Voelker (2000), Potential links between surging ice sheets, circulation changes, and the Dansgaard-Oeschger cycles in the Irminger Sea, 60–18 kyr, *Paleoceanography*, *15*(4), 425–442.

Veiga-Pires, C. C., and C. Hillaire-Marcel (1999), U and Th isotope constraints on the duration of Heinrich events H0-H4 in the southeastern Labrador Sea, *Paleoceanography*, *14*(2), 187–199.

Verbitsky, M., and B. Saltzman (1995), A diagnostic analysis of Heinrich glacial surge events, *Paleoceanography*, *10*(1), 59–65.

Vidal, L., L. Labeyrie, E. Cortijo, M. Arnold, J. C. Duplessy, E. Michel, S. Becqué, and T. C. E. van Weering (1997), Evidence for changes in the North Atlantic Deep Water linked to meltwater surges during the Heinrich events, *Earth Planet. Sci. Lett.*, *146*, 13–27.

Vidal, L., L. Labeyrie, and T. C. E. van Weering (1998), Benthic $\delta^{18}O$ records in the North Atlantic over the last glacial period (60–10 kyr): Evidence for brine formation, *Paleoceanography*, *13*(3), 245–251.

Voelker, A. H. L. (2002), Global distribution of centennial-scale records for Marine Isotope Stage (MIS) 3: A database, *Quat. Sci. Rev.*, *21*(10), 1185–1212.

Voelker, A. H. L., M. Sarnthein, P. M. Grootes, H. Erlenkeuser, C. Laj, A. Mazaud, M.-J. Nadeau, and M. Schleicher (1998), Correlation of marine ^{14}C ages from the Nordic Seas with the GISP2 isotope record: Implications for ^{14}C calibration beyond 25 ka BP, *Radiocarbon*, *40*(1–2), 517–534.

Voelker, A. H. L., P. M. Grootes, M. J. Nadeaue, and M. Sarnthein (2000), Radiocarbon levels in the Iceland Sea from 25–53 kyr and their link of the Earth's magnetic field intensity, *Radiocarbon*, *42*(3), 437–452.

Waelbroeck, C., J. C. Duplessy, E. Michel, L. Labeyrie, D. Paillard, and J. Duprat (2001), The timing of the last deglaciation in North Atlantic climate records, *Nature*, *412*, 724–727.

Waelbroeck, C., L. Labeyrie, E. Michel, J. C. Duplessy, J. F. McManus, K. Lambeck, E. Balbon, and M. Labracherie (2002), Sea-level and deep water temperature changes derived

from benthic foraminifera isotopic records, *Quat. Sci. Rev.*, *21*(1–3), 295–305.

Wang, Y. J., H. Cheng, R. L. Edwards, Z. S. An, J. Y. Wu, C.-C. Shen, and J. A. Dorale (2001), A high-resolution absolute-dated late Pleistocene monsoon record from Hulu Cave, China, *Science*, *294*, 2345–2348.

Willamowski, C., and R. Zahn (2000), Upper ocean circulation in the glacial North Atlantic from benthic foraminiferal isotope and trace element fingerprinting, *Paleoceanography*, *15*(5), 515–527.

Wunsch, C. (2003), Determining paleoceanographic circulations, with emphasis on the Last Glacial Maximum, *Quat. Sci. Rev.*, *22*(2–4), 371–385.

Yokoyama, Y., T. M. Esat, K. Lambeck, and L. K. Fifield (2000), Last ice age millennial scale climate changes recorded in Huon Peninsula corals, *Radiocarbon*, *42*(3), 383–401.

Yokoyama, Y., T. M. Esat, and K. Lambeck (2001), Coupled climate and sea-level changes deduced from Huon Peninsula coral terraces of the last ice age, *Earth Planet. Sci. Lett.*, *193*, 579–587.

Zahn, R., J. Shönfeld, H.-R. Kudrass, M.-H. Park, H. Erlenkeuser, and P. Grootes (1997), Thermohaline instability in the North Atlantic during meltwater events: Stable isotope and ice-rafted detritus records from core SO75-26KL, Portuguese margin, *Paleoceanography*, *12*(5), 696–710.

—————————

S. R. Hemming, Lamont-Doherty Earth Observatory of Columbia University, Route 9W, Palisades, NY 10964, USA. (sidney@ldeo. columbia. edu)